

4.1 Sampling, quantization and next signal reconstruction

The technical world is becoming more and more digital because digital signals are very convenient for information processing. However, most physical phenomena are analog and the sensors measure analogue quantities. For that reason, the *digital signal processing DSP* is often realized in the following sequence: conversion of the analogue signal to digital form \Rightarrow digital signal processing \Rightarrow conversion of the digital signal back to the analogue one. The conversion is realized by the *analog-to-digital converters ADC* while the reverse process is realized by *digital to analog converters DAC*.

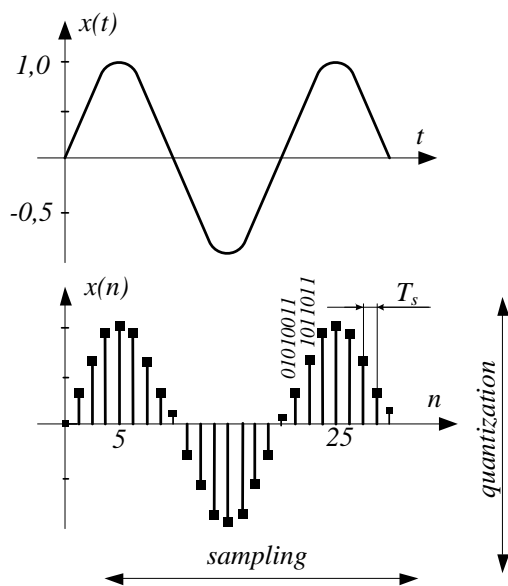


FIGURE 4.1
The analog signal and its conversion to the discrete form.

The analogue signals are of *continuous time* – the value of such signal is determined in every instant of time. An example of the analogue signal is presented in Figure 4.1a. The conversion of the analogue signal $x(t)$ to the digital form is realized in such a way that in

assumed moment of time the value of the signal $x(n)$ is determined and represented by a number. We can say that the digital signal is determined in *discrete time*, which means that the value of the signal is known only in selected moments. Usually the discrete time is realized by collecting the samples of the analogue signal at the constant interval called the *period of sampling* T_s (Figure 4.1b).

The process of collection of the samples is called the *sampling process* of analog signals. The frequency $f_s=1/T_s$ is called the *sampling frequency* and it is described in *Hz* or *sps – samples per second*. The process of determination of the digital value of the samples is called the *quantization* of the signals. The sampling is the digitization of the time, while the quantization is the digitization of the signal value.

As the result of sampling the time on the axis x is substituted by the number (index) n and every sample is described by its index n . The analog signal described by the equation $x(t) = X_m \sin \omega t$ is converted to the signal $x(n) = \sum X_n$ (where X_m is the magnitude of analogue signal while the X_n is the value of the signal of the index n).

The conversion from the index n to the time t is obvious because index n indicates the time with the period $T_s = 1/f_s$. For example, if we are sampling the signal of the frequency 50 Hz and we would like to obtain the discrete signal represented by 64 samples per the period of signal¹ the sampling frequency should be $f_s = 3200 \text{ Hz}$ (and period of sampling is $T_s = 312.5 \mu\text{s}$).

Thus the $n = 50$ corresponds with the time $50 \times 312.5 \mu\text{s} = 15.625 \text{ ms}$. If we would like to have 128 samples per period of the measured signal then the sampling frequency should be two-times larger (6400 Hz in our case).

Important question is: how many samples per period is the best? Simple answer is: as much as possible because in such case the analogue signal is the best represented by digital one and further analogue signal reconstruction is more exact. But as more samples per period (as higher speed of sampling) as more expensive is digital to analog converter. Therefore the more

¹ It is advantageous to have 2^n samples per period – this subject is discussed later.

appropriate answer to above question is: sufficient number of samples.

The sufficient number of samples describes the fundamental law of DSP – the Nyquist-Shannon theorem²: *the sampling frequency should be at least two times larger than the highest frequency component of the sampled signal* (two times larger than the bandwidth w).

Thus on other words we can say that the number of samples per period should exceed two³. Indeed although sampling theorem has reach mathematical grounds we simply can note that by three points it is possible to draw only one sinusoid and therefore to correct reconstruct sampled signal it is sufficient to have only three point per period.

It should be noted that in sampling theorem we say about the *highest frequency component*. It means that if we have distorted signal for example rectangular one then to correct describe this signal we should take into account sufficient large number of harmonics and the sampling frequency should be two times larger than the highest harmonic.

The analog sinusoidal signal of the frequency f_x can be by the equation:

$$x(t) = X_m \sin 2\pi f_x t \quad (4.1)$$

and is represented by only one spectral line of the frequency f_x (Figure 5). After sampling with the period T_s the same signal is described as

$$x(n) = X_m \sin 2\pi f_x nT_s \quad (4.2)$$

But because the sinusoid is identical with the period 2π ($\sin \varphi = \sin(\varphi \pm 2k\pi)$) the equation (5.2) should be rewritten in the form

$$x(n) = X_m \sin(2\pi f_x nT_s \pm 2k\pi) \quad (4.3)$$

After introducing the value $m = k/n$ we obtain

$$\begin{aligned} x(n) &= X_m \sin 2\pi \left(f_x \pm \frac{k}{n} f_s \right) nT_s = \\ &= X_m \sin 2\pi (f_x \pm mf_s) nT_s \end{aligned} \quad (4.4)$$

² Shannon theorem (sampling theorem) is also known as Nyquist-Shannon theorem. Before the Shannon the sampling theorem was analyzed by mathematicians Whittaker and Ferrar. Independently similar theorem was introduced by a Russian scientist Kotelnikov. Therefore the Shannon theorem is sometimes also called as the WKS sampling theorem (WKS – Whittaker, Kotelnikov, Shannon).

³ When CD technology started the sampling frequency was selected as 44.1 kHz because human ear is able to detect the sound of frequency to about 20 kHz.

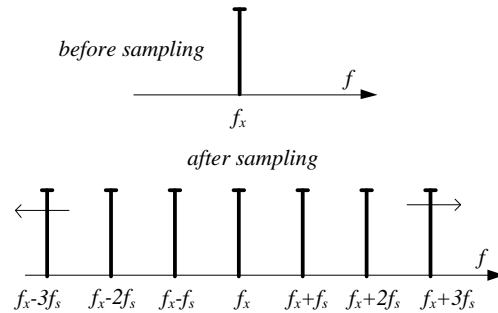


FIGURE 4.2
The spectrum line of the sinusoidal signal and its replication after sampling.

Thus after sampling of the signal of frequency f_x at the output of analog to digital converter appear the infinity number of components $f_a \pm mf_s$ - component representing input signal and mirrored around signals with distance f_s (Figure 4.2).

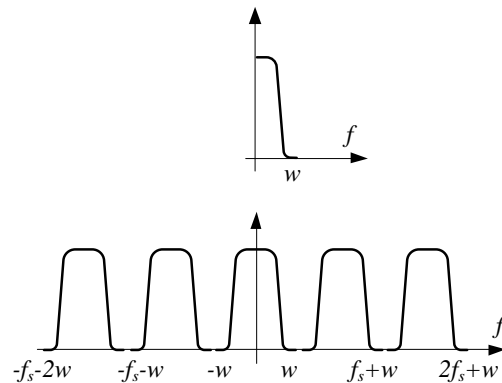


FIGURE 4.3
The signal of the bandwidth w and its replication after sampling.

Similarly, if instead of one sinusoidal signal we have the signals within a bandwidth w (Figure 4.3) after sampling we obtain the multiplication of this bandwidths with the frequency f_s . We obtain a lot of signals of the frequencies $w \pm mf_s$.

The signal presented in Figure 4.3 was sampled with the frequency $f_s > 2w$ (according to the Nyquist rule). Thus in the frequency range $0 < f < w$ the signals before and after sampling are the same – it is possible to remove the other signals of the frequency $f > w$ with a filter. But if the sampling frequency is smaller than $2w$ the duplicated signals are covered mutually and in the frequency range around the sampling frequency exist two signals of the same frequency (Figure 4.4).

We are not able to recognize which one is true. This effect is called *aliasing*.

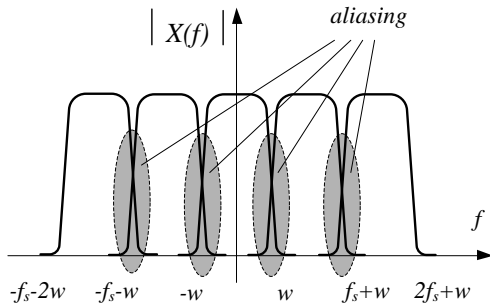


FIGURE 4.4
The replication of the signals (aliasing) when the sampling frequency is too small.

The aliasing effect is not only a mathematical problem because it exists and is very troublesome in practice. Figure 4.5 presents a simple experiment – we perform spectral analysis of a signal for a sampling frequency of 10 kHz. The testing range on the screen is half a sampling frequency – thus a signal of 2.5 kHz appears exactly in the middle of the screen. But if we increase later the frequency of the tested signal after exceeding 5 kHz, this signal appears again as returning one. The signal corresponding with 7.5 kHz appears exactly in the same place as 2.5 kHz. Only the difference is that the true signal is moving to the right while the false (alias) signal is moving to the left.⁴



FIGURE 4.5
Experimental detection of an aliasing signal during spectral analysis.

By analyzing Figures 4.3 and 4.4 we can say that a sufficient condition to avoid an aliasing effect is to fulfill the Nyquist rule. Indeed, if we are sure that we have only tested a signal such condition could be sufficient. But we know that in real world the useful signal is commonly accompanied by parasitic signals, for example noises and interferences. This parasitic signal can return as an alias one.

⁴ But false 12.5 kHz behaves similarly to 2.5 kHz and both signals are difficult to distinguish.

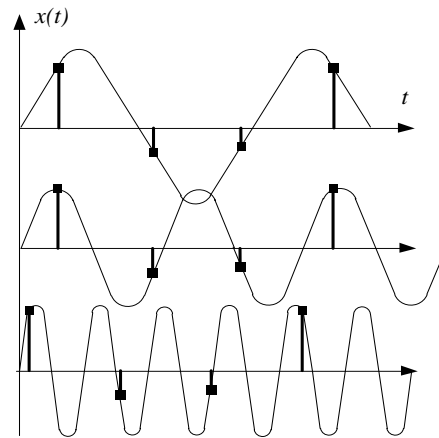


FIGURE 4.6
The same sampling result of various frequency signals.

Figure 4.6 presents the possibility that we obtain due to aliasing the same result for signals of different frequencies. Let us consider the following example. The sampling frequency used in CD technology is $f_s = 44.1 \text{ kHz}$. According to the Nyquist theorem the sampling frequency is sufficiently high (more than two times larger than 20 kHz). However, if in the processed acoustic signal there is a parasitic signal of the frequency 45 kHz, this signal is in analog technique not a danger – it is inaudible (beyond the audibility of the human ear). But according to equation (4.4) after sampling the parasitic signal appears as $f_x - f_s = 45 \text{ kHz} - 44 \text{ kHz} = 1 \text{ kHz}$. Thus, after sampling a new distorted very loud audible signal of 1 kHz appears due to the aliasing.

To avoid such ambiguity caused by the aliasing effect before the analog-to-digital converter there should be introduced a special *anti-alias lowpass filter* with the cut-off frequency equal to the *Nyquist frequency* (Figure 4.7). The Nyquist frequency f_N is half of the sampling rate $f_N = f_s / 2$. The frequency bandwidth till $f_s / 2$ is often called as *Nyquist band* or *Nyquist zone*.

The cut-off frequency of the anti-alias filter depends on the dynamics of the signal⁵. As was discussed in the previous chapter the typical slope of the M^{th} -order filter is $M \times 10 \text{ dB/decade}$ (or 6 dB/octave). If our sampled signal exhibits the dynamics of 100 dB (what is in the case of symphonic orchestra sound) then to limit this signal to a decade bandwidth above w it is necessary to use a tenth order filter, which is rather difficult in

⁵ Take into account that as the bandwidth of the amplifier we assume the frequency range where the amplitude of the signal does not drop more than 3dB. Thus even outside the bandwidth there are signals with quite large amplitude.

practical realization. We can see that for large dynamics of the signal the filter should exhibit very large steepness of the frequency characteristic in the transition band. Therefore as the anti-alias filter often elliptical (Cauer) filters with large steepness of the frequency characteristic are used. But high-order filters with large steepness introduce phase distortion, which in the case of acoustic signals is unacceptable.

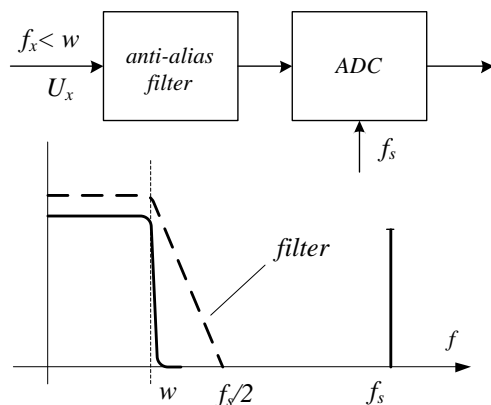


FIGURE 4.7
The sampling of the signal with the anti-alias filter at the input.

Figure 4.7 presents the principle of application of the anti-alias filter. According to the Nyquist theorem the sampling frequency f_s should be two times larger than the bandwidth w . But if we use anti-alias filter for the full attenuation of the signal is necessary to include small margin (taking into account slope of the filter characteristic). For that reason it is safer to set the sampling frequency f_s two times larger than the frequency when the anti-alias filter sufficiently attenuates the signals (thus the Nyquist frequency $f_s/2$ is slightly larger than the bandwidth w).

For example in the CD audio system the sampling frequency was chosen as 44.1 kHz what means that the Nyquist frequency is 22.05 kHz. Thus we have small margin for filter assuming that the human ear sensing border is about 16 kHz.

Higher sampling frequency means less critical requirements of the filter performances. Such conclusion results in the technique of sampling called *oversampling* technique (Figure 4.8). This method is currently applied in high quality sound processing especially because on the market appeared sigma-delta AD converters with high sampling frequency. For example in SACD system introduced by Sony (*SACD – Super Audio Compact Disc*) the sampling frequency is 2.82 MHz which means the oversampling factor $K = 64$.

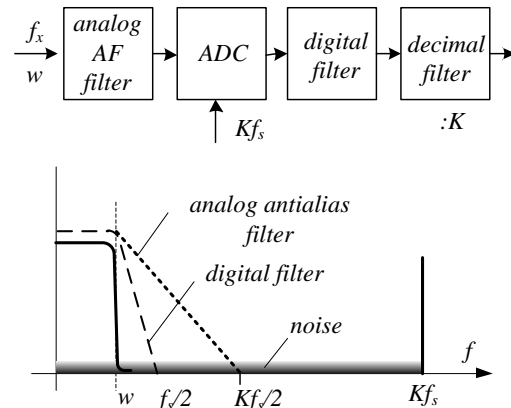


FIGURE 4.8
The digital to analog conversion with oversampling technique

By applying the oversampling we can use the analogue anti-alias filter of lower order. After conversion to the digital signals we can use much better digital anti-alias filter and then the decimal filter recovering the lower sampling rate. The profit related to the application of the cheaper and less complicated anti-alias filter is at the expense of the necessity of application of the analogue-to-digital converter of higher sampling speed.

It is also other important advantage of oversampling technique. The energy of noises is distributed in the whole bandwidth therefore as larger sampling frequency as lower noise level. If we next (after sampling) cut-off the frequency useful bandwidth we eliminate some part of noises. And decrease of noises in the useful bandwidth is crucial for AD conversion because the dynamics and resolution of this conversion is much better.

Let us consider another case when we process the signal in the bandwidth 450 MHz – 460 MHz. Such case we can meet often in telecommunication signal transmission. Applying the sampling frequency 920 MHz (according to the Nyquist theorem) seems to be extravagance. It is possible to reconstruct the sampling signal with modified the Nyquist rule: *the sampling frequency should be at least two times larger than the bandwidth (not the largest frequency signal)*. In our case of the signals in bandwidth 450 MHz – 460 MHz it is sufficient to use sampling frequency 20 MHz instead of 920 MHz. This technique is called the *undersampling technique* (or sometimes band-pass sampling).

In the quantization process to each sample a digital value is assigned, most often in the binary code. Figure 4.9 presents the quantization with 2-bit resolution. In 2-

bit quantization the converted value can be represented by four possible levels: 00, 01, 10 and 11. The value of the continuous signal is rounded to the nearest possible level of quantization – thus the maximal value of the quantization error is half of a quant. In our case of 2-bit quantization this error is equal to 12.5% of full value. It is obvious that the larger is the digital word representing the quantized value (as more bits are used) the better is the quality of quantization (lower quantization error and larger quantization dynamics)⁶. Table 4.1 presents the performances depending on the number of bits of various AD converters.

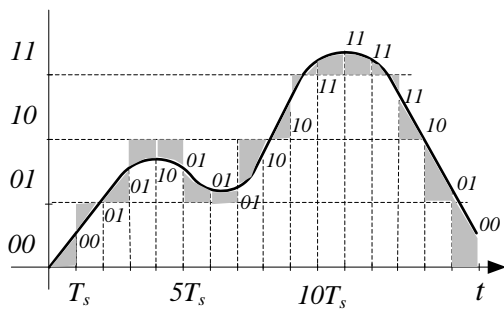


FIGURE 4.9
The quantization of the continuous signal with 2-bit resolution (the error of quantization is indicated with the grey color)

TABLE 4.1
The performances of the quantization process depending on the number of bits N (determined under assumption, that the range of the conversion is 0 – 2V).

Number of bits N	Quantization levels 2^N	Quantum value q [μ V]	Resolution % FS
8	256	8 000	0.39
10	1 024	2 000	0.098
12	4 096	500	0.024
16	65 536	31	0.0015
24	16 777 216	0.12	0.000006

Figure 4.10 presents the example of the conversion with a 3-bit converter. The *LSB* (*LSB* – *least significant bit*) is the abbreviation assigned to the smallest quantity of converted value and for N-bit converter it is equal to the resolution $1/2^N$. On the other hand the smallest quantity of the measured value is one quantum q determined as the smallest part of the *FS* value (*FS* – *full scale*)

$$q = \frac{FS}{2^N} \quad (4.5)$$

⁶ But the larger is the number of bits the more expensive is the analogue-to-digital converter.

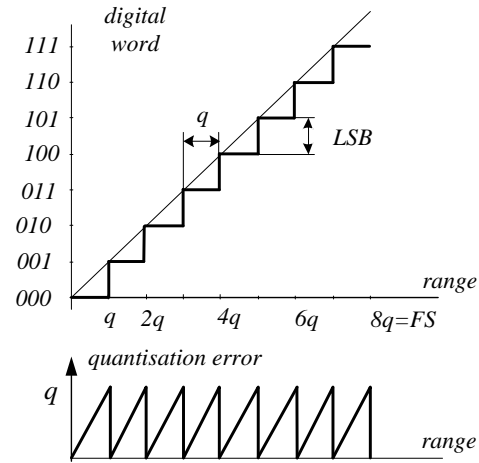


FIGURE 4.10
The characteristic of quantization of the 3-bit ADC

The resolution can be determined as $1/2^N$ 100% and for the 8-bit converter the resolution is $100/2^8 = 100/256 = 0.39\%$. From Figure 4.10 results that the quantization error is varying between 0 and q value. It is possible to decrease this error by shifting the quantization steps by the $q/2$ value - thus the error of quantization is then varying between $-q/2$ and $+q/2$ (Figure 4.11).

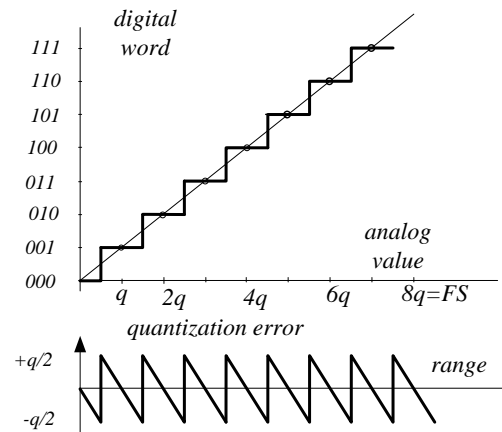


FIGURE 4.11
The modified characteristic of quantization of the 3-bit ADC

According to the characteristic presented in Figure 4.11 the error of quantization ε is $\pm q/2$ and the probability distribution $p(\varepsilon)$ is uniform for all values of errors between $-q/2$ and $+q/2$ (Figure 4.12).

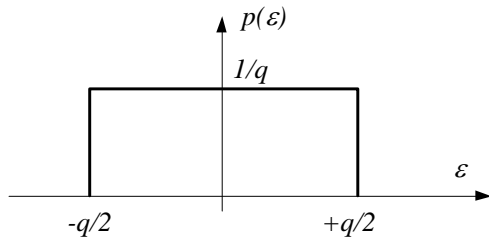


FIGURE 4.12
The probability distribution of the error of quantization.

The mean square value (*rms value*) of the error is:

$$\epsilon_{rms} = \sqrt{\int_{-q/2}^{q/2} \epsilon^2 p(\epsilon) d\epsilon} = \sqrt{\frac{1}{q} \int_{-q/2}^{q/2} \epsilon^2 d\epsilon} = \frac{q}{\sqrt{12}} \quad (4.6)$$

The ϵ_{rms} value is often described as the noise of quantization. The signal to noise ratio SNR is:

$$SNR = 20 \log \frac{rms \ signal}{rms \ noise} = 20 \log \frac{2^N \frac{q}{2\sqrt{2}}}{q / \sqrt{12}} = 20 \left(\log 2^N - \log \frac{2}{\sqrt{6}} \right) \quad (4.7)$$

$$SNR = 6.02N + 1.76 \text{ dB} \quad (4.8)$$

The relationship (4.8) is determined in bandwidth from DC to $f_s/2$. If the signal bandwidth w is less than $f_s/2$ then the expression (4.8) can be modified to the form:

$$SNR = 6.02N + 1.76 + 10 \log \left(\frac{f_s}{2w} \right) \quad (4.9)$$

The expression (4.9) reflects the effect of noise reduction due to oversampling – for given signal bandwidth doubling of sampling frequency increases the SNR ratio by 3dB.

The noises level is important for the dynamics of conversion. This dynamics can be calculated as the ratio of a signal $2^N q$ to the resolution of quantization q

$$dynamics = 20 \log \frac{2^N q}{q} = 6.02N \quad (4.10)$$

The equation (4.10) is often expressed as “six dB per one bit”. For example, in acoustic signal processing

it is assumed that the bandwidth is 20 kHz while dynamics is 100 dB. Thus the sampling frequency should be about 40 kHz and to obtain the dynamics 100 dB the number of bits should be: $100/6.02=16.6$. Thus to obtain correct dynamics of the audio signals the converter should be the 16-bit one.

TABLE 4.2
The performances of the quantization process depending on the number of bits N (determined under assumption, that the range of the conversion is 0 – 2V).

Number of bits N	Resolution % FS	rms noises $q / \sqrt{12}$ [μ V]	Dynamics dB
8	0.39	2 300	48
10	0.098	580	60
12	0.024	144	72
16	0.0015	8.9	96
24	0.000006	0.034	144

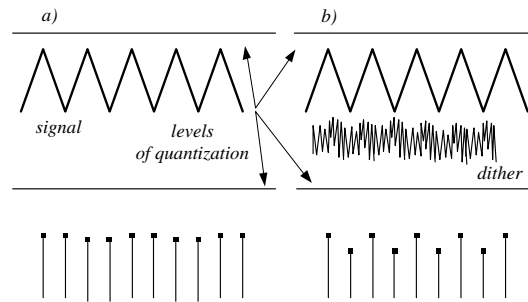


FIGURE 4.13
Improvement of the resolution by dithering.

We can improve the resolution of quantization in artificial way. If the changes of the signal are less than the level of quantization they are converted into pulses of the same value (Figure 4.13a). But if we add to the signal noise of the level small than level of quantization the maximum and minimum values of the signal can be detected as it is illustrated in Figure 4.13b. This technique is known as *dithering*.

Beside described earlier conversion of the analog signal into digital code exist also other method of A/D conversion – for example conversion to number of pulses in dual slope converters (described later) and one-bit conversion used in sigma-delta converters (also described later).

In one-bit conversion the output pulses are of the same magnitude $-U_{ref}$ - $+ U_{ref}$ and the value of converted analog signal is described by the half-pulse width. For zero input signal both halves have the same width and average value is zero. As the input signal increases the width of one half increases and average value also increases (Figure 4.14). It is principle of

delta modulation (or Δ modulation) – some kind of PWM modulation (pulse width modulation).

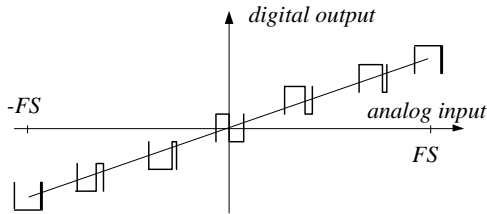


FIGURE 4.14. The one-bit conversion.

One-bit conversion realized by using of the sigma-delta converter is closely related to oversampling principle. Its main advantages are simplicity of converter and large dynamics due to *noise shaping*. Therefore it is commonly used in multimedia applications but also in measurements.

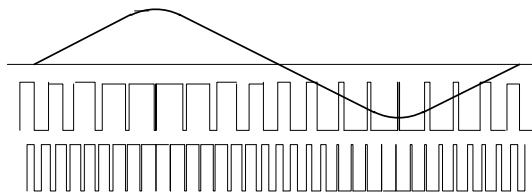


FIGURE 4.15. The one-bit conversion of sinusoidal signal (two speed of sampling).

It is a question if one-bit conversion is really analog to digital conversion. Indeed we have sampling of the analog signal but the quantization is some kind of digital/analog hybrid. We can easy convert one-bit signal into multi-bit one by applying a decimation filter. But on the other hand the average value of this signal represents the analog value and the analog value can be easy reconstructed by applying lowpass filter.

When we buy the AD converter the two main important parameters to choice are: sampling frequency and number of bits. It is not possible to select both parameters as high as possible because converter with high speed has poor resolution (number of bits) and the reverse. Therefore we usually look for compromise in selection of parameters taking into account following factors:

- As higher sampling frequency as higher frequency bandwidth of converted signal (according to Nyquist rule). Thus the sampling frequency should be at least two times larger than the bandwidth. If we have

distorted signal we should consider number of harmonics necessary to correct convert this signal.

- As larger number of bits as better resolution and the same better accuracy of conversion. With 8-bit converter it is not possible to obtain accuracy better than 0.4%.

- In some applications accuracy is less important than dynamics – for example in media processing. In such case important is the rule: 6 dB per bit. To convert signals with 100 dB dynamics it is necessary to use at least a 16-bit converter.

As the result of quantization the value of the sampled signals is usually represented by the binary code. There are various systems of number encoding – generally we use two formats of the number: *fixed point number* (sometimes called integer number) and *floating point number* (called also real number).

In the *fixed point format* every bit is in fixed position, starting from the largest one (*MSB – most significant bit*) and ending by the smallest one (*LSB – least significant bit*). In natural binary code called *unsigned integer* every bit represents the digit 2^N . Thus the digit of the analog value with range FS is represented as by the dependence:

$$x = FS(a_1 2^{-1} + a_2 2^{-2} + \dots + a_n 2^{-in}) \quad (4.11)$$

Thus for the FS = 1 V the number 0101 is corresponding to the:

$$x = 0 \cdot 0.5 + 1 \cdot 0.25 + 0 \cdot 0.125 + 1 \cdot 0.0625 = 0.3125 \text{ V}$$

TABLE 4.3 Various formats of the fixed point numbers.

deci- mal	unsigned integer	offset binary	sign and magnitude	two's complement
7	0111	1110	0111	0111
6	0110	1101	0110	0110
5	0101	1100	0101	0101
4	0100	1011	0100	0100
3	0011	1010	0011	0011
2	0010	1001	0010	0010
1	0001	1000	0001	0001
0	0000	0111	1000	0000
-1		0110	1001	1111
-2		0101	1010	1110
-3		0100	1011	1101
-4		0011	1100	1100
-5		0010	1101	1011
-6		0001	1110	1010
-7		0000	1111	1001

The unsigned binary format cannot represent negative numbers. This problem can be solved by the *offset binary* format where the decimal value is shifted to obtain the negative number. The digit in this format is described by the equation

$$x = FS(a_1 2^{-1} + a_2 2^{-2} + \dots + a_n 2^{-in} - 0.5) \quad (4.12)$$

Another format also enabling to represent the negative number is the *format sign and magnitude*. In this format the first left bit is reserved for the sign (zero for positive number and one for negative one). These two formats (binary offset and sign and magnitude) are difficult to implement in operational unit. Moreover in sign and amplitude format there are two representations of decimal zero.

The most popular is *format two's complement* that is easy to implement in the computer arithmetic unit. In this format the positive numbers are represented similarly to the unsigned integer format and the sign and magnitude format. Also, similarly as in the sign and magnitude format, the first bit is reserved for sign. For negative numbers the following algorithm is used: the decimal number is taken as the absolute value \Rightarrow next this number is convert to binary format \Rightarrow all bits are complemented: ones become zero, zero becomes one \Rightarrow a 1 is added to this number. For example -5 is converted in following way: $-5 \Rightarrow 0101 \Rightarrow 1010 \Rightarrow 1011$. The most important advantage of the format two's complement is that the arithmetic unit in the same way adds positive and negative numbers (by subtracting it automatically counts in two's complement).

Many limitations of the fixed point numbers (especially in the case of large numbers) can be avoided in *floating point format*. Floating point format is similar to the scientific notation of numbers: *mantissa M* is multiplied by 2^E , where *E* is *exponent*. Additionally whole number is multiplied by $(-1)^S$ where *S* is the sign bit

$$x = (-1)^S \times M \times 2^E \quad (4.13)$$

The most popular is the ANSI/IEEE 754-1985 standard where in a 32-bit representation of the number the first bit is a sign bit, next 8 bits are assigned to the exponent and last 23 bits are assigned to the mantissa according to the formula

$$x = (-1)^S \times 2^{E-127} \times M \quad (4.14)$$

The mantissa is represented by the following notation

$$M = 1 + m_{22} 2^{-1} + m_{21} 2^{-2} + \dots + m_1 2^{-22} + m_0 2^{-23}$$

For example the number: 1 0000101 011100000000000000000000 corresponds to:

$$(-1) \times 1.4375 \times 2^{-122} = -2.70363 \times 10^{-37}.$$

The floating point format enables representation of the numbers with better dynamics but with worse resolution.

It is possible in every moment to convert the binary numbers into decimal, hexadecimal or other format. But if the signal is being further processed digitally the binary format is the most convenient to use.

Although modern AD converters are very fast they need certain time to perform sampling and quantization process. Therefore, the AD converters are usually preceded by a special circuit holding the processed signal for the time necessary for the conversion. These circuits are called *SH – sample-and-hold circuits*.

An example of the SH circuit is presented in Figure 5.16. After closing of the switch the capacitor C is charged to the voltage value equal to the input voltage. After disconnection of the switch the capacitor C stores (holds) the voltage. In the holding time the conversion (processing) of the signal is performed. The working cycle of the SH circuit consists of three parts: sampling time, short transient time when the holding value is fixed and holding time.

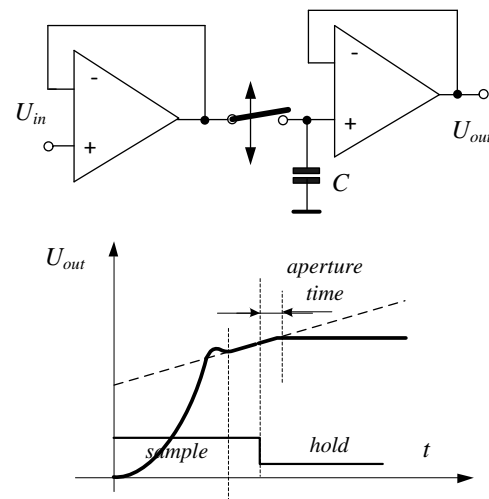


FIGURE 4.16 The simple sample-and-hold circuit and its time characteristic.

The sampling time can be as short as possible, only to equalize the input voltage and the capacitor voltage. This time can be extended and the changes of the voltage on the capacitor can follow-up the input voltage. Such circuits are called *track-and-hold circuits*.

The simple circuit presented in Figure 4.16 is often substituted by slightly more complex circuits with feedback. The example of the circuit with feedback is presented in Figure 4.17. The SH circuits with

feedback operate slower than the simple circuits, but the accuracy of signal processing is better.

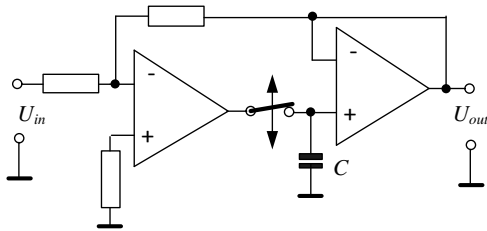


FIGURE 4.17
The sample-and-hold circuit with feedback.

The sample-and-hold circuits are indispensable parts of many digital processors, among them AD and DA converters. In the latter case they help in smoothing of the signal and elimination of the pulse interferences. On the market, there are also available amplifiers with SH circuit – *SHA* – *sample-and-hold amplifiers*. Important parameter of SH circuit is the *aperture time*. Aperture time is the time between hold command and disconnection of the signal from the hold capacitor (Figure 4.16). The typical times of sampling are of about $1 \mu s$ and the aperture time is not larger than several *ps*. There are also very fast sample-and-hold circuits with sampling time of about $10 ns$ and aperture time less than $1 ps$.

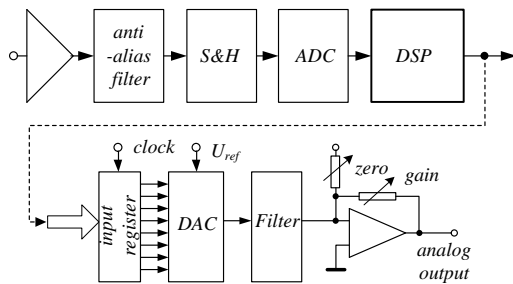


FIGURE 4.18
The chain of digital signal processing DSP elements.

The main purpose of analog to digital conversion is the next *digital signal processing DSP*. The digital signal processing offers many unique possibilities not available in the analogue signal processing (Antoniou 2005, Deziel 2000, Lai 2004, Lyons 2004, Madisetti and Williams 1998, Mitra 2002, Smith 2003, Stranneby 2001). The most popular application of digital signal processing techniques is Fast Fourier Transform FFT and Digital Filtering. A large area of digital signal processing application is image processing and

multimedia applications (Bovik 200, Jähne 2004, Vaseghi 2007, McClellan et al 1998).

Often DSP is finished with sending the processed data. But sometimes is necessary to come back to the original analogue form after digital signal is processed it. As example can be considered an audio application where the last step is an analog loudspeaker. Therefore often the signal is converted into digital one; next it is processed and then again is converted into analogue signal as presented in Figure 4.18.

At the input of digital to analog conversion usually is inserted a *register circuit (latch circuit)*, which is required to save the signal for the time necessary for conversion of the last digit (*the settling time*). The input register plays the same role as in the case of analog to digital conversion the sample-and-hold circuit. An analogue signal is generated as the sum of the component signals corresponding to appropriate levels of quantization. At the output the filter circuit and eventually the amplifier are inserted.

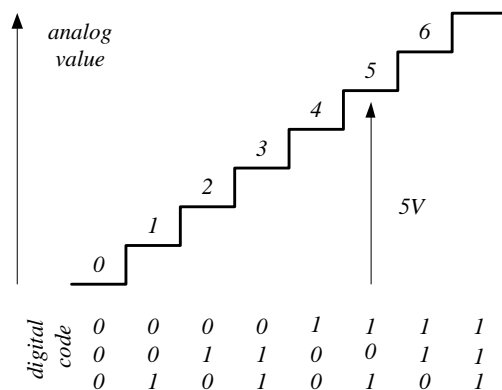


FIGURE 4.19
The conversion of the digital code to the analog value.

The *digital to analogue converters DAC* are used for the recovery of original analogue signals from the digital code. Hence, this process is sometimes called *the reconstruction of the analogue signal*. Each digital value of the code is related to the defined value of the analogue signal resulting from the partition of the full range to the number of quantity – as it is illustrated in Figure 4.19.

Beside presented above de-quantization also the de-sampling process is necessary to reconstruction of the signal. As result of AD conversion we obtain a series of pulses with the amplitudes proportional do the digital values of the signal in the moments of sampling (Figure 5.20a). In the simplest case we can complete the lack of the signal between the pulses by the holding the

magnitude of the pulse until the delivery of the next pulse. This process is called *ZOH – zero order hold – or staircase reconstruction* (Figure 4.20b).

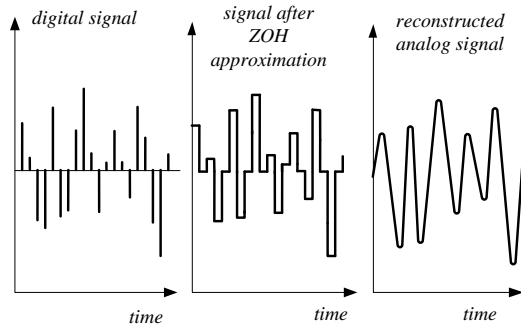


FIGURE 4.20
The reconstruction of the analog signal.

For the reconstruction of the signal the best would be to apply the ideal low-pass filter. If we use the zero order hold we realize following relationship

$$x(t) = \begin{cases} 1 & \text{for } 0 \leq t \leq T_s \\ 0 & \text{for other moments} \end{cases} \quad (4.15)$$

The function (5.15) in the frequency domain is described as

$$X(j\omega) = \int_{-\infty}^{\infty} x(t) e^{-j\omega t} dt = T_s e^{-j\omega \frac{T_s}{2}} \frac{\sin\left(\omega \frac{T_s}{2}\right)}{\omega \frac{T_s}{2}} \quad (4.16)$$

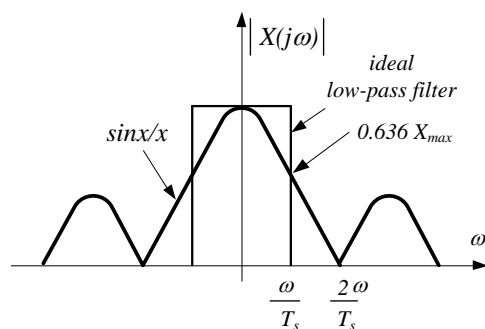


FIGURE 4.21
Amplitude response of the ideal and real ZOH filter.

The function (4.16) is presented in Figure 4.21. The magnitude of the signal decreases with the frequency (as compared to the flat horizontal characteristic of the

ideal low-pass filter). For that reason, at the output of the DA converter a correcting filter of the characteristic $x/\sin x$ is sometimes inserted.

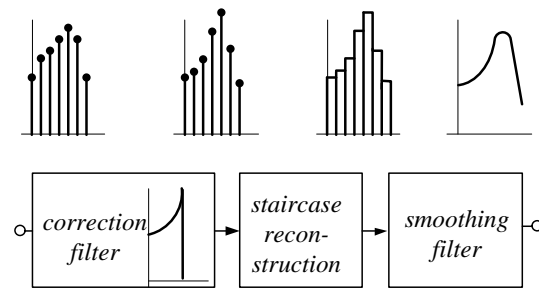


FIGURE 4.22
The reconstruction of the analogue signal from the series of pulses.

As result of the presence of side leaves of the $\sin x/x$ characteristics at the output can appear false residual images near the $f_s, 2f_s, 3f_s$ frequencies (Maloberti 2007). Thus the lowpass smoothing filter at the output of D/A converter should remove these signals – similarly as it is in the case of anti-aliasing filter at the input of D/A converter.

4.2 Analog to digital converters

Many years various AD converters have been designed and developed (Candy 1991, Goeshele 1994, Jespers 2001, Norsworthy 1996, van de Plasche 2003, Schreier 2004). However, currently on the market there are only a few main types of them: successive approximations register SAR, pipeline, delta-sigma, flash and dual slope (integrating) converters.

Figure 4.23 and Table 4.4 present the comparison of two important parameters of the AD converters: the sampling frequency (speed) and number of bits (resolution). We can see that there is no one universal AD converter – the converters of high speed are of the poor resolution and *vice versa* – accurate (large number of bits) converters are rather slow.

Various converters serve other part of the market. The SAR converters are very accurate, operate with relatively high accuracy (16-bit) and wide range of speed – up to 10 MSPS⁷. Therefore these converters are usually applied to data acquisition boards.

For much higher frequencies (up to several GHz) the flash converters are used. As SAR converter needs for conversion $3 - 30 \mu s$, the flash converters need only $10 ns$. Flash converters seldom are with higher that 8 bits

⁷ MSPS – mega samples per second.

resolution. They are mainly used for oscilloscope and telecommunication applications.

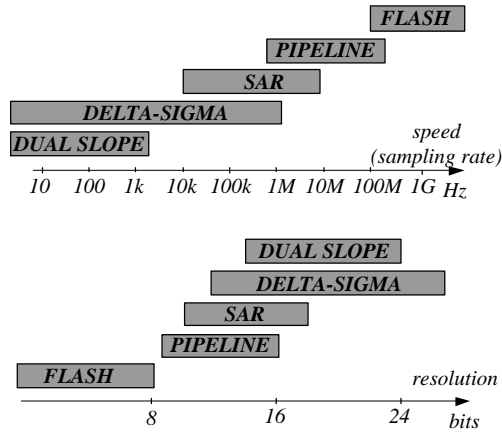


FIGURE 4.21
The comparison of the performances of the main AD converters.

TABLE 4.4
The best performances of the market available AD converters.

resolution bits	speed sps	type	model	approx. price
31	4k	$\Delta\Sigma$ 4th	ADS1282	34
24	16k	$\Delta\Sigma$ 2nd	ADS1211	13
24	2.5M	$\Delta\Sigma$	AD7760	25
24	4M	$\Delta\Sigma$	ADS1675	18
18	100s	integr	MAX132	10
18	2M	SAR	AD7641	29
16	10M	$\Delta\Sigma$	ADS1610	21
16	10M	SAR	AD7620	35
16	1M	SAR	ADS8329	7
16	250M	pipeline	AD9467	100
14	10M	pipeline	ADS850	17
14	250	pipeline	ADS4129	72
12	1G	pipeline	ADS5400	775
12	500M	pipeline	AD9434	85
8	2.2G	flash	MAX109	20
8	40M	half-flash	TCL5540	2.5
6	800M	flash	MAX105	36

The pipeline converters can exhibit both - high resolution and high speed. But they are rather complex and expensive and therefore used for special purposes.

The integrating – dual slope converters enable to obtain very high resolution and accuracy. But because their conversion time is relatively long $10 - 150\text{ ms}$ they are mainly used for conversion of DC signals. Due to high accuracy these converters are usually used in digital measuring instruments.

The best resolution and dynamics exhibit delta-sigma converter. Recently these converters are in significant progress and gradually substitute the dual-slope converters in many applications. Also in measuring converters, including data acquisition boards these

converters are often used. The main area of application of delta-sigma converters are the multimedia, due to their high dynamics and low noise level.

Successive Approximation Register –SAR converters

Figure 4.22 presents the principle of operation of the SAR converter. The SAR (*Successive Approximation Register*) is one of the most commonly used AD converters in scientific instrumentation. It is because their performances (resolution 16- or 18-bit, speed up to 10 MSPS, time of conversion $1\ \mu\text{s}$ for 16-bit) are acceptable for the most of applications.

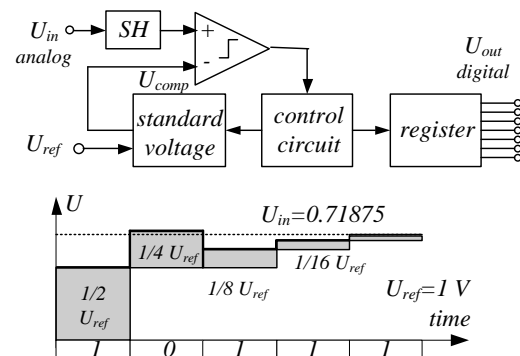


FIGURE 4.22
The principle of operation of SAR converter.

The principle of operation of the SAR device resembles the weighting on the scale. Successively the standard voltages in sequence: $U/2, U/4, U/8...U/2^N$ are connected to the comparator. These voltages are compared with converted U_{in} voltage. If the connected standard voltage is smaller than the converted voltage in the register this increment is accepted and the register sends to the output signal “1”. If the connected standard voltage exceeds the converted voltage the increment is not accepted and register sends to the output signal “0”.

Figures 4.23 and 4.24 present the example of the SAR converter – model AD7667 of Analog Devices. The standard voltages are obtained using the array of 16 binary weighted capacitors. During the acquisition phase all switches are connected to analog input U_{in} and the capacitors are charged. In the conversion phase the capacitors are disconnected from the U_{in} and connected to the reference ground. This way the captured voltage is applied to the comparator input. Next, the switches connect successively the capacitor array to the standard voltage U_{ref} (thus we realized digital to analog conversion DAC of input voltage). This difference is connected to the comparator input. The control logic unit toggles switches as the comparator is balanced. As

this process is completed the control logic sends the code to the digital output.

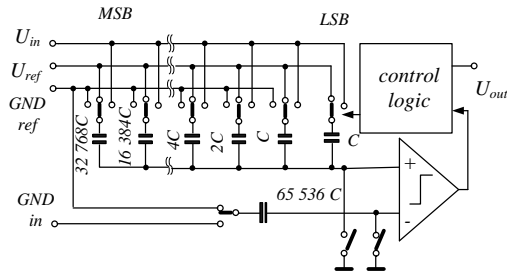


FIGURE 4.23
The principle of operation of the PulSAR converter of the Analog Devices (model AD7667).

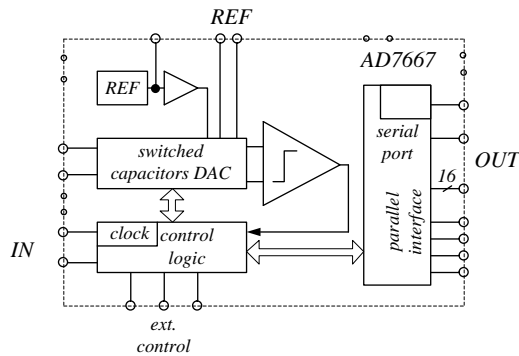


FIGURE 4.24
Functional block diagram of the AD7667 PulSAR converter of Analog Devices.

The main advantages of the presented converter are its high accuracy and low consumption of power – only one comparator is used for the conversion. Figure 4.24 presents the functional diagram of this converter. The 16-bit device enables conversion of the 0 – 2.5 V voltage to the digital output (serial or parallel) with uncertainty 0.004%FS, dynamics 88 dB and sampling rate 800 kSPS (conversion time 1.25 μs). The power consumption is only 80 mW (130 μW for $f_s = 1$ kSPS).

Flash converters

In the *flash converters* instead of successively connecting weighted binary voltages to one comparator (as in SAR devices) there are connected at the same time binary weighted voltages to 2^N comparators (each possible states). The example of flash converter is presented in Figure 4.25.

In the case of the 8-bit converter it is necessary to connect 255 resistors to the 255 comparators (in the case of 16-bit converters it would be 65 535

comparators!). No wonder that the flash converters are designed as at most 8-bit converters. The main advantage of the flash converters is that the conversion is performed in one step. Therefore the time of conversion is very small (less than 1ns) and the sampling rate above 1 GSPS is possible. The main drawback of the flash converter is its poor resolution (number of bits) and large power dissipation (due to great number of comparators).

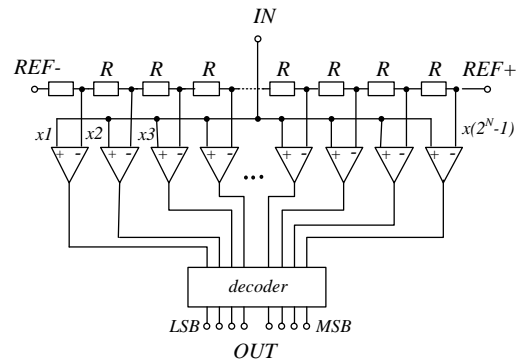


FIGURE 4.25
Functional block diagram of the AD7667 PulSAR converter of Analog Devices.

As an example of flash converter we can consider the MAX109 model of Maxim. It is an 8-bit converter (effective number of bits ENOB = 6.9 for 1.6 G GSPS) with a sampling rate up to 2.2 GSPS and conversion time 0.5 ns. The uncertainty of this converter is 0.25 LSB and the power consumption is 6.8 W.

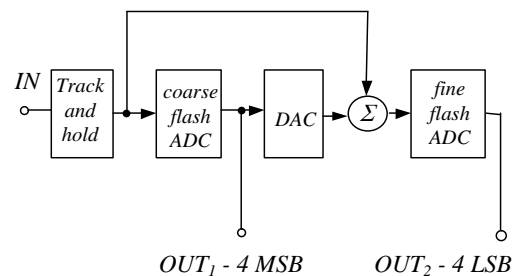


FIGURE 4.26
An example of the half-flash type AD converter.

It is possible to decrease the number of converters in the half-flash type converter – presented in Figure 4.26. In such converter the sampling is performed in two sub-ranges. The first 4-bit flash converter processes roughly the first four bites. The converted voltage is subtracted from the input voltage (from the track-and-

hold circuit) and this voltage difference is converted by the second fine 4-bit flash converter. Due to this solution the number of converters in 8-bit device is diminished to 30 (from the original 255).

As an example of the half-flash converter we can consider TCL5540 converter of Texas Instruments. This converter enables 8-bit conversion with the sampling rate 40 MSPS and conversion time 9 ns. The uncertainty of this converter is 1 LSB.

Pipeline converters

Pipeline converters extends the idea of the half-flash converter to many subranges (these converters are sometimes also called as “subranging”). The main differences between half-flash and pipeline converters are as follows: in a half-flash converter there are two stages while in pipeline converters there can be several stages; after each stage there are inserted amplifiers for improving the resolution of the next stage; between the stages there are inserted track-and-hold circuits.

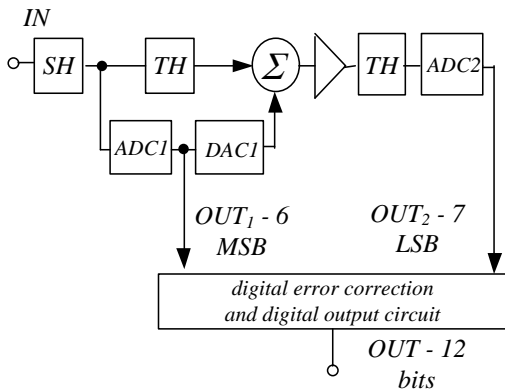


FIGURE 4.27
The example of 12-bit pipeline converter.

An example of two-stage pipeline converter is presented in Figure 4.27. The input signal after SH circuit is converted to digital signal by ADC1 converter – 6 most significant bits. The remaining signal is again converted to a digital one by DAC1 circuit and it is subtracted from the input signal. This residual analogue signal is amplified to obtain better resolution in the next stage. The signal is converted again to a digital signal by ADC2 converter – 7 least significant bits. The important is the error correction logic circuit. In a 12-bit converter both converting stages, 6 bits and 7 bits, have common 1 bit. This overlapped additional bit is used for the eventual error correction. As the signal is going sequentially stage by stage the converter can exhibit latency time depending on the number of stages. This latency can be a problem in some

applications, for example including feedback. If the sampling rate is too slow the hold time of track and hold parts can be disturbed causing conversion error. Therefore pipeline converters has also limited minimum sampling rate.

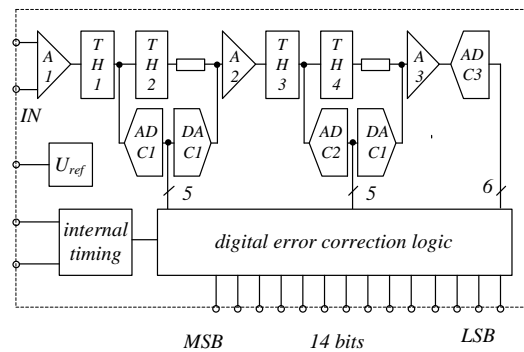


FIGURE 4.28
The functional block diagram of AD6645 pipeline converter of Analog Devices.

The multistage operation enables to perform the conversion with relatively high resolution 14 – 18 bits and sampling rate up to 100 MSPS. In comparison with flash converters a much smaller number of comparators is required – for example four-stage 16-bit converter requires only 60 comparators. Figure 4.28 presents the three-stage pipeline converter of Analog Devices (model AD6645). It enables the conversion with 14-bit resolution and sample rate 105 MSPS (minimum sampling rate 30 MSPS). The time of conversion is 10 ns, power consumption 1.5 W and uncertainty 1.5 LSB.

The dual slope converters

The integrating converters are often realized as the *dual slope converters*. The principle of operation of dual slope converter is presented in Figure 4.29. The integrating circuit is connected to the comparator that detects the zero-level of the integrator signal. This comparator controls the logic gate connecting the clock generator to the counter.

The dual slope converter operates in two half-cycles. In the first one to the integrating circuit the measured voltage is connected for the fixed time T_1 . At the same time the clock oscillator of frequency f_{cl} is connected to the counter. The first half-cycle is finished when the counter indicates assumed value, for example $N_1 = 1000$. The voltage at the output of the integrating circuit increases with a fixed slope to the value

$$U_{int} = \frac{1}{RC} \int_0^{t_1} U_x dt = \frac{U_x}{RC} \frac{1}{f_{cl}} N_1 \quad (4.17)$$

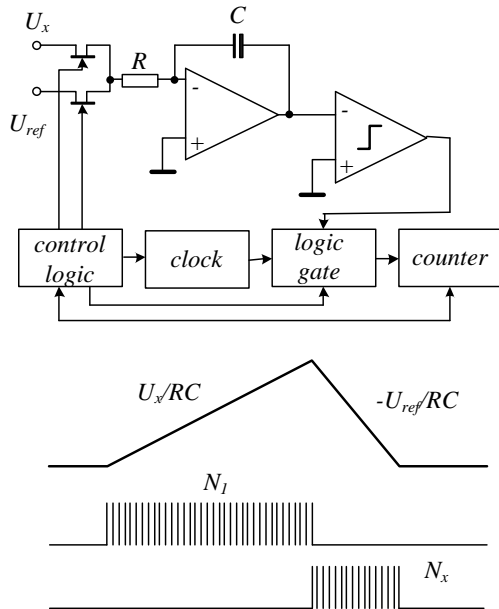


FIGURE 4.29
The principle of operation of the dual slope integration ADC.

In the second half-cycle the reference voltage of the reverse polarization is connected to the integrating circuit and the counter starts counting the clock oscillator pulses. The voltage at the integrator output is decreased to the moment when the comparator detects zero. The zero state is when the following condition is fulfilled

$$\frac{U_x}{RC} \frac{1}{f_{cl}} N_1 = \frac{U_{ref}}{RC} \frac{1}{f_{cl}} N_x \quad (4.18)$$

and the number of counted pulses is

$$N_x = \frac{N_1}{U_{ref}} U_x \quad (4.19)$$

Thus the final state of the counter depends on the N_1 value (this we is fixed very precisely), on the reference voltage value U_{ref} and of course on the converted voltage value U_x . The value indicated by the counter does not depend on the RC value and the frequency of clock oscillator.

The important feature of the integrating converters is the rejection of AC noises. Consider the case that the measured DC voltage U_x is accompanied by the interference AC voltage $U_{int} = U_m \sin(\omega t + \phi)$. After integration we obtain

$$U_{int} = \frac{1}{T} \int_0^T [U_x + U_m \sin(\omega t + \phi)] dt = U_x - \frac{U_m}{\omega T} [\cos(\omega T + \phi) - \cos \phi] \quad (4.20)$$

Thus if the integration period T is fixed in such a way that $T = 2\pi/\omega$ then the second term (AC interference) is equal to zero. The noise rejection ratio $RSNR$ is (Tran Tien Lang 1987)

$$RSNR = \frac{noise}{error} = 20 \log \frac{\omega T}{\cos(\omega T + \phi) - \cos \phi} \quad (4.21)$$

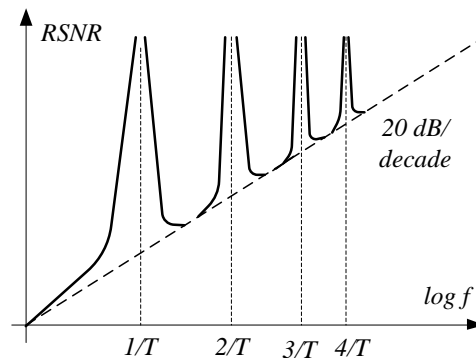


FIGURE 4.30
The noise rejection ratio in the integrating AD converter.

Figure 4.30 presents the dependence of the $RSNR$ factor on the frequency. The integration converter behaves like a selective filter rejecting not only the component of the frequency $f = 1/T$ but also the harmonics of this signal. Usually, the value of T is fixed to be equal to 20 ms , which enables rejection of the 50 Hz signal and its harmonics. In practical circuits the T period is sometimes synchronized with the frequency of the supply AC voltage.

The relatively long time of integration is a drawback of the dual slope converter. This problem can be overcome by applying the multislope converter (Figure 4.31).

There are three-fold-slope and quad-slope devices. In the three-fold-slope device the second cycle (of dual slope device) is divided to the two steps. In the second step the reference voltage is connected to the integrator with smaller R resistance (for example 100 times smaller). This way the time necessary to decrease the output voltage of the integrator is 100 times shorter. After the integrator output voltage reaches a defined

threshold voltage it is again connected the R resistor for precise detection of the zero state. Thus after these three phases the following relationship is realized

$$\frac{U_x}{RC} \frac{1}{f_{cl}} N_1 = \frac{U_{ref}}{RC} \frac{1}{f_{cl}} 100N_{x1} + \frac{U_{ref}}{RC} \frac{1}{f_{cl}} N_{x2} \quad (4.22)$$

and

$$U_x = \frac{U_{ref}}{N_1} (100N_{x1} + N_{x2}) \quad (4.23)$$

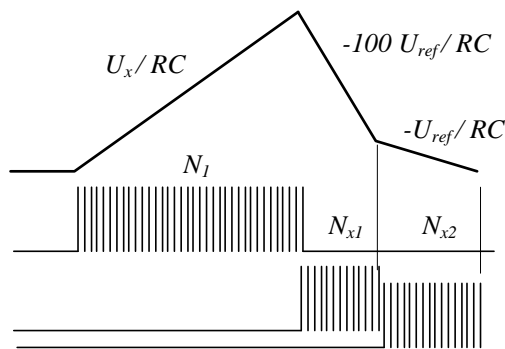


FIGURE 4.31 Principle of operation of a three-fold-slope converter.

The multi-slope integrating technique offers improvement of the conversion speed (or resolution in the same time) at the expense of more complexity and the need to apply two precise resistors.

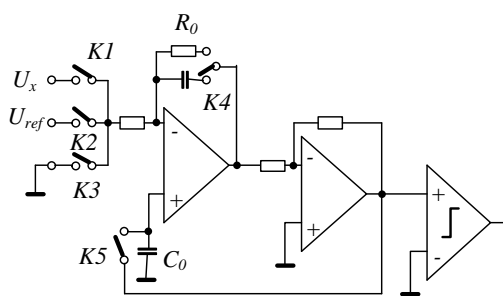


FIGURE 4.32 The integrating converter with the auto-zero correction (Tran Tien Lang 1987).

Another problem appearing in the integrating converters is a zero drift. The minimization of this effect is possible in quad-slope converters, where an additional cycle is performed for the short-circuited

input, which enables us to introduce the required correction. Another method is the application of the auto-zero function. An example of such a converter is presented in Figure 4.32. The conversion time is divided into four cycles – in the first one for the short-circuited input and connected resistor, instead of the capacitor (switch K4), the capacitor C_o (connected by the switch K5) is charged to the offset voltage. In the two next cycles (typical dual slope operation) this voltage across the capacitor C_o is subtracted automatically, introducing the zero correction. In an additional fourth cycle the capacitor is short-circuited in order to remove the charged voltage.

The integrating converters are typically used as the end part of DC digital voltmeters. Therefore they are usually equipped with a digital display. Currently, the the integrating converters are often substituted by cheaper delta-sigma converters. The important drawback of the integrating converter (apart from the long time of conversion) is the necessity of use of the expensive, high quality capacitors. Although there is no capacity C in the equation 4.19, the accuracy of the converter depends on the quality of this capacitor (the effect of memorizing the residual voltage).

Typical integrating converters operate as 12-bit or 15-bit ($3 \frac{1}{2}$ or $4 \frac{1}{2}$ digit displays). The 18-bit integrating converter of Maxim (model MAX132) exhibits an uncertainty of 0.006%.

Delta-Sigma converters

The *delta-sigma* $\Delta\Sigma$ converters called also *1-bit converters* or *bitstream converters*⁸ utilize the oversampling technique. Due to many advantages (most of all the best resolution – even up to 31-bit) these converters are currently very intensively developed (Candy 1991, Norsworthy 1996, Schreier 2005). The typical architecture of delta-sigma converter is presented in Figure 4.33 and the principle of operation of such converters is illustrated in Figure 4.34.

In delta-sigma conversion is used the delta modulation (hence the name of this device). In delta modulation the width of the impulse is proportional to the value of converted signal. As the 1-bit ADC quantizer operates the comparator and latch switched with the frequency Kf_s , forced by the clock (K is the oversampling factor). The output voltage is converted again to analogue form by 1-bit DAC. The adder in the input compares the input value and the output signal.

The simplified picture of signals in delta-sigma converter is presented in Figure 4.34. The operation is controlled by clock oscillator (point E). If the input

⁸ or sigma-delta converters.

signal is equal to $0.5 U_{ref}$ (point A) the output of 1 bit DAC generates pulses of the same width (corresponding of the signal of a clock generator). This signal is subtracted from the input signal (sigma operation) and difference is connected to the input of integrator (point B). Note that due to the feedback mean value of 1-bit DAC is always equal to the input signal.

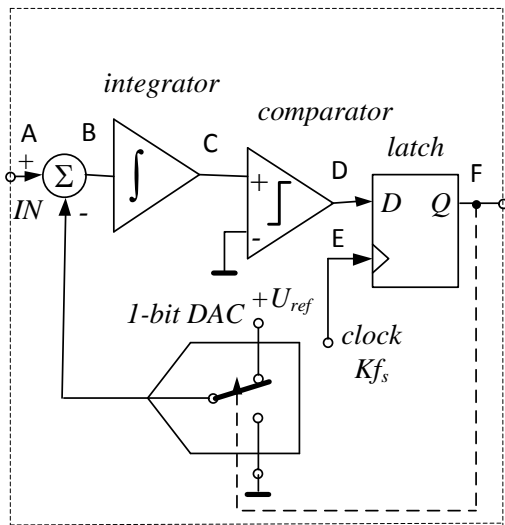


FIGURE 4.33
The architecture of typical delta-sigma modulator.

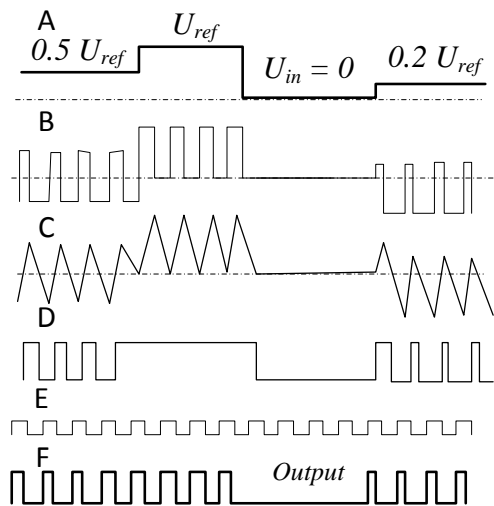


FIGURE 4.34
The signals in selected point of delta-sigma converter presented in Figure 4.33.

At the output of integrator is triangular signal that is next converted to rectangular one by the comparator. Output signal is additionally formed by the latch flip-flop converter (in the output is signal “1” if both clock and input signals are “1”).

When the input signal is equal to U_{ref} we again obtain triangular signal after integrator but the comparator does not change the output state because the integrator signal is always larger than zero. Similarly is when the input signal is equal to zero – the integrator signal is always smaller than zero (compare both cases in point D. For $U_{in} = 0.2 U_{ref}$ we obtain at the output pulses of smaller width.

There are various solutions of delta-sigma converter (1 bit DAC can switch between U_{ref} and zero as well between $-U_{ref}$ and $+U_{ref}$) but always the mean value of output bitstream corresponds with input signal value as it is presented in Figure 4.35..

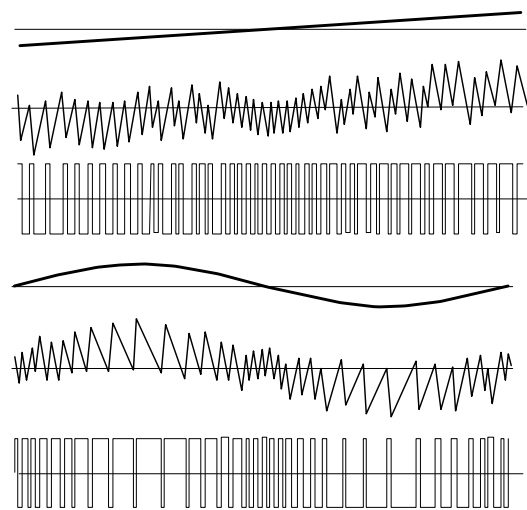


FIGURE 4.35
The 1-bit converter signals of increased linearly input voltage and sinusoidal input voltage.

The important advantage of the delta-sigma converter is the noise suppression. In the previous chapter it was shown that the increase of the output signal of 1 bit results in increase of dynamics of 6 dB. This conclusion can be inverted – an increase of the dynamics (SNR – signal to noise ratio) of 6 dB would give the possibility of increasing the resolution by one bit. Thus the SNR of about 140 dB enables us to obtain a 24-bit converter.

Figure 4.36 presents the equivalent circuit of the delta-sigma converter with the source of noises. The output signal value is

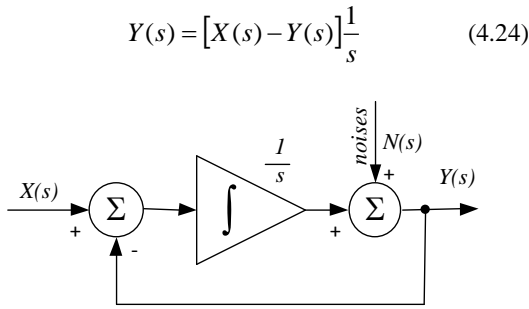


FIGURE 4.36
The equivalent circuit of the delta-sigma converter.

For $N(s) = 0$ we can describe the transmittance of the converter as:

$$\frac{Y(s)}{X(s)} = \frac{1}{s+1} \quad (4.25)$$

The relationship (4.25) is the transmittance of the low-pass filter. If the $X(s) = 0$ we obtain:

$$Y(s) = -Y(s) \frac{1}{s} + N(s) \quad (4.26)$$

and transmittance for the noise source is

$$\frac{Y(s)}{N(s)} = \frac{s}{1+s} \quad (4.27)$$

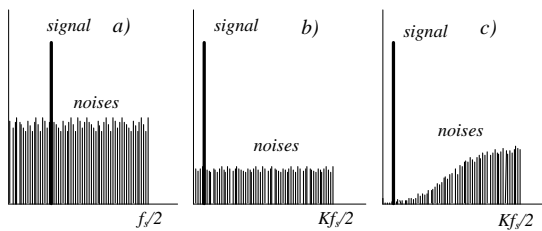


FIGURE 4.37
The noise in delta-sigma converter: suppression due to oversampling (b) and noise shaping (c).

The circuit operates for the noises as a high-pass filter and reduces the noises for low frequency (Figure 4.37c). This feature is called *noise shaping*. Thus the delta-sigma converter suppresses the noises in two ways. Due to oversampling the noises are decreased, because the noises energy is distributed in the larger bandwidth (Figure 4.37b). And additionally the noises are attenuated, because the signal is filtered as low-pass while the noises are filtered as high-pass (Figure 4.37c).

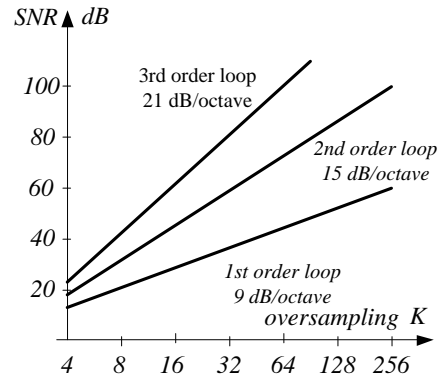


FIGURE 4.38
The dependence of SNR on the order of delta-sigma modulator and the oversampling factor

To obtain a noise suppression of about 40 dB it is necessary to apply a oversampling factor equal to 64 (Figure 4.38). Further noise suppression is possible by increasing the order of the modulator. From the graph presented in Figure 4.38 we can see that to obtain a 24-bit converter (140 dB dynamics) it should be to apply a third order modulator. Figure 4.39 presents the circuit of the second order delta-sigma converter.

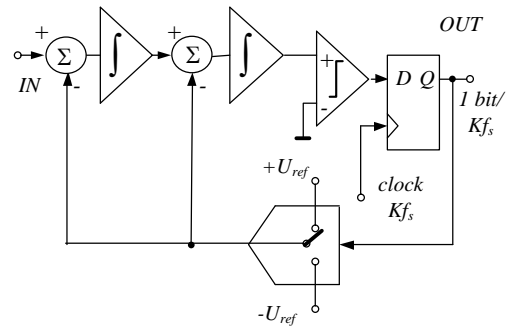


FIGURE 4.38
The second order delta-sigma converter

It is also possible to obtain improvement of dynamics and SNR by cascade connecting several converters of first order. In such circuit it is necessary to apply the differentiating circuits in order to add the output signals of the subsequent steps. The technique of multistage converting is called *MASH (Multistage Noise Shaping)* and these converters are used in high quality audio devices to obtain excellent dynamics. Figure 4.39 presents the circuit of the MASH type converter.

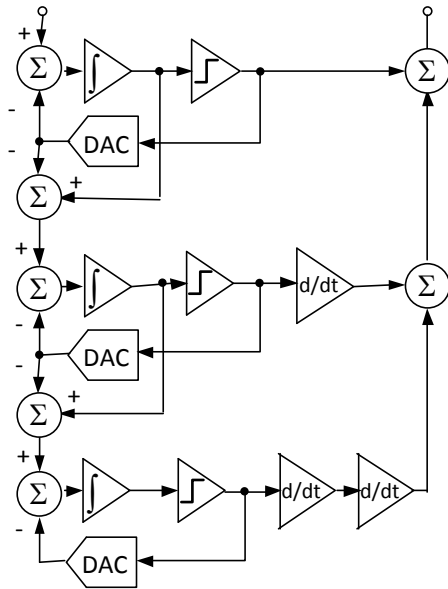


FIGURE 4.39
The MASH type multistage delta-sigma converter.

Recently on the market is available huge choice of delta-sigma converters of excellent performances: high resolution up to 30 bits, high dynamics to 130 dB, high accuracy and even large frequency bandwidth of several MBPS (see Table 4.4). No wonder that delta-sigma converters practically excluded integration converters and also are competitive to SAR devices.

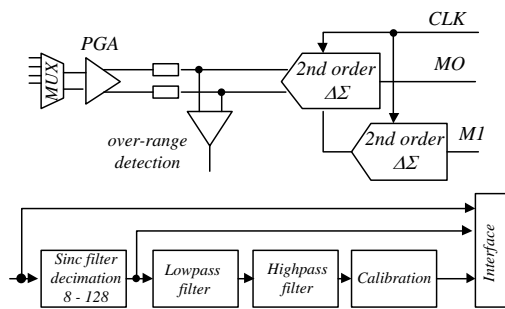


FIGURE 4.40
The architecture of high resolution delta sigma converter – model ADS1282 of Texas Instruments.

As an example we can consider high resolution delta-sigma converter ADS1282 of Texas Instruments with resolution 130 dB – 31 bits, nonlinearity INL 0.5 ppm and sampling frequency 4 kSPS. It consists of fourth order delta sigma converter – two second order stages in pipeline structure (Figure 4.40).

Many one-bit converters are equipped with decimation filters enabling to change of the sampling rate – for example from $64f_s/1$ bit to $f_s/16$ bits. The decimation process is realized by using the low-pass digital filter (removing of high frequency quantization noises) and by removing of excess samples.

As the decimation filter commonly are used sinc filters ($\sin x/x$ filters) with the transfer function:

$$|H(f)| = \frac{\sin \frac{N\pi f}{f_{mod}}}{N \sin \frac{\pi f}{f_{mod}}} \quad (4.28)$$

or

$$H(z) = \frac{1 - z^{-N}}{N(1 - z^{-1})} \quad (4.29)$$

where N is the decimation ratio and f_{mod} is the sampling frequency of delta-sigma modulator.

Figure 4.41 presents the transfer characteristic of typical decimation filter.

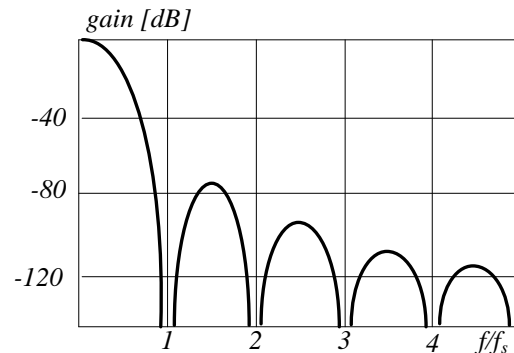


FIGURE 4.41
An example of the frequency response of sinc decimation filter.

Similarly as in the case of analogue signal processing the digital signal processing can be influenced by the zero drift of the amplifier (especially the temperature zero drift) and the gain error. Therefore some converters are equipped with calibration tools, as it is presented in Figure 4.40.

Figure 4.42 illustrates the main errors of linearity. The *integral nonlinearity INL* is the deviation of the values of the actual transfer function from a straight line. The *differential nonlinearity DNL* is the incorrect quantization resulting in not equal quanta. If the elementary quant is LSB the DNL is deviation from the ideal 1 LSB code. The special case of the large differential nonlinearity is the *missing code error*. This error occurs when the quantization step is larger than 2

LSB. For example due to large DNL the number 100 (in Figure 4.42) is not indicated during the conversion. Because this error is dangerous for accuracy of conversion many of manufactured converters are described as “no missing code”.

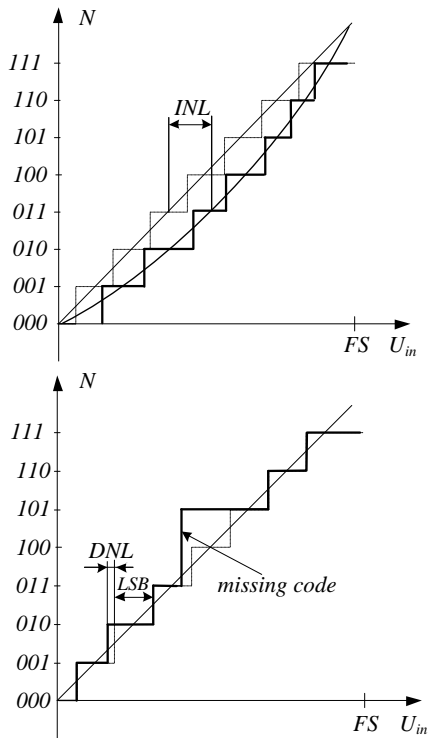


FIGURE 4.42 The transfer characteristic of the 3-bit converter with the integral nonlinearity error INL and the differential nonlinearity error DNL

The performances of the analog-to-digital converters are described by many parameters presented in data sheets. Below are presented main of these parameters.

SNR is the described earlier *signal to noise ratio* (usually it is the ratio of amplitude of the signal to the amplitude of the noises but also the ratio of *rms* values is used).

SINAD (*signal to noise and distortion ratio*) is defined as the ratio of *rms* value of the sine wave to the *rms* value of noises plus all harmonics of the signal.

THD (*total harmonic distortion*) is the ratio of *rms* sum of the harmonics to the fundamental component.

IMD (*intermodulation distortion*) appears when the input signal contains two signals of similar magnitude and frequencies f_1 and f_2 . After the sampling process there can be generated components of the frequencies $f_1 - f_2, f_1 + f_2, 2f_1 - f_2$ etc. IMD is defined as the ratio of the

rms of intermodulation components to the signal without distortion.

SFDR (*spurious free dynamic range*) is defined as the ratio of *rms* value of fundamental signal component to the *rms* value of the largest spurious component (mainly spurious pulses).

Transient response is the response of the converter after the step unit change of the input signal.

FPBW (*full power bandwidth*) is defined as the point of the frequency characteristic where the amplitude of the digitized conversion result is decreased by 3 dB.

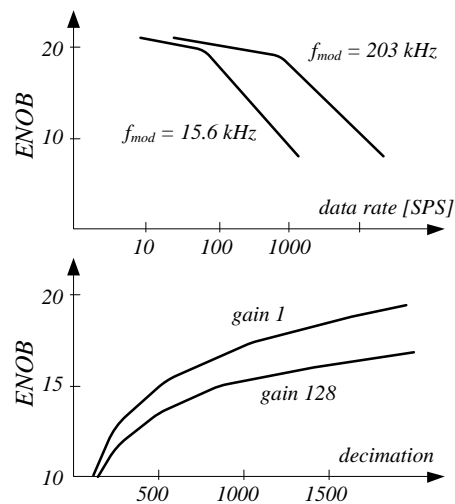


FIGURE 4.43 The dependence of the ENOB factor on the parameters of delta-sigma converter (ADC model MSC1210 of Texas Instruments)

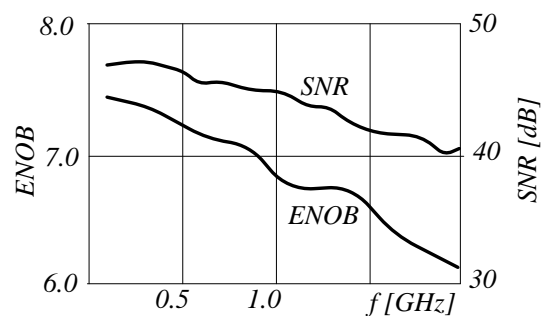


FIGURE 4.44 The dependence of the ENOB factor on the input frequency (ADC model AdC08D1020 of Texas Instruments)

Special importance is related to the ENOB (*effective number of bits*) factor. In an ideal analogue-to-digital converter there is only the quantization error. But in the

real converters with the increased frequency additional noises and distortion can be quite significant.

In delta-sigma converters the customer has usually possibility to select parameters, as frequency of modulation, gain, decimation factor etc. Thus it should feel the consequences of the choice of parameters as it is presented in Figure 4.43.

The ENOB factor is closely related to the dynamic of the converter measured by SINAD factor:

$$ENOB = \frac{SINAD - 1.76}{6.02} \quad (4.30)$$

Especially noise influences the dynamics in the very high speed flash converters. As it is presented in Figure 4.44 the effective number of bits declared as 8-bit converter decreased to almost six for 2 GHz signals.

4.3 Digital to analog converters

In digital to analog conversion it is necessary to perform de-sampling operation and de-quantization also. The de-sampling operation consisting of zero-order hold and filtering was described earlier (see Figure 4.22). The de-quantization operation can be realized by the circuit with the summation of the voltages corresponding to binary code saved in register, as it is presented in Figure 4.45.

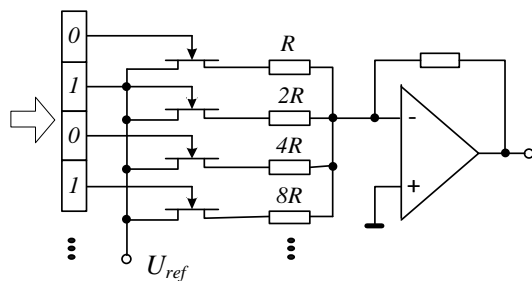


FIGURE 4.45 The digital to analogue converter with weighted resistors

The converter presented in Figure 4.45 is rather difficult to manufacture because it requires precise resistors with a very wide range of values. Technologically simpler is to use the same value of resistors, although it means that the number of these resistors can be huge.

The converter built from single-valued resistors requires 256 resistors for 8-bit conversion and as much as 65 536 of them for 16-bit conversion. In practical circuits the voltage divider can be composed of two dividers – one for coarse conversion (the first 8 bits) and the second for fine conversion (last 8-bits).

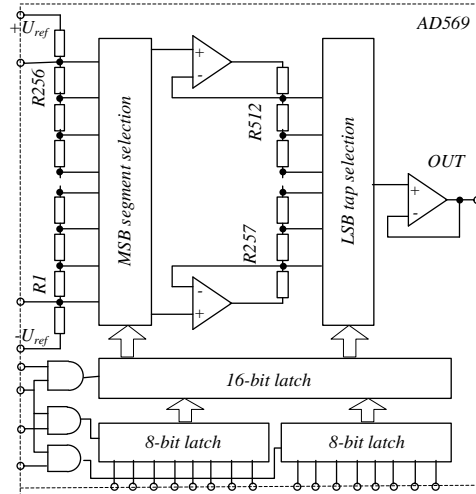


FIGURE 4.46 The functional block diagram of the string digital-to-analog converter AD569 of Analog Devices

In such design in order to achieve 16-bit conversion only (!) 512 resistors are required. Although such a number of resistors seems to be great these converters (called *segmented converters* or *string converters*) are available on the market – as an example we can consider the DA converter model AD569 developed by Analog Devices (Figure 4.46). The main advantage of the string converter is relatively large speed and very good linearity of conversion. The AD569 converter enables 16-bit conversion with nonlinearity less than 0.01% and settling time 3 μs.

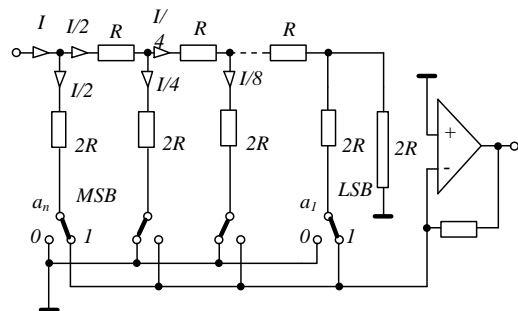


FIGURE 4.47 The R-2R digital to analogue converter with ladder network

Further simplification of the converter circuit is possible in the *R-2R converter* presented in Figure 4.47. In this case also the resistors of the same value *R* are used (*2R* can be composed from two resistors). At each node the current splits into halves. The resulting output voltage is proportional to the total current

summed at the inverting input of the amplifier. It is advantageous that the whole network is consuming the same current from the supply source independently of the positions of the switches.

In the *R-2R* converter it is not required to have precise value of the resistors – it is only necessary to have the resistors with precisely the same value of each resistance. Recently are available converters based on *R-2R* principle with 20 bit resolution and settling time equal to 1 μ s – as for example AD5791 converter of Analog Devices.

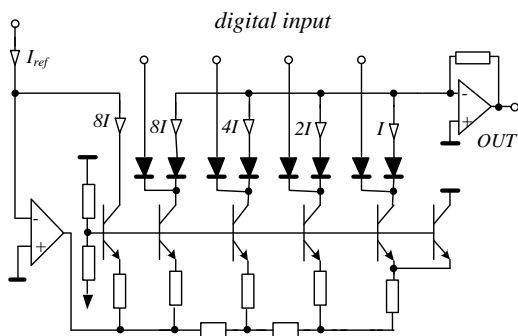


FIGURE 4.48
Digital-to-analog converter with weighted currents

Instead of applying of the current divider we can simply switch the current sources as it is presented in Figure 4.48. The advantage of the converter with switched currents (called a *current steering converter*) is relatively high speed (up to 500 *MSPS*). For example, the 8-bit converter model DAC08 of Analog Devices converts data with an update rate up to 12 *MSPS* and settling time 85 *ns*.

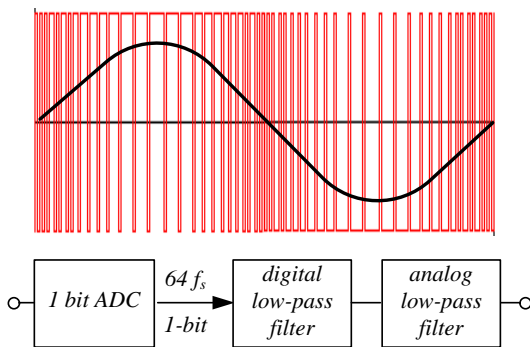


FIGURE 4.49
The reconstruction of the analog signal after oversampling and PWM modulation

Advantages of delta-sigma converters with 1-bit bitstream as high dynamics, noise shaping and linearity are also commonly used in reverse digital-to-analog conversion. If the signal is represented by great number of samples per period, it is practically continuous (Figure 4.49) because in pulse with modulation the average value of digital signal is proportional to primary analog signal and can be reconstructed only by using the low-pass filter. In practice to obtain pure signal (to remove noises and distortion) more complex multi bit delta-sigma converters are used but the idea of simple analog signal reconstruction by using only low-pass filter is applied.

The conventional audio CD technique uses PCM (*Pulse Code Modulation*) technique with 44.1 kHz sampling frequency and 16 – 24 bit resolution. Therefore using oversampling technique it is necessary to use decimation filter to recover such digital signal from the 1-bit bitstream (as presented in Figure 4.50).

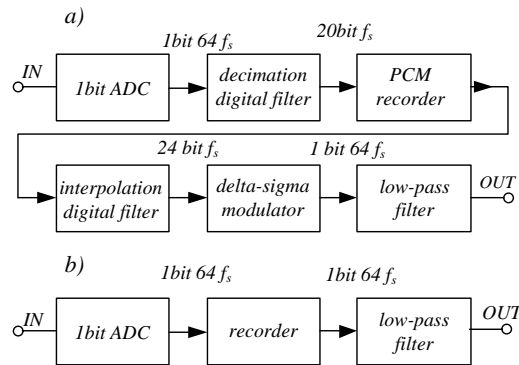


FIGURE 4.50
Conventional (a) and DSD (b) techniques of audio signal recording and reproduction

In the DSD (*Direct Stream Digital*) technique introduced by SONY audio system the 1-bit stream of the oversampling frequency 2.82 MHz is directly recorded on the DVD type disc profiting high density of this disc and enhanced speed of data transmission.

Signal converted by applying of the oversampling technique often needs to be converted again to “ordinary” sampling form with sampling frequency decreased to f_s and the same time the resolution increased to multi-bit form (for example 20-bit resolution as it is presented in Figure 4.50). To perform such operation special filters called *decimation filters* can be used (see Figure 4.41).

Sometimes to improve the possibility of signal reconstruction the increase of the number of samples in is recommended. Such an operation can be performed

using various kinds of *interpolation filters*. Figure 4.51 presents the relatively simple technique of increasing of number of samples by inserting additional samples. In first step the zero value additional samples are added and next after using the low-pass filter we obtain the signal with more samples.

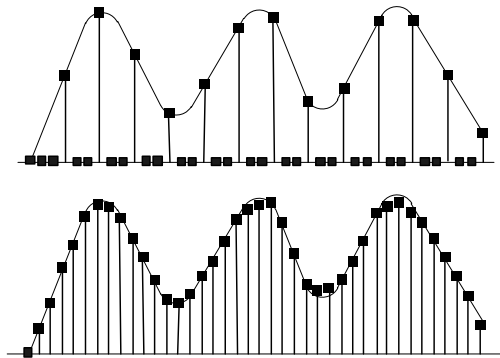


FIGURE 4.51
The increase of number of samples by insertion of additional zero samples

The delta-sigma oversampling DSD converters are mainly used in high quality sound processing. As the example in the Figure 4.52 is presented audio 24 bit, 192 kHz multibit delta-sigma converter model AD1852 of Analog Devices. It exhibits 117 dB dynamic range and 102 dB THD+N.

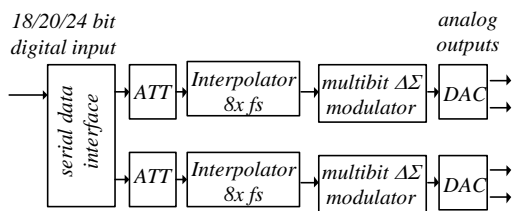


FIGURE 4.52
Simplified functional block diagram of audio stereo delta sigma DAC

In the data sheets describing the performances of digital-to-analog converters similar parameters are used as in the case of analog-to-digital converters. Figure 4.53 describes the *integral nonlinearity error INL* and *differential nonlinearity error*.

The integral nonlinearity is the difference between a real transfer function and an idealized straight line. The differential nonlinearity is the difference between ideal step equal to 1 LSB code and the real step.

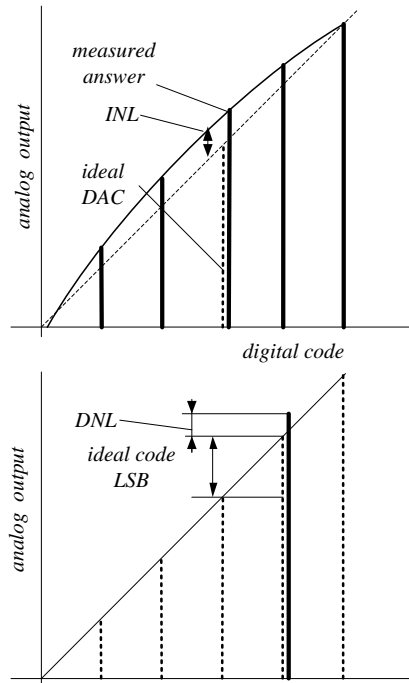


FIGURE 4.53
Integral nonlinearity error INL and differential nonlinearity error DNL of DAC

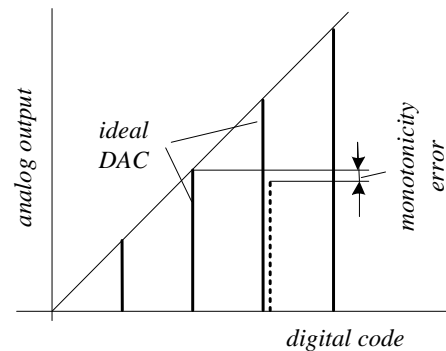


FIGURE 4.54
The error of monotonicity

The *error of monotonicity* is corresponding to the differential nonlinearity error. The DAC is monotonic if the analogue output always increases as the input code increases. Because this error deteriorates the DAC performances the manufacturers often mention “guaranteed monotonicity”. An example of the monotonicity error is presented in Figure 4.54.

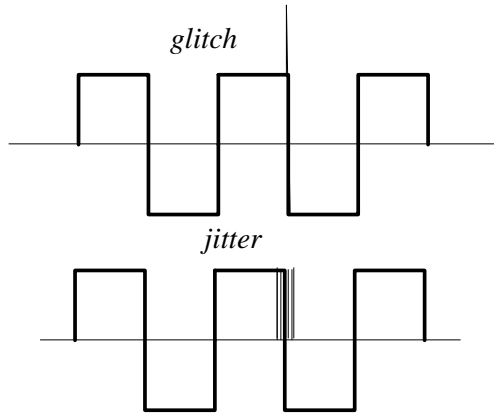


FIGURE 4.55
The glitch and jitter disturbing the signal

As the converter performs the switching operations in the transition state can appear short spikes called *glitches*. These pulses are dangerous because they are not observable on the standard (poor quality) oscilloscopes, although they can disturb the signal processing. Therefore at the output of converter often is inserted a special filter called a *deglitcher*. One of the techniques to eliminate glitches is to use sample-and-hold circuits holding the signal during the switch process. Another error related to the switch process is a jitter (Figure 4.55). The *jitter error* means the unrepeatability of the pulse slope, pulse duration or pulse phase.

4.4 Tools of digital signal processing

The *digital signal processing DSP* requires the knowledge of several new specific mathematical methods although most of the methods used in analogue signal analysis have equivalents in digital signal analysis. For example the Fourier Transform in the analog technique is equivalent to the Discrete Fourier Transform DFT, analog convolution is equivalent to the digital one, Laplace *s*-operators are sometimes supplemented by the *z*-transform. In this chapter the main term of DSP technique are collected or reminded.

One bit can be represented by one impulse. If this impulse exhibits a short duration time it can be represented by the *Dirac delta function* denoted by $\delta(t)$. The delta function is a normalized impulse with a value of one

$$\delta(n) = \begin{cases} 1 & n = 0 \\ 0 & n \neq 0 \end{cases} \quad (4.31)$$

This impulse can be shifted (Figure 4.56) and this operation is denoted as $\delta(n-k)$

$$\delta(n-k) = \begin{cases} 1 & n = k \\ 0 & n \neq k \end{cases} \quad (4.32)$$

Thus the impulse of the discrete function of the value $x(k)$ can be described as

$$x(k) = x(n)\delta(n-k) \quad (4.33)$$

where first part $x(n)$ represents value of the impulse and the second one $\delta(n-k)$ informs about position or shift of the impulse.

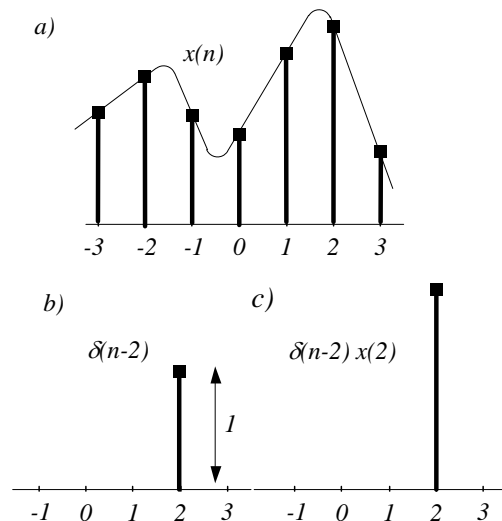


FIGURE 4.56
The discrete function (a), shifted unit impulse (b) and the selected impulse $x(k)$ (c)

The discrete signal is composed of the series of impulses with the magnitude proportional to the sampled signal $f(t)$ and with the period T_s

$$x(nT_s) = f(nT_s)\delta(t-nT_s) \quad (4.34)$$

or generally

$$x(n) = \sum_{k=-\infty}^{\infty} x(k)\delta(n-k) \quad (4.35)$$

We can perform the mathematical operations on the discrete signals. We can add discrete signals $y(n) = x_1(n) + x_2(n)$ as well we can multiply such signals $y(n) = x_1(n) \cdot x_2(n)$. We can also shift the signal by n_0 thus $y(n) = x(n-n_0)$. We can describe relation between output and input of digital system as differential equation:

$$\sum_{k=0}^N a_k y(n-k) = \sum_{k=0}^M b_m x(n-k) \quad (4.36)$$

or more generally

$$y(n) = \sum_{k=1}^N a_k y(n-k) + \sum_{k=0}^M b_m x(n-k) \quad (4.37)$$

These operations are possible if the system is *linear time invariant LTI*. The system is *linear* if the additive relation called as the *superposition principle* is valid. The superposition principle is described as

$$f(x_1) + f(x_2) = f(x_1 + x_2) \quad (4.38)$$

Thus if $y_1(n)$ is the system response to the input signal $x_1(n)$ and $y_2(n)$ is the system response to the input signal $x_2(n)$ and

$$x(n) = a_1 x_1(n) + a_2 x_2(n) \quad (4.39)$$

the output of a linear system is

$$y(n) = a_1 y_1(n) + a_2 y_2(n) \quad (4.40)$$

The superposition is very important in DSP. Let us assume that the input signal $x(n)$ can be *decomposed*, which means that it can be converted into two or more additive components $x_1(n), x_2(n), \dots$. We can determine the output signal component of each input signal $y_1(n), y_2(n), \dots$. Next the output signal can be *synthesized* as the sum of each component. The synthesized output signal is identical as calculated directly $y(n) = f(x(n))$. Thus if the system is complex we can analyze it as superposition of simpler components.

The system is *time invariant* (stationary) if the delay (shift in the time domain) of the input signal causes appropriate delay of the output signal. Thus if $x(n) = x_1(n-n_0)$ the response is $y(n) = y_1(n-n_0)$.

For the analysis of the discrete signal it is required if the system is casual. In the *casual system* the output signal depends only on the previous or present values of the input signals. Thus if input samples are $x(n)$ for $n < n_0$ the output signal does not depend on the samples $n > n_0$.

The LTI circuit is completely characterized by the answer to the delta impulse input known as impulse response $h(n)$ – Figure 4.57. The number of output impulses (corresponding with one input impulse) depends on the order of the digital circuit.

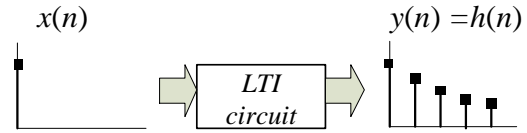


FIGURE 4.57 The impulse response of the 5th order digital system

The discrete signal can be also represented in frequency domain. If this signal is periodical we can perform the conversion from the time domain to frequency domain by using Discrete Time Fourier Transform DTFT⁹:

$$X(\omega) = X(e^{j\omega}) = \sum_{n=-\infty}^{\infty} x(n) e^{-jn\omega} \quad (4.41)$$

or for limited number of samples N Discrete Fourier Transform DFT:

$$X(k) = \sum_{n=0}^{N-1} x(n) e^{-j2\pi nk/N} \quad (4.42)$$

as polar function or as trigonometric function¹⁰

$$X(k) = \sum_{n=0}^{N-1} x(n) [\cos k(2\pi nk/N) - j \sin(2\pi nk/N)] \quad (4.43)$$

For signals sampled with frequency f_s (thus $x(nT_s)$) the relationship (4.42) can be rewritten as

$$X(k) = X(\omega_s) = \sum_{n=0}^{N-1} x(n) e^{-jn\omega_s/N} \quad (4.44)$$

or

$$X(k) = X\left(\frac{\omega_s}{N}\right) = \sum_{n=0}^{N-1} x(n) e^{-jn\omega_s} \quad (4.45)$$

The frequency representation of discrete signal is a complex number consisting of real cosines part and imaginary sinus part (or modulus and phase

⁹ The signals in time domain we describe usually by using small letters e.g. $x(n)$ while in frequency domain by using large letters e.g. $X(m)$.

¹⁰ According to Euler rule: $e^{j\phi} = \cos \phi - j \sin \phi$.

components). Sometimes, for example for spectral analysis it is sufficient to present only modulus of the result of Fourier transform. Figure 4.58 presents an example of signal in the frequency domain – note that some samples can be equal to zero.

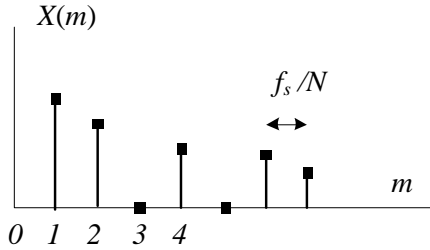


FIGURE 4.58
An example of the signal presentation in the frequency domain.

Of course we can always return from frequency domain to the time domain by using the Inverse Discrete Fourier Transform IDFT:

$$x(n) = \frac{1}{N} \sum_{m=0}^{N-1} X(m) e^{jm\omega_s} \quad (4.46)$$

or more generally

$$x(n) = \frac{1}{N} \sum_{m=1}^{N-1} X(m) e^{j2\pi nm/N} \quad (4.47)$$

$$x(n) = \frac{1}{N} \sum_{m=1}^{N-1} X(m) [\cos(2\pi nm/N) + j \sin(2\pi nm/N)] \quad (4.48)$$

For describing discrete signals and operations very convenient is to use the *z-Transform*:

$$X(z) = Z[x(n)] = \sum_{n=-\infty}^{\infty} x(n) z^{-n} \quad (4.49)$$

where $z = re^{j\omega}$. By comparing with relationship (4.41) describing DFT we see that the *z-Transform* is the same as Fourier Transform for $r = 1$.

The z^{-1} is equivalent to the delay of the signal by one sample

$$Z[x(n-1)] = z^{-1} X(z) \quad (4.50)$$

while z^{-m} means the delay by m samples

$$Z[x(n-m)] = z^{-m} X(z) \quad (4.51)$$

The differential equation (4.37) we can now rewritten in simplified form as:

$$Y(z) = Y(z) \sum_{k=1}^M a(k) z^{-k} + X(z) \sum_{k=0}^N b(k) z^{-k} \quad (4.52)$$

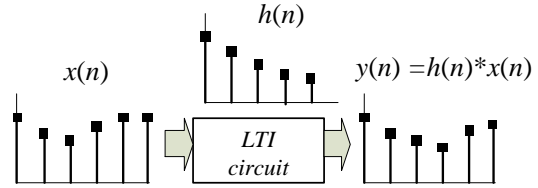


FIGURE 4.59
The relation between input and output signal of linear discrete system.

If we have linear DSP circuit treated as the “black box” we are able to determine the output signal if earlier the impulse response $h(n)$ was defined. The relation between output $y(n)$ and input $x(n)$ signals is described by the relationship:

$$y(n) = \sum_{k=-\infty}^{\infty} x(k) h(n-k) \quad (4.53)$$

[This relation is known as the *convolution* and denoted by the symbol *:

$$y(n) = \sum_{k=-\infty}^{\infty} x(k) h(n-k) = x(n) * h(n) \quad (4.54)$$

or

$$y(n) = \sum_{k=-\infty}^{\infty} x(n-k) h(k) = h(n) * x(n) \quad (4.55)$$

The convolution is the relationship between input signal and output signal of LTI systems and enables to determine the response signal if the impulse response $h(n)$ is known. The reverse operation known as *deconvolution* enables to determine the input signal if the output signal and impulse response are known. The *z-transform* of the impulse response is

$$H(z) = \sum_{k=0}^{\infty} h_k z^{-k} \quad (4.56)$$

and the relation between input and output is:

$$Y(z) = H(z)X(z) \tag{4.57}$$

Thus in time domain the linear digital circuit is completely described by its impulse response $h(n)$ and the same in the frequency domain by frequency impulse response $H(z)$ (or $H(\omega)$).

The convolution can be realized in the z -domain as simply multiplication. The transfer function $H(z)$ explicitly describes the properties of the casual system.

In general case the transfer function can be described by differential equation:

$$H(z) = \frac{Y(z)}{X(z)} = \frac{a_1z^{-1} + a_2z^{-2} + a_3z^{-2} \dots}{1 + b_1z^{-1} + b_2z^{-2} + b_3z^{-3}} \tag{4.58}$$

or

$$H(z) = \frac{Y(z)}{X(z)} = \frac{\sum_{k=0}^{N-1} a(k)z^{-k}}{1 + \sum_{k=1}^M b(k)z^{-k}} \tag{4.59}$$

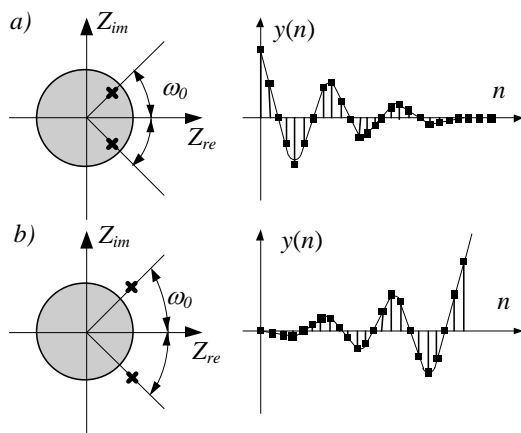


FIGURE 4.60
The system is stable because poles are inside the unit circle (a) and the system is unstable with the poles outside of the circle (b) (ω_0 – frequency of oscillations)

It is possible that the denominator can be equal to zero what means non-stability of the system. Therefore the analysis of the transfer function is important to check if digital circuit is stable. We can rewrite the relationship (4.59) in a form:

$$H(z) = \frac{(z - z_1)(z - z_2)(z - z_3) \dots}{(z - p_1)(z - p_2)(z - p_3) \dots} \tag{4.60}$$

where z_1, z_2, z_3 values are the zeros (values of the z when the numerator is equal to zero) and p_1, p_2, p_3 are poles (the values of z when the denominator is equal to zero).

The zeros ($z_1, z_2, z_3 \dots$) and poles ($p_1, p_2, p_3 \dots$) are complex numbers. If we analyze the position of the poles in the z -plane we can test the conditions of stability. The casual system is stable if the poles are located inside the unit circle $|z|=1$ in the z -plane (Figure 4.60).

The convolution is a very important operation in digital signal processing – practically all digital filters perform this operation. In calculation of the convolution we repeat many times elementary operation – $h(k)x(n-k)$. Looking at the figure 4.56 it is obvious that elementary operation consists of shifting our impulse by k and multiply by $h(k)$. Next according to the relationship (4.55) it is necessary to add results of these elementary operations to obtain output impulse $y(n)$.

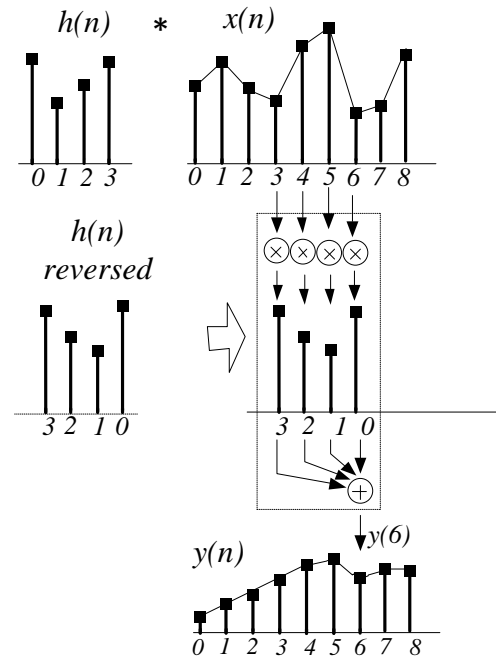


FIGURE 4.61
The “convolution machine” as a tool for calculation of the convolution (after Smith 2003)

The convolution operation as computer algorithm is relatively simple. The calculate of the $y(n)$ output impulse it is necessary to perform following steps:

- a) reversing left-for-right the signal $h(n)$
- b) shift this signal by n samples

- c) multiply this signal by corresponding impulses in the input signal: $h(k)x(n-k)$
- d) to add all multiplied results.

Figure 4.61 presents the illustration of the convolution calculation is the “convolution machine” proposed by Steven Smith (Smith 2003). As an example the calculation of an output impulse $y(6)$ is demonstrated. Translation this operation to computer algorithm is presented in Figure 4.62. We have fixed register with impulse response (filter) coefficients. Data of this register is multiplied by the moving register with input signal and adding results are transferred do the moving register with output data.

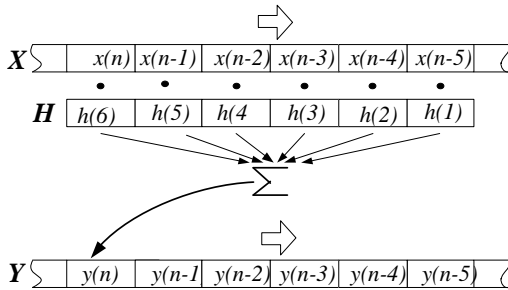


FIGURE 4.62
The computer algorithm of the convolution operation

The convolution has the following properties (Figure 4.63)

$$y(n) = x(n) * h(n) = h(n) * x(n) \quad (4.61)$$

$$[x(n) * h_1(n) * h_2(n)] = x(n) * [h_1(n) * h_2(n)] \quad (4.62)$$

$$h_1(n) * x(n) + h_2(n) * x(n) = [h_1(n) + h_2(n)] * x(n) \quad (4.63)$$

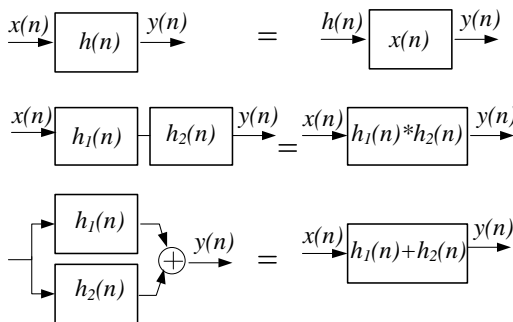


FIGURE 4.63
Properties of the convolution operation

The calculation of the convolution in the time domain can be substituted by the operation in the frequency domain. It is especially important in the case of deconvolution operation which is very difficult to perform in time domain. Both operations can be realized in the frequency domain taking into account the relationship

$$y(n) = x(n) * h(n) \quad Y(f) = X(f)H(f) \quad (4.64)$$

To perform the convolution operation in the frequency domain it is necessary:

- to calculate the Fourier transform of input signal and impulse response $X(f), H(f)$
- to multiply both transform,
- return to the time domain by using the inverse Fourier transform.

Figure 4.64 illustrates the realization of the convolution operation in time and frequency domain. In the frequency domain we should take into account both real and imaginary part of the signal. Thus the multiplication of signals in the frequency domain can be performed according to the relationships

$$Y(f) = H(f) \times X(f) \quad (4.65)$$

$$\text{Re } Y(f) = \text{Re } X(f)\text{Re } H(f) - \text{Im } X(f)\text{Im } H(f)$$

$$\text{Im } Y(f) = \text{Im } X(f)\text{Re } H(f) + \text{Re } X(f)\text{Im } H(f)$$

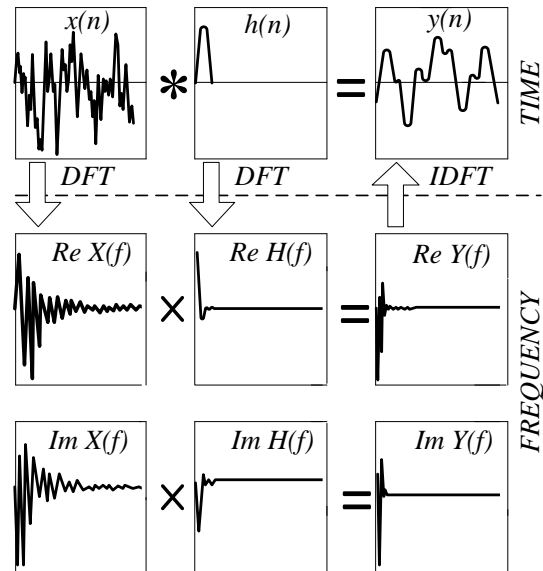


FIGURE 4.64
Realization of the convolution operation in the time domain and the frequency domain (after Smith 2003)

The deconvolution can be realized in the frequency domain as the division operation, according to the relationships

$$H(f) = Y(f) : X(f) \quad (4.66)$$

$$\operatorname{Re} H(f) = \frac{\operatorname{Re} Y(f) \operatorname{Re} X(f) + \operatorname{Im} Y(f) \operatorname{Im} X(f)}{[\operatorname{Re} X(f)]^2 + [\operatorname{Im} X(f)]^2}$$

$$\operatorname{Im} H(f) = \frac{\operatorname{Im} Y(f) \operatorname{Re} X(f) - \operatorname{Re} Y(f) \operatorname{Im} X(f)}{[\operatorname{Re} X(f)]^2 + [\operatorname{Im} X(f)]^2}$$

Both, convolution and deconvolution operations are very useful in the image processing. In this case the impulse response is often called as *point spread function PSF*. By using digital filter known also as *mask* or *kernel* we can change various features of a picture: the edges (smoothing or enhancement), contrast, color, etc. The deconvolution algorithm is very useful for image processing, for example when the picture is blurred. When the PSF is unknown or poorly determined then special iterative techniques called *blind deconvolution* can be used for the picture reconstruction.

The deconvolution operation can be also used in sound processing. We can assume that a virtual filter with impulse response $h_{noise}(n)$ is responsible for the noises and interferences. For example if we analyze the noisy pause between musical parts of recording we can determine such filter parameters. Next we can try to remove the noise from the musical record performing the deconvolution (asking what is the input signal $x(n)$ if we know the output signal $y(n)$ and impulse response).

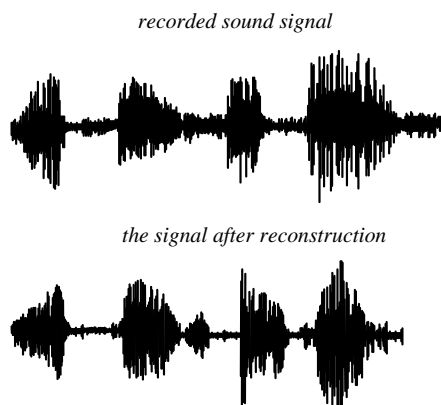


FIGURE 4.65
The sound signal reconstructed after application of the deconvolution algorithm (Czyzewski 1998)

Figure 4.65 presents the example of applying of deconvolution operation to improve the sound. In the

first step, the impulse response of the filter representing the original signal was determined for a musical instrument (from the Baroque time). Next, this impulse response was used for reconstruction of the old, disturbed and damaged record. As a result pure sound was obtained (without noises and distortion); moreover, this reconstruction was not only technical one, but it also recovered the musical character of the Baroque period.

Another important digital operation is the *correlation function*, used for the comparison of two signals $x_1(n)$ and $x_2(n)$. The correlation function is described by following relation

$$r_{12}(k) = \frac{1}{N} \sum_{n=0}^{N-1} x_1(n) x_2(n+k) \quad (4.67)$$

The correlation is a mathematical operation very similar to the convolution:

$$y(n) = \sum_{k=-\infty}^{\infty} x(k) h(n-k) \quad (4.68)$$

By comparing equations 4.67 and 4.68 it is clear that only the sign +/- is the difference. Thus although convolution and correlations are different functions they can be calculated by using similar computer algorithm – in example of the “machine” presented in Figure 4.64 we only omit the reverse operation of the second function. If we compare two signals we determine the *cross-correlation*, and if we compare the signal with itself we determine the *autocorrelation*.

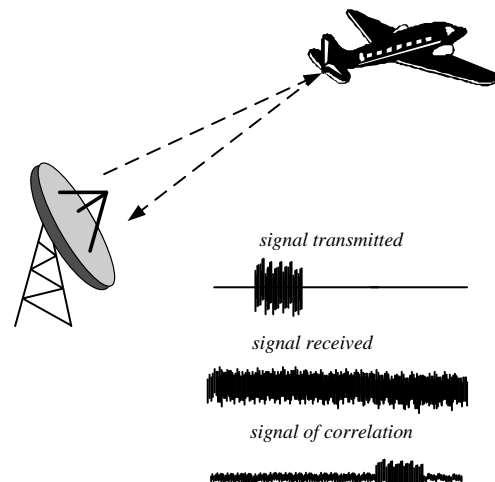


FIGURE 4.66
The signal reconstructed after application of the correlation algorithm

A typical application of correlation function is searching for the radar signal covered by noises (Figure 4.66). Because we know the wave shape of transmitted signal it is possible to find it even if the noises are larger than the useful signal.

The autocorrelation function is a best method to test the periodicity of the signal – see relationship (2.44).

4.5 Discrete Fourier Transform DFT

The Discrete Fourier Transform DFT is one of the most important operations in digital signal processing.

-It enables conversion between time and frequency domain (as it was presented sometimes the signal processing can be easier performed in the frequency domain).

- It is a toll for signal analysis – we can obtain almost full information about the signal, including determination of Total Harmonic Distortion THD.

- It is a gate to digital world. If we have series of data we can convert them to mathematical digital representation. For example the bitmap figure representation (of large volume) can be converted to two-dimensional Fourier transform. This is a basis for image processing in digital tomography [Guy *et al* 2005].

As it was described earlier the equivalent of continuous time Fourier transform:

$$X(\omega) = \frac{1}{2\pi} \int_{-\infty}^{+\infty} x(t) e^{-j\omega t} dt \quad (4.69)$$

For a discrete time is a Discrete Time Fourier Transform DFTT:

$$X(\omega) = \frac{1}{2\pi} \sum_{n=-\infty}^{+\infty} x(n) e^{-j\omega n} \quad (4.70)$$

The summation from infinity is possible theoretically for only simple cases therefore we usually limit the number of samples to N in a Discrete Fourier Transform DFT:

$$X(k) = \sum_{n=0}^{N-1} x(n) e^{-j\frac{2\pi nk}{N}} \quad (4.71)$$

In this way we assume that the discrete signal is periodical and the selected samples are a good its representation¹¹.

Sometimes the DFT is presented in form:

$$W_N^{nk} = e^{-j\frac{2\pi nk}{N}} = (W_n)^{nk} \quad (4.72)$$

where coefficient $W_N = \exp(-j2\pi/N)$ thus:

$$W_N^{nk} = e^{-j\frac{2\pi nk}{N}} = (W_n)^{nk} \quad (4.73)$$

The Fourier transform allows the conversion of the signal from the time domain to the frequency domain and *vice versa*. Below, are presented the main properties of the discrete Fourier transform.

If $x_1(n)$ is represented by the Fourier transform $X_1(k)$ and accordingly $x_2(n)$ by $X_2(k)$ then

$$x(n) = ax_1(n) + bx_2(n) \Leftrightarrow X(k) = aX_1(k) + bX_2(k) \quad (4.74)$$

This relation describes the *linearity* properties of the DFT.

The DFT is *periodic* with a period of N also if the $x(n)$ is non-periodic.

$$X(k) = \sum_{n=0}^{N-1} x(n) e^{-j2\pi kn/N} = \sum_{n=0}^{N-1} x(n) e^{-j2\pi kn/N} e^{-j2\pi Nn/N} = X(k+N) \quad (4.75)$$

If the input signal is real then the real part of the DFT is an even function and the imaginary part of DFT is an odd function. This kind of symmetry is sometimes called *hermitian symmetry*.

$$x(n) = x^*(n) \Leftrightarrow X(k) = X^*(-k) \quad (4.76)$$

If $x(n)$ is an even function then $X(k)$ is also even. If $x(n)$ is an odd function then $X(k)$ is also odd. Furthermore, if $x(n)$ is real and even then $X(k)$ is real and even. And if $x(n)$ is real and odd then $X(k)$ is imaginary and odd.

$$x(n) = x(-n) \Leftrightarrow X(k) = X(-k) \quad (4.77)$$

This relationship describes the *symmetry properties* of DFT.

$$x(n) = x_1(n) * x_2(n) \Leftrightarrow X(k) = X_1(k) X_2(k) \quad (4.78)$$

The relationship (4.78) is very important in DSP, because it means that the convolution operation can be performed by DFT of both components, then by multiplication of the results, and finally, by the inverse

¹¹ Or we can assume that all samples outside selected range are equal to zero.

transform to the time sequence (*circular convolution*). And inversely we can perform the deconvolution of $x(n)$ by transforming it to $X(k)$ and by dividing it by one component $X_r(k)$.

$$\sum_{n=0}^{N-1} |x(n)|^2 = \frac{1}{N} \sum_{k=0}^{N-1} |X(k)|^2 \quad (4.79)$$

The relationship (4.79) known as the *Parseval theorem* states that the energy of the signal in time domain is the same as the energy in the frequency domain. Thus the time domain representation of the signal is fully transformable to the frequency domain if the system is linear time invariant.

$$x(n-m) \Leftrightarrow W_N^{kn} X(k) \quad (4.80)$$

The *shift m in the time domain (time delay)* is equivalent to the multiplication in the frequency domain by the component $\exp(-j\omega m)$. Thus, the phase component of the complex representation is increased by ωm .

$$X(k-M) \Leftrightarrow W_N^{Mn} x(n) \quad (4.81)$$

The *shift M in the frequency domain* is equivalent to the multiplication of the signal in time domain by the component $\exp(-j\omega M)$.

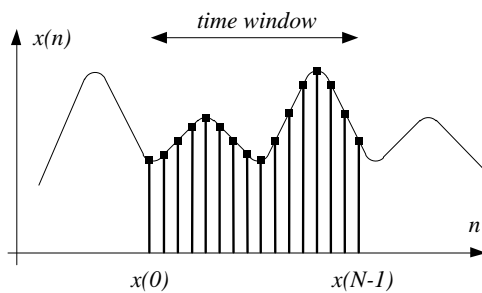


FIGURE 4.67
The selection of N samples for Fourier analysis

To select N number of samples it is used time window method illustrated in Figure 4.67. We select samples by multiplying the signal by the window function. For example the rectangular window function (presented in Fig. 4.66) is in the form:

$$w(n) = \begin{cases} 1 & \text{for } n_0 \leq n \leq n_0 + N \\ 0 & \text{for other samples} \end{cases} \quad (4.82)$$

where n_0 is the starting point of the window and N is the number of samples.

The use of rectangular window causes some unwanted effects. The Fourier transform of the rectangle signal is described by the equation

$$X(k) = \frac{\sin(\pi k N / M)}{\sin(\pi k / M)} \quad (4.83)$$

where M is the number of samples, and N is the number of selected samples in the time window.

The equation (4.83) is called the *Dirichlet kernel*. For usually $M=N$ and for small values of $\pi k/M$ (when $\sin x \approx x$) this equation can be presented in a simplified form

$$X(k) = \frac{\sin \pi k}{\pi k} \quad (4.84)$$

It means that even if samples in time domain are the same value in the frequency domain they are modulated by sinc function.

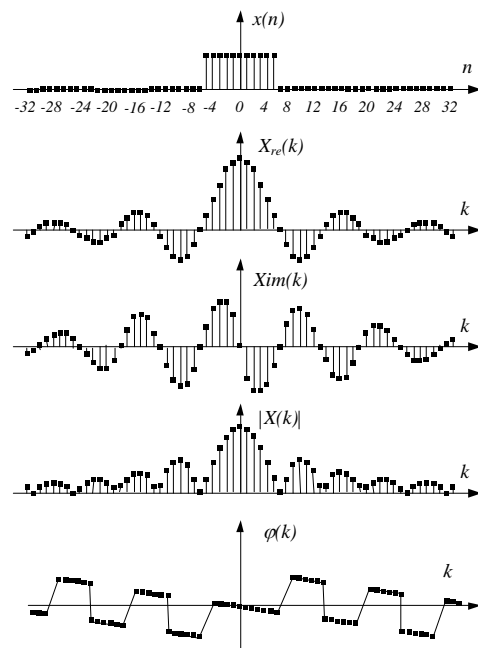


FIGURE 4.68
An example of the results of DFT analysis of rectangle window (after Lyons 2004)

In Figure 4.68 various components of the results of Fourier transform are presented: real and imaginary part (see Eq. (4.43)) or modulus and phase:

$$|X(k)| = \sqrt{X_{re}^2(k) + X_{im}^2(k)} \quad (4.85)$$

$$\varphi(k) = \arctg \frac{X_{im}(k)}{X_{re}(k)} \quad (4.86)$$

If we perform spectral analysis sufficient is to present only modulus but generally (for example if we analyze impedance) we should take into account complex number. From Figure 4.68 results that the all components are influenced by the form of window function.

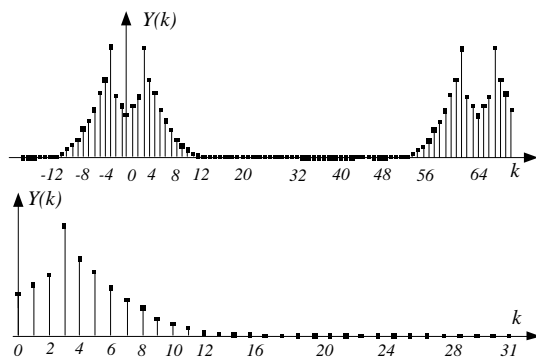


FIGURE 4.69
An example of the results of DFT analysis for selected 64 samples of the signal and the first 32 samples representing the analyzed signal

Figure 4.69 presents the example of the Fourier analysis of the selected 64 samples of the signal. The result is periodical with period $N/2$. Due to symmetry of obtained results only first $0 - (N/2)$ samples are useful because the remaining samples are meaningless (also the samples of negative frequencies do not introduce new information).

If we select series of N samples with sampling period T_s :

$$x(kT_s) = x(0), x(T_s), x(2T_s), \dots, x((N-1)T_s) \quad (4.87)$$

as result of Fourier transform we obtain series of $N/2$ samples distanced by f_s/N :

$$X\left(\frac{nf_s}{N}\right) = X(0), X\left(\frac{f_s}{N}\right), X\left(\frac{2f_s}{N}\right), \dots, X\left(\frac{(N-1)f_s}{N}\right) \quad (4.88)$$

what is illustrated in Figure 4.70. Thus the samples of DFT analysis do not represent harmonics but they result form the relation f_s/N . If we for example select sampling frequency 3200 Hz and number of samples $N = 32$ the distance between $X(k)$ samples is 100 Hz and the first harmonics 50 Hz is not represented.

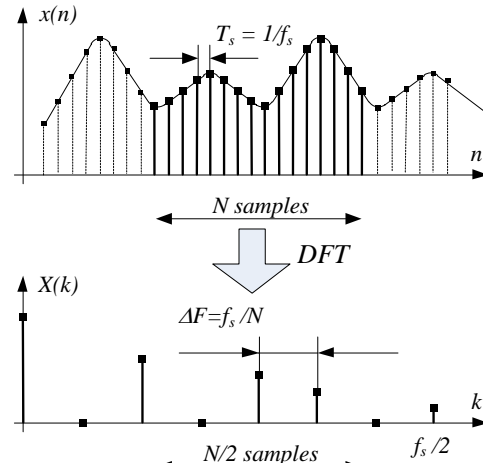


FIGURE 4.70
Input and output signal of DFT analysis.

If the sample f_s/N corresponds exactly with the frequency of harmonics we have *synchronous analysis* and it is represented by one line. But if the harmonics does not have representative line in DFT analysis it is represented by several spectral lines around the frequency nearest to the frequency of the signal. This effect of spectral line broadening is called as *leakage* and we have *asynchronous analysis*.

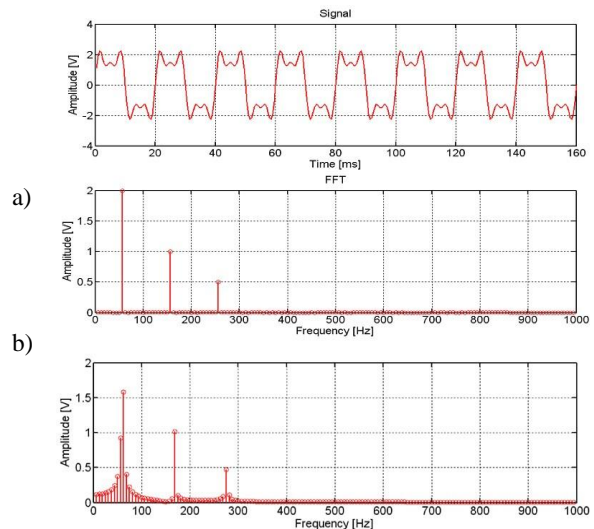


FIGURE 4.71
The example of spectral representation of the distorted signal for synchronous (a) and asynchronous (b) DFT analysis (Matlab simulation for $f_s = 2 \text{ kHz}$, $N = 320$, $A_1 = 2V$, $A_2 = 1V$, $A_3 = 0.5V$, $f_1 = 50 \text{ Hz}$ (case a), $f_1 = 54 \text{ Hz}$ (case b))

For synchronous analysis the sinc function (see Figure 4.68) practically does not influence the result. Figure 4.72 presents the example of DFT analysis of cosine function. If the analysis is synchronous then the samples correspond exactly to the zero values of side lobes and only one spectral line is visible (Figure 4.72a). But for the asynchronous analysis (what occur more often) the positions of the samples can meet various places of the side lobes and the leakage is more wide (Figure 4.72b).

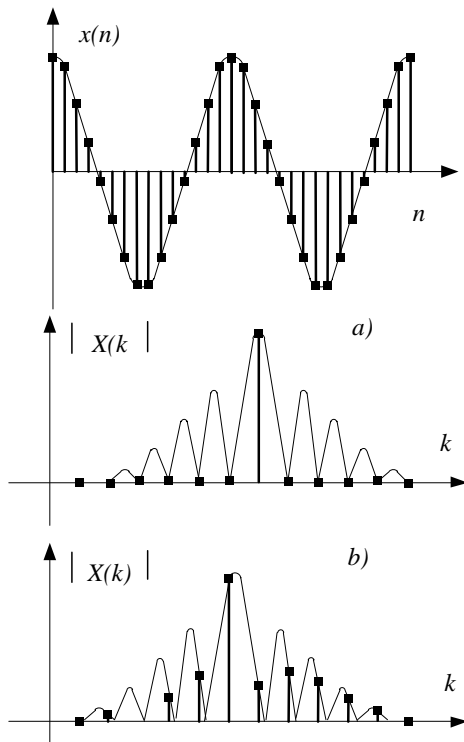


FIGURE 4.72
The Fourier transform of the cosine function in the case of synchronous (a) and asynchronous (b) analysis (after Lyons 2004)

The side lobes appear due to the sharp border of the rectangle window. We can reduce the amplitude of the side lobes using other shapes of the window, when the border is smoother. Figure 4.73 presents the effect of applying of the Hanning window described by the relationship:

$$w(n) = 0.5 - 0.5 \cos(2\pi n / N) \quad (4.89)$$

We can see that after application of the Hanning window the side lobes have reduced amplitude but at the expense of widening the main window. There are various kinds of windows: Hanning, Hamming, Chebyshev, Keiser, etc. and by choosing a correct window it is possible to improve the quality of the spectral analysis.

Chebyshev, Keiser, etc. and by choosing a correct window it is possible to improve the quality of the spectral analysis.

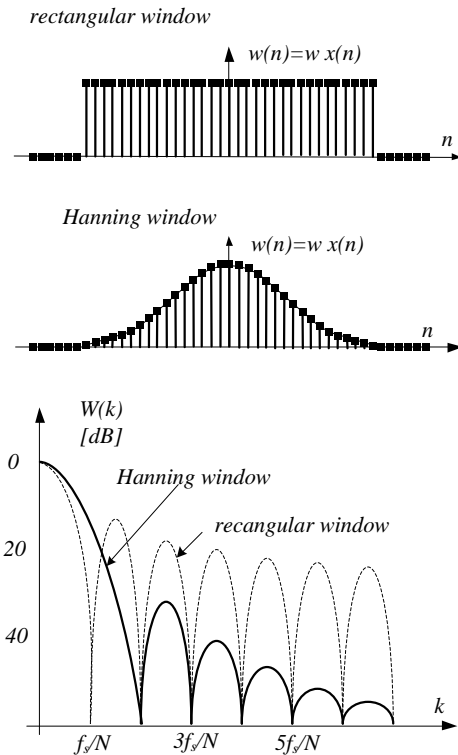


FIGURE 4.73
The effect of applying of the Hanning window

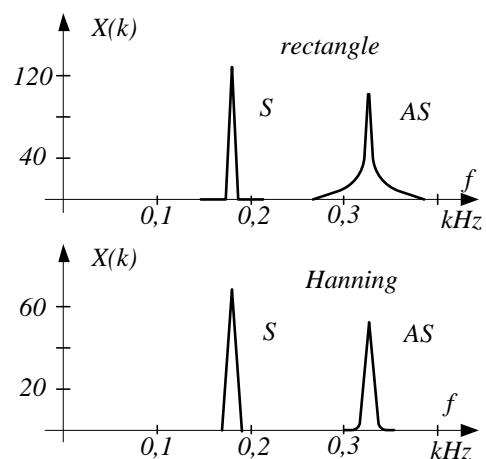


FIGURE 4.74
The effect of applying of the Hanning window for synchronous S and asynchronous AS case (Smith 2003)

Figure 4.74 presents the example of the spectral analysis results obtained without and with the Hamming window. After use of the Hamming window the tails of the spectral line decrease in the case of asynchronous analysis, but in the case of synchronous analysis the application of the Hamming window increases the broadband of the spectral line.

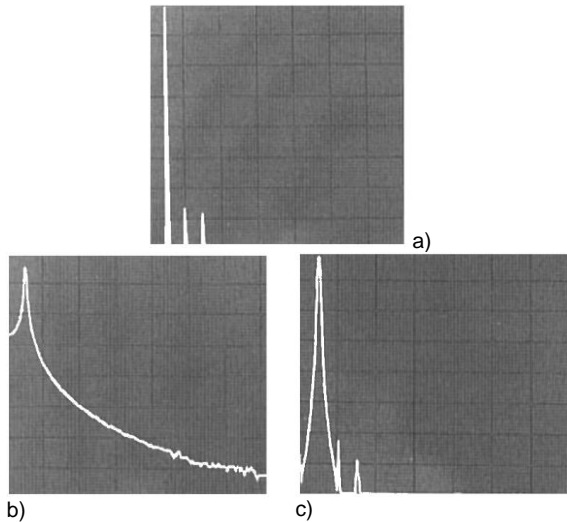


FIGURE 4.75
The example of synchronous spectral analysis (a), asynchronous with rectangular window (b) and asynchronous one with Hanning window (c) (Agilent 150 2005) (permission of Agilent)

analysis the first line due to leakage practically covers the other harmonics. But after application of the Hanning window the results of asynchronous analysis are significantly improved. Thus during the analysis it is important to find (experimentally) the best shape of the window.

The resolution of spectral lines depends on the relation f_s/N . Sometimes if we have small number of samples we can improve resolution artificially by adding some zero samples as it is presented in Figure 4.76.

The computation of the N-point Fourier transform requires huge number complex multiplication operations. Thus, the calculation of the Fourier transform is not a trivial task even for fast processors, because the time of computations practically excludes this analysis in the real time systems. The turning point was the invention of Cooley and Tukey (Cooley 1965). They proposed a special algorithm allowing faster Fourier transform calculation. This algorithm with some modifications is used currently in the Fourier analysis and is called *FFT – Fast Fourier Transform*. By applying the FFT analysis it is possible to decrease the number of multiplication from 2^N to $0.5 N \log_2 N$. For example to realize the 1024-sample DFT it is necessary to perform 1 048 576 multiplication operations and 1 047 552 addition operations, while the FFT analysis requires in such a case only 5 120 multiplications (around 200 times less than in the DFT) and 10 240 additions (around 100 times less).

The FFT algorithm profits from the symmetry and periodicity of Fourier transform to increase the computational efficiency by diminishing the number of operations. The DFT equation is divided into two parts, even and odd sequence

$$X(k) = \sum_{n=0}^{N/2-1} x(2n)W_N^{2nk} + W_N^k \sum_{n=0}^{N/2-1} x(2n+1)W_N^{2nk} \tag{4.90}$$

The factor W_N^{kn} , known as the *twiddle factor*, appears in both parts of the equation and it is sufficient to be computed just once. Moreover, there are only four different values of this factor and there is no need to compute them so many times. The computation of N-point transform is a rather difficult, therefore the sequences described by Eq. (4.90) are decomposed into several sub-sequences finishing on the two-point DFT. The flow-graph of this algorithm is presented in Figure 4.77.

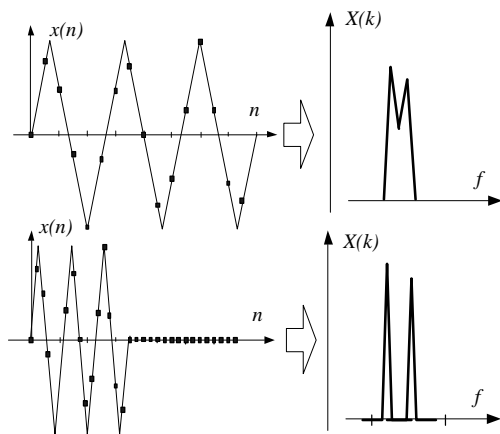


FIGURE 4.76
The improvement of resolution of DFT analysis by increase of the number N of samples

Figure 4.75 presents the comparison of the results of the analysis of the same signal. In the synchronous case the results are excellent. In the case of asynchronous

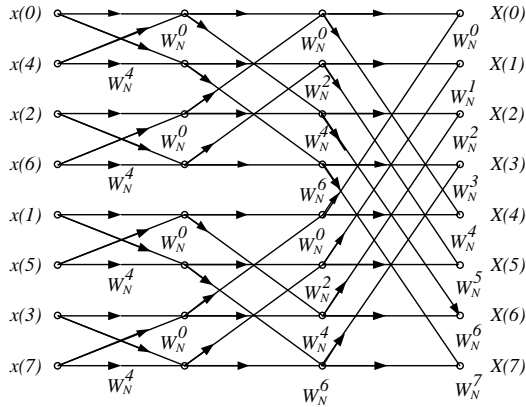


FIGURE 4.77
The flow-graph of the decimation-in-time 8-point FFT algorithm (Mitra 2003)

The calculation of two-point transform is relatively simple and for example the first transform from Figure 4.77 can be expressed as:

$$X_{00}(k) = \sum_{n=0}^1 x_{00}(n) W_2^{nk} = x(0) + W_2^k x(4) \quad (4.91)$$

This two-point DFT consisting of one multiplication and two additions can be expressed by the butterfly flow-graph presented in Figure 4.78.

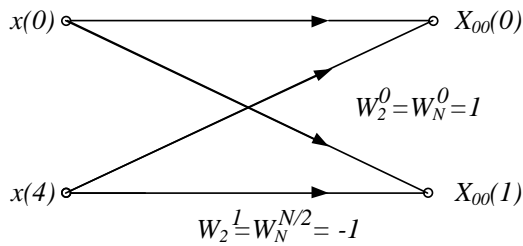


FIGURE 4.78
The butterfly operation of the two-point DFT

The decomposition of the data sequence can be performed in the time domain (*decimation-in-time*) or in the frequency domain (*decimation-in frequency*). Figure 4.77 presents the example of the flow-graph of the decimation-in-time FFT algorithm for N=8. By using such algorithm it is possible to determine the 8-point DFT by applying 24 multiplication operations.

The FFT algorithms are described in detail elsewhere (Bracewell 1999, Chu 2000, James 2002, Mitra 2002, Sneddon 1995). Most of these algorithms

required to provide 2^N samples. If there is a smaller number of samples it is recommended to complete them by supplementing the samples by the appropriate number of zero samples.

Currently, tools for computing the FFT (and *Inverse Fast Fourier Transform – IFFT*) are available in ready-to-use form in many computing platforms (for example in MatLab or LabVIEW), many measuring instruments are equipped with FFT (for example digital oscilloscopes). The calculation of the FFT is possible using scientific calculators or spreadsheets (for example MS Excel).

It is important to note that FFT algorithm is not a simplification of DFT analysis – it is a method of simply calculation of DFT. The results of calculation of both FFT and DFT should be the same.

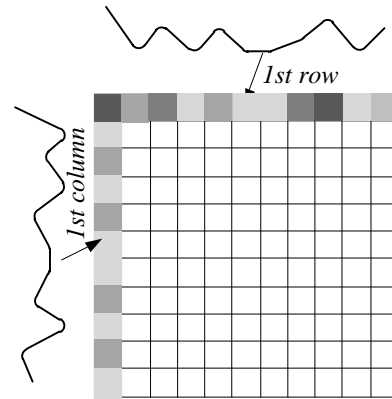


FIGURE 4.79
Substitution of bitmap picture by vector picture by means of FFT.

In analysis of electrical signal FFT analysis is usually performed as one-dimensional $x(t) \leftrightarrow X(F)$ form. But in image processing, for example computer tomography [Kak and Slaney 1988] the two- and three-dimensional Fourier analysis plays a crucial role because it enables to convert huge bitmap picture to small vectorial form, easy next to process. The two-dimensional DFT can be described as [Kak and Slaney 1988]:

$$F(u, v) = \frac{1}{MN} \sum_{m=0}^{M-1} \sum_{n=0}^{N-1} f(m, n) \exp \left[-j2\pi \left(\frac{mu}{M} + \frac{nv}{N} \right) \right] \quad (4.92)$$

while inverse DFT is:

$$f(m, n) = \sum_{u=0}^{M-1} \sum_{v=0}^{N-1} F(u, v) \exp \left[j2\pi \left(\frac{mu}{M} + \frac{nv}{N} \right) \right] \quad (4.93)$$

The relationship (4.92) can be presented as:

$$F(u, v) = \frac{1}{M} \sum_{m=0}^{M-1} \left[\frac{1}{N} \sum_{n=0}^{N-1} f(m, n) \exp\left(-j \frac{2\pi}{N} nv\right) \right] \exp\left(-j \frac{2\pi}{M} mu\right) \quad (4.94)$$

Thus the equation in square brackets is one-dimensional transform representing m th row. We can compute two-dimensional DFT by representing each row by its one-dimensional transforms and next by calculation transforms of each column.

It is required that the transform should be *reversible*. This means that we should be able to reconstruct the primary time varying signal from the frequency spectrum – for example using the Inverse Fourier Transform. But Fourier transform is correct only for *stationary signals* – signals not varying in the time or the frequency. We only obtain the information on which frequency component exists in the signal and not how it varies. Thus it would be not possible to recover music passage as presented in Figure 4.80 because it varies in frequency but also in time.

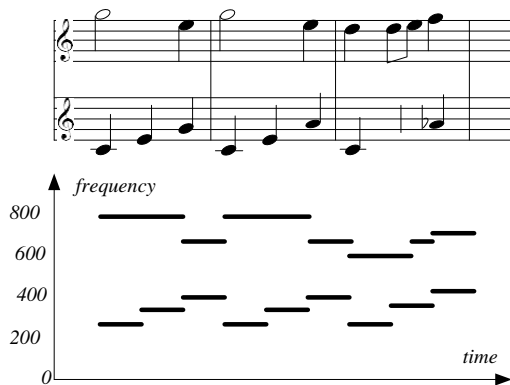


FIGURE 4.80
Music signal as a function of time and frequency.

Important limitation of the Fourier transform is that this operation is off-line. We need to collect data, insert to memory and next compute it. Fortunately modern signal processing devices are very fast and we are able to compute also *real time FFT*.

The digital FFT usually requires certain time for analysis of the packet of samples and during this time incoming samples can be unavailable for analysis. To avoid losing the data between the ADC and FFT devices a time buffer can be inserted (Figure 4.81). The time buffer should be dynamically fitted to the time of

analysis, which depends on the frequency span. Sometimes, for very short signals the time buffer can be substituted by several overlapping buffers, as shown in Figure 4.81b.

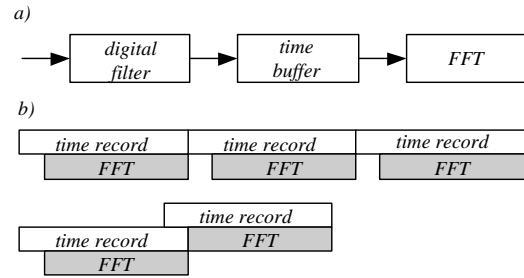


FIGURE 4.81
The time buffer for real time FFT analysis.

To analysis of non-stationary signals can be used special Fourier Transform called the time-dependent Fourier transform or *Short-time Fourier Transform STFT*. In this transform the time window of the analyzed signal is shifted in time – the analyzed signal is multiplied by shifted time window function (*Moving Window Method – MWM*). Thus, the non-stationary signal can be further reconstructed by the results of STFT distributed in time.

The short Fourier time is expressed by the equations:

$$X(n, k) = \sum_{m=0}^{N-1} w(m)x(n-m)e^{-jm(2\pi k / N)} \quad (4.95)$$

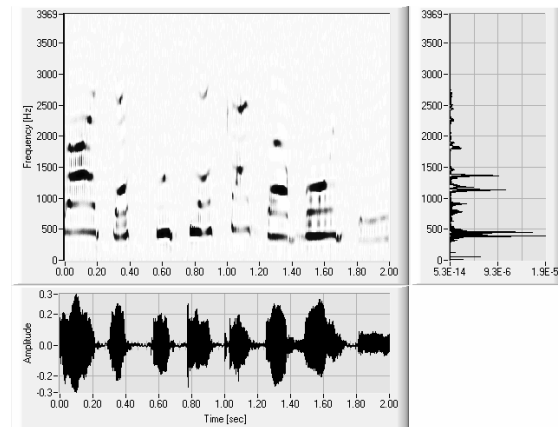


FIGURE 4.82
The result of analysis of human voice performed with Short Time Fourier Transform (Rak 2004).

The function $w(m)$ is the function of the time window. The results of the time/frequency analysis can be presented as a 3D picture. Usually it is presented as the frequency/time $F(t)$ 2D picture called a spectrogram – sometimes supplemented by the $x(t)$ and $X(F)$ dependence – as presented in Figure 4.82.

4.6 Digital filters

In comparison to the analogue filters described earlier (built from the RC elements and the amplifiers) the digital filters exist mainly as computer programs (thus they are some kind of virtual instruments) – although, there are digital filters available in the form of integrated circuits. The digital filters can be easily modified by the software, including also the possibility of the alteration of the parameters during the filter operation, in special kinds of filters, called adaptive filters. The performance of the filter does not depend on the quality of RC elements, but some hardware factors can limit their implementation (organization of the memory, speed of the processor etc).

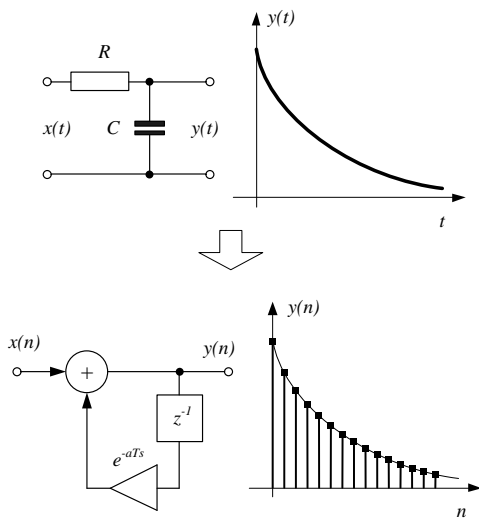


FIGURE 4.83
The analog RC low-pass filter and its digital equivalent.

The digital filters (as the analogue ones) should exhibit relatively flat characteristics in the passband, the transition band should be as narrow as possible, the filter should be linear (without the phase distortions), and the step response in time should be fast and without overshoot. Additionally, it is recommended to apply the optimal design (relatively simple), taking into account the necessary time and number of numerical operations. A correctly designed digital filter has a

performance of filtering much better than its analogue counterpart.

Figure 4.83 presents the digital equivalent of analog filter – the function of RC elements is realized by shifting z^{-1} part. By comparing this digital circuit with Figure 4.61 it can be easily observed that to receive the digital filter the operation of convolution should be performed (shifting, multiplying and adding). By increasing number of shifting-multiplying-adding operators we can increase order of filter.

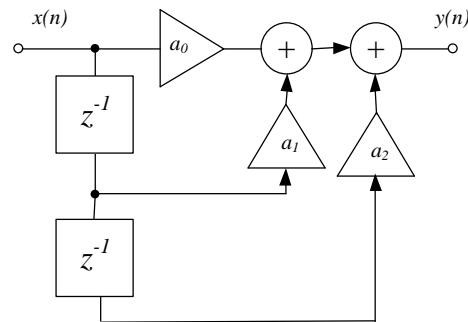


FIGURE 4.84
The example of the FIR filter.

In the filter presented in Figure 4.84 the response depends only on the input signal – this filter is without the feedback. This filter is called the *Finite Response Filter FIR* or *non-recursive filter*.

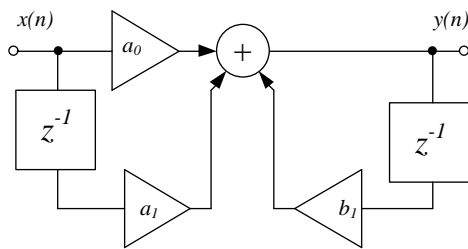


FIGURE 4.85
The example of the IIR filter.

By applying of the feedback we can improve performances of the filter. In the filter presented in Figure 4.85 the response depends not only on the input signal, but also on the output signal due to the feedback. Therefore, such filters are called *recursive filters* or *Infinite Response Filters IIR*.

The FIR filters are simpler in design and since they are without feedback there is no problem with the stability of the filter. The IIR filters, due to the feedback exhibit better steepness of the filter frequency characteristic in the transition band. This enable to

design the filters with a lower number of the multiplier elements and therefore such filters can be faster and less demanding for the processing power and memory requirements. The main drawback of recursive filters is the danger that they can be unstable. It is necessary to perform analysis of the stability conditions – mainly the position of the poles in the z -plane.

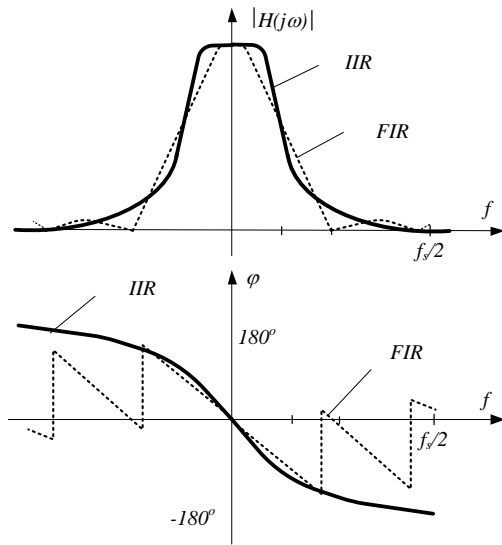


FIGURE 4.86
The comparison of amplitude and phase characteristics of 5th order FIR and IIR filters [Lyons 2004].

Figure 4.86 presents the comparison of the frequency characteristics of recursive and non-recursive digital filters. IIR filter exhibits better amplitude characteristic (more steepness, less ripples) although FIR filter has better phase linearity.

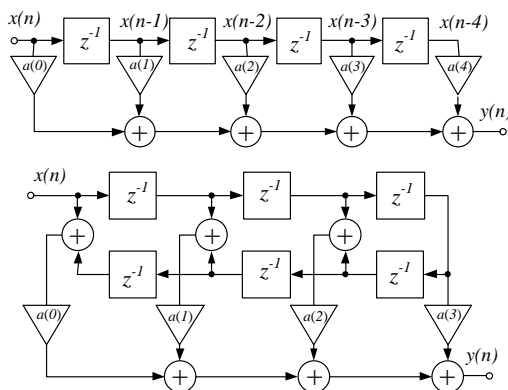


FIGURE 4.87
Two examples of the FIR filters.

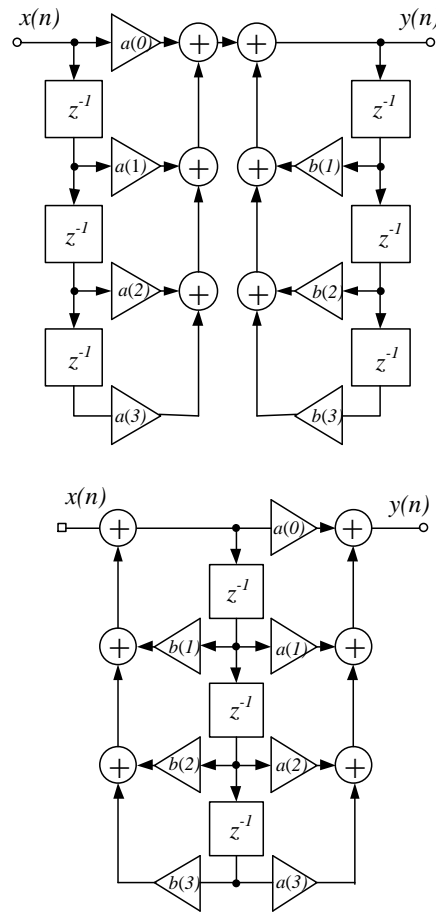


FIGURE 4.88
Two examples of the IIR filters.

As the digital filter realizes the convolution operation it can be described by the relationships:

- in time domain

$$y(n) = h(n) * x(n) \tag{4.96}$$

- or in frequency domain

$$Y(k) = H(k) \cdot X(k) \tag{4.97}$$

The transmittance of a digital filter is described by the dependence

$$H(z) = \frac{Y(z)}{X(z)} = \frac{\sum_{k=0}^{N-1} a(k)z^{-k}}{1 + \sum_{k=1}^M b(k)z^{-k}} \tag{4.98}$$

The samples with coefficients $b(k)$ are the feedback samples, while the samples with coefficients $a(k)$ are the input samples. In the case of FIR filter the coefficients $b(k) = 0$ and the transmittance is expressed by:

$$H(z) = \sum_{k=0}^{N-1} a(k)z^{-k} = a_0 + a_1z^{-1} + a_2z^{-2} + \dots \quad (4.99)$$

or by the relationship

$$y(n) = \sum_{k=0}^{N-1} a(k)x(n-k) = a_0x(n) + a_1x(n-1) + a_2x(n-2) + \dots \quad (4.100)$$

The characteristic of the filter is explicitly described by its *impulse response* $h(n)$ called also the *filter kernel*. Therefore the sequence of coefficients $h(n)$ (or a and b coefficients in equations 4.98-4.100) are also called the *filter coefficients*.

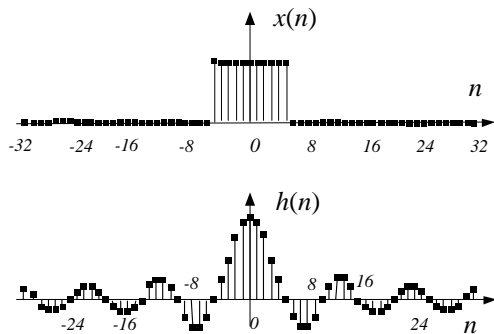


FIGURE 4.89 Rectangular window in time domain and corresponding signal in frequency domain.

In analysis of DFT presented in previous section it was observed that if we select the samples in the form of rectangular window the output signal was represented by the relation $X(k) \approx \text{sinc}x/x$. We can invert this relation and ask which time window of the input impulses of the filter guarantees that the output impulse sequence is represented by the rectangular window (thus close ideal output of the filter).

It can be expected if the pulse response form $\text{sinc}x/x$ relation than the response in the frequency domain is the same as the frequency response of the ideal filter. Due to limited number of samples in the impulse response we can only approximate the $\text{sinc}x/x$ relation. The higher the order of the digital filter, the better is the frequency characteristic (close to the rectangular

one). But even a large number of coefficients of the impulse response do not guarantee that the response is rectangular with the flat part in the pass-band. There are always oscillations in passband and stopband called *Gibbs phenomenon* (Figure 4.90).

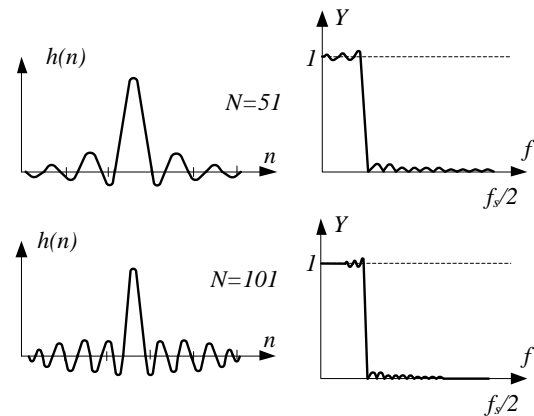


FIGURE 4.90 Impulse response and frequency output of the filter of 51 and 101 order (Lai 2004).

Similarly as in the case of DFT operation we can weaken of the effect of rectangular window by changing its shape (mainly borders). Various windows have been proposed - Blackman, Keiser, Chebyshev etc. Figure 4.91 presents an example of application of Blackman window.

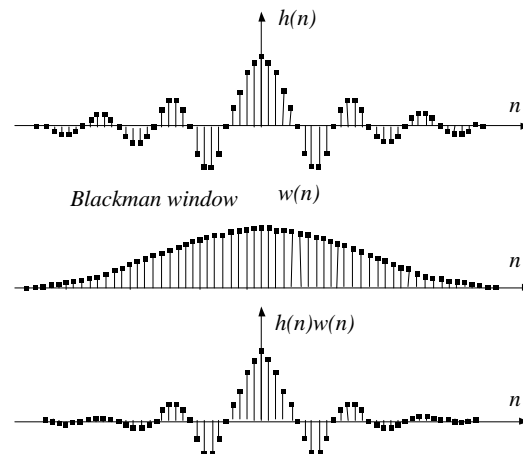


FIGURE 4.91 The impulse response of the filter with the Blackman window.

The application of the Blackman window decreases the ripples in the frequency characteristic, but at the expense of the steepness of this characteristic (Figures

4.92 and 4.93). Very useful are the Keiser and Chebyshev windows, because such windows enable shaping of the window by appropriate choice of the window coefficients.

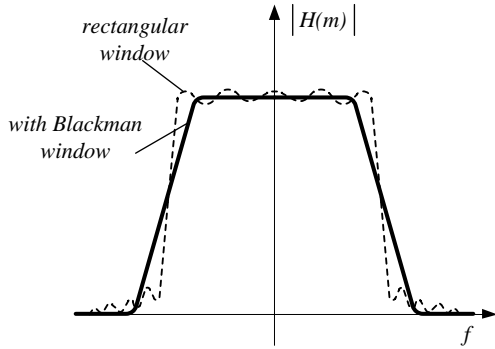


FIGURE 4.92 The transfer characteristic of the filter after applying of the Blackman Window [Lyons 2004].

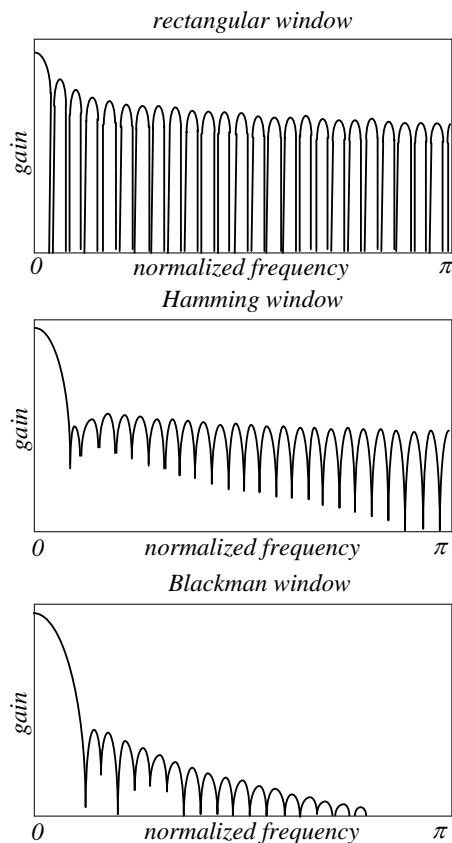


FIGURE 4.93 The gain response of the filters with various fixed windows [Mitra 2002].

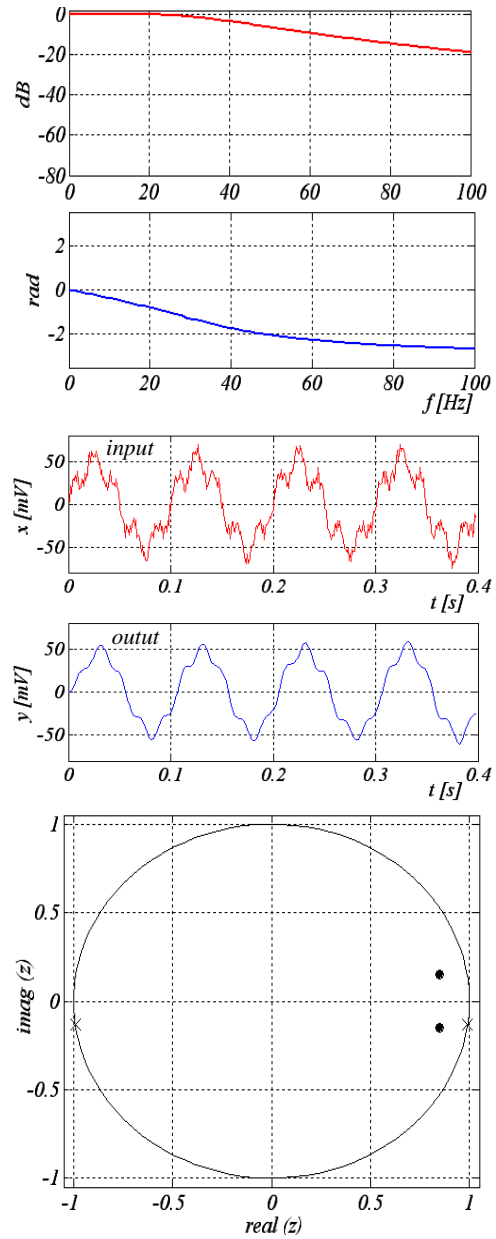


FIGURE 4.94 Design of 2nd order digital filter by Matlab tools (amplitude and phase characteristics, input and output signals, zeros and poles).

We can design of the digital filters considering all remarks presented in the Section devoted to analog filters. Thus we can design Butterworth, Bessel, Cauer or Chebyshev filyters. There are developed various methods of design of digital filters (Thede 2004, Winder 2002). Because procedures of design of analogue filters are very well developed, sometimes it

is reasonable to design an appropriate analogue filter and then to convert it into digital one. There are tools enabling conversion between analogue and digital techniques, for example the bilinear transformation from the s -plane to the z -plane

$$s = \frac{2}{T} \left(\frac{1 - z^{-1}}{1 + z^{-1}} \right) \quad (4.101)$$

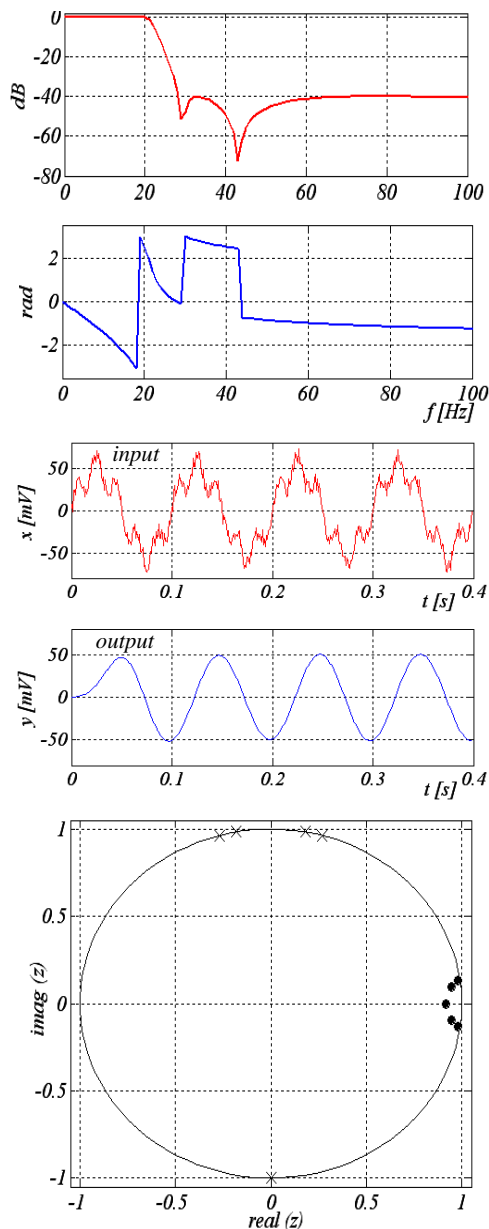


FIGURE 4.95 Design of 5th order digital filter by Matlab tools

On the market there are available professional software for filter design as well as free programs on the Internet. Also, programming platforms, like LabVIEW offer user-friendly tools for filter realization. Developed tools for filter design are also available in MatLab (Jackson 1995, Lutovac 2000).

Figures 4.94 and 4.95 present the examples of the digital filters design by using the Matlab tools¹². This design was performed for following assumption: useful signal 50 mV and 10 Hz, disturbed by interference 15 mV and 50 Hz and noise 10 mV. Sampling was performed with sampling frequency 1 kHz for 400 samples. We would like to design the FIR filter fulfilling conditions:

- distortion in pass-band less than 0.1 dB V_{pp} ,
- attenuation in stop-band better than 40 dB.

Assuming that as the filter we use the elliptic one to obtain values of coefficients a and b we can use the command $[B,A] = \text{ellip}[nf, rp, rs, fzn, low]$, where nf –s an order of the filter, rp is the level of ripples in the pass-band, rs is the attenuation of the stop-band, fzn is the cutoff frequency and low means that it is low-pass filter.

After calculation we obtain coefficients of the filter:

$$A = [1.000 \quad -4.765 \quad 9.106 \quad -8.724 \quad 4.190 \quad -0.807]$$

$$B = [0.003 \quad -0.010 \quad 0.007 \quad 0.007 \quad -0.010 \quad 0.003]$$

Poles of the filter are:

$$R = [-1, 00 \quad 0.96+i0.27 \quad 0.96 -i0.27 \quad 0.98+i0.18 \quad 0.98-i0.19]$$

thus all poles are inside the unit circle and the filter is stable.

Zeros of the filter are:

$$Z = [0.98+i0.13 \quad 0.98-i0.13 \quad 0.94=i0.09 \quad 0.94-i0.09 \quad 0.92]$$

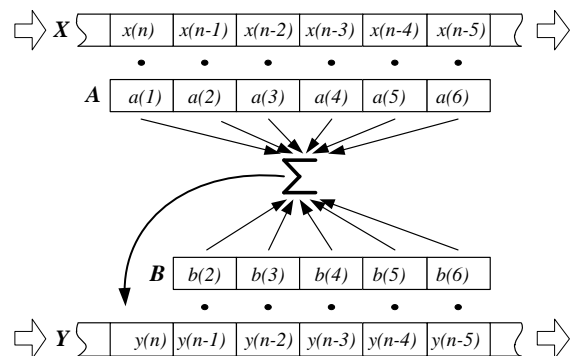


FIGURE 4.96 Algorithm of the operation of the filter.

¹² These examples have been prepared by Slawomir Baranowski.

The results of simulation are presented in Figures 4.94 and 4.95. The filter of the second order not sufficiently removes noise and distortion but the filter of fifth order is stable and effectively removes interferences.

The algorithm of the operation of the filter is presented in Figure 4.96. We have two registers with data coefficients and two moving registers with input and output data. It is necessary to multiply the appropriate coefficient by the data and next to add the results and write sample to output register.

Digital filters can be realized practically in all computers equipped with a data acquisition board. The *digital signal processors DSP* in comparison with usual microcontrollers are equipped with a special module MAC (multiplier/accumulator) suitable for digital filter realization. The manufacturers of DSP usually enclose suitable Application Notes enabling design of the digital filter – an example is Application Note No. SPRA669 published by Texas Instruments for digital signal processor TMS320C54x.

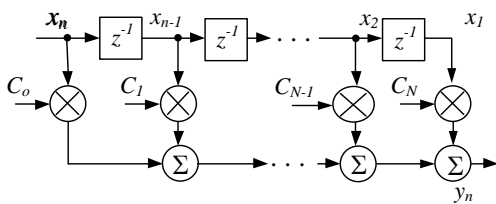


FIGURE 4.97
The mathematical operations in digital filtering process.

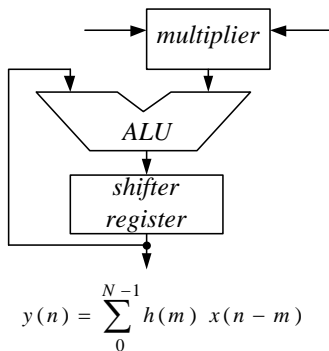


FIGURE 4.98
The CALU unit.

According to the circuit presented in Figure 4.97 it is necessary to perform operations:

$$y_n = (x_n \times C_0) + (x_{n-1} \times C_1) + \dots + (x_2 \times C_{N-1}) + (x_1 \times C_N) \quad (4.102)$$

Figure 4.98 presents the CALU module performing MAC operation (multiplication and summation) in one clock cycle. To perform such a filtering operation it is convenient to use a circular buffer in which newly acquired sample replaces the oldest sample in the memory (Figure 4.99).

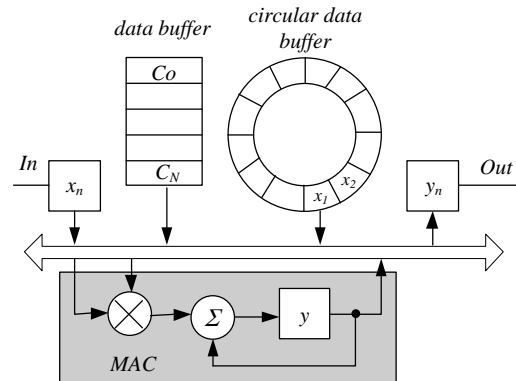


FIGURE 4.99
The filtering operation with MAC unit.

Figure 4.100 presents the comparison of analog and digital filters. Steven Smith (Smith 2003) has compared two low-pass filters: analogue six pole Chebyshev filter with 1 kHz cut-off frequency and digital filter with sampling frequency 10 kHz and 128 samples in the time window. The analogue filter was constructed using 3 op-amps, 12 resistors and 6 capacitors.

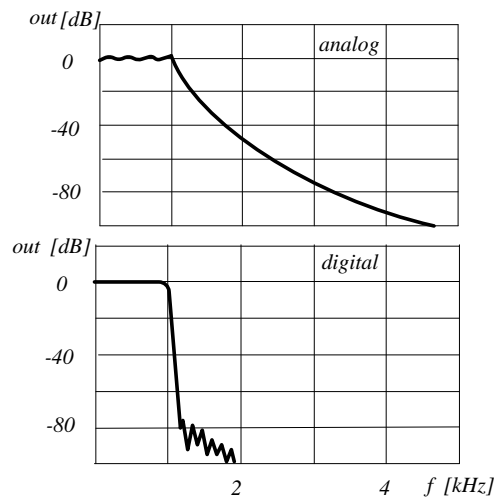


FIGURE 4.100
Comparison of frequency characteristics of analog and digital filters [Smith 2003]

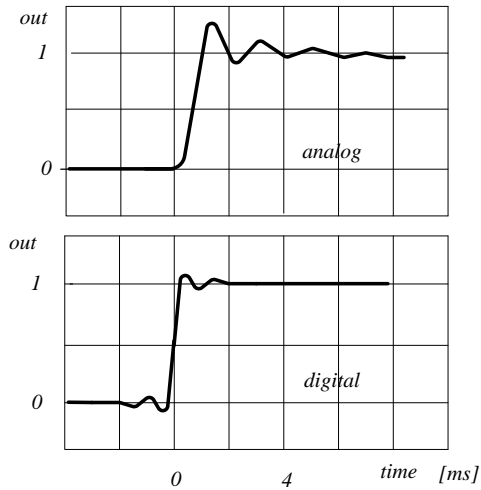


FIGURE 4.101
Comparison of time characteristics of analog and digital filters [Smith 2003]

The comparison of both filters without doubt indicated that the digital filter is much better. Its characteristic is flat in the pass-band while for the analogue filter 6% ripples are detected. In digital filter we can observe 100 dB attenuation of the signal in the transition band between 1 kHz and 2 kHz while in analogue filter such effect is for about 4.5 kHz. Also the time response of digital filter is more linear and with smaller overshoot.

However, in this comparison Smith also pointed out several advantages of the analogue filters. The first advantage is the speed – to obtain fast digital filter large sampling frequency is required while an analogue filter can operate without problems up to about 1 MHz.

Also the amplitude dynamics of the analogue filter can be better. In 12-bit ADC the quantization noise is 0.29 LSB for 4095 bits which results in dynamics of about $14 \cdot 10^3$. In comparison, the dynamics of a typical op-amp is about $10 \cdot 10^6$. The frequency range of an op-amp is between 0.01 Hz and 100 kHz which is about seven decades. To obtain the same frequency range in a digital filter for the sampling frequency 200 kHz it is necessary to process 20 million samples.

Important advantage of digital filters is possibility to change their parameters by software – practically in on-line mode. This possibility is used in special kind of filters – adaptive filters.

By applying digital filters it is possible to obtain much more complex transfer characteristics in comparison with analog filters. For example we can easily realize comb filters commonly used in digital TV

for separation of luminance and chrominance signal. An example of such filter is presented in Figure 4.102.

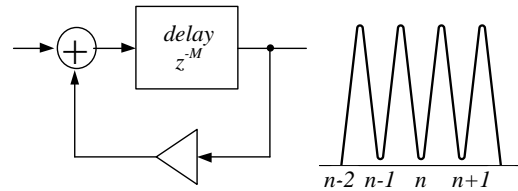


FIGURE 4.102
Digital comb filter.

Digital filters are commonly used to reject noises and interferences from the useful signal (see Figure 4.95). One of the most frequently used averaging digital filter is the moving average filter. This filter calculates the average value from the sample and M neighboring samples – it averages the samples in the window around the sample. Thus it performs the following operation

$$y(i) = \frac{1}{M} \sum_{j=0}^{M-1} x(i+j) \quad (4.103)$$

The value M can be selected that M previous samples or M next samples are used, but the best results are for the samples around the processed sample ($M/2$ previous samples and $M/2$ next samples). Figure 4.103 presents the examples of moving averaging results.

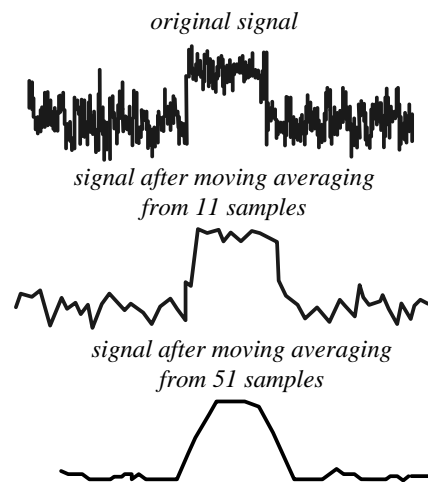


FIGURE 4.103
The rejection of noises by application of moving average filter (Smith 2003).

The averaging filters are very useful for the improvement of the images affected by noises. The moving average filter calculates the average value of the pixel and neighboring pixels, for example from the 3×3 area as demonstrated in Figure 4.104a. The area used for averaging can be of various values and shapes (not necessary the square one).

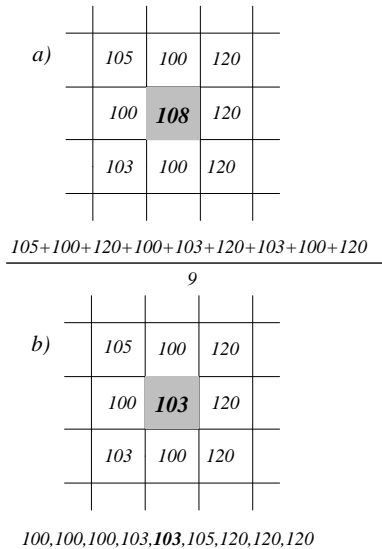


FIGURE 4.104
The principle of averaging (a) and median (b) filter.

Sometimes better results can be obtained with the *median filter*. The median value is a value calculated in such a way, that 50% of samples are larger than processed sample and 50% of samples are smaller. Practically, the median value is calculated as follows: the samples are ordered from smallest one to the largest, and next the central value is selected (Figure 4.104b).



FIGURE 4.105
The improvement of the image quality of the noisy picture (a) by applying of the median filter (b) (Young 1998) (permission of Ian T. Young)

The median value is more efficient in noise rejection because extreme values of the samples are rejected (in the case of average filter this samples influence the processed value). Moreover, the median filters in better way improve the sharp edges in the picture, while the average filters smooth the edges. Figure 4.105 presents two examples of the picture improvement after application of the appropriate filter.

Digital filters are especially useful in digital image processing. Most off tool available in programs as Photoshop use the digital filters.

4.7 Digital measuring instruments

As the digital measuring instrument we do not mean the instruments where the pointer is substituted by the digital display but the instrument where most of the operations of signal processing are performed digitally (Rathore 2004). In some areas digital measuring instruments have practically replaced analogue ones. For example portable, universal measuring instruments (Figure 4.106) are available everywhere with prices comparable to analogue ones but with performances much better. Similarly precise voltmeters, ammeters, ohmmeters (multimeters) have practically supplanted the analogue instruments.



FIGURE 4.106
An example of digital portable multimeter

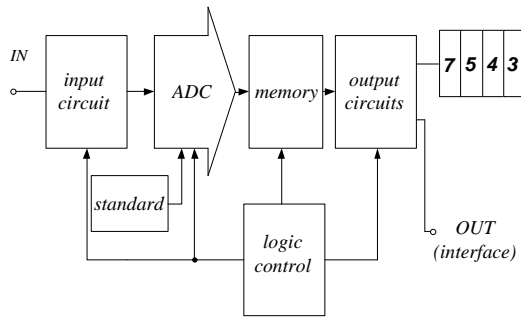


FIGURE 4.107
The functional block diagram of typical digital measuring instrument

Figure 4.107 presents the block diagram of a typical digital instrument. The input circuit contains the conditioning circuits: voltage dividers or amplifiers for measuring the voltage in various ranges, shunt resistors for current measurement, supply source for resistance measurement, DC/AC converters. The example of a typical input circuit of a digital multimeter is presented in Figure 4.108.

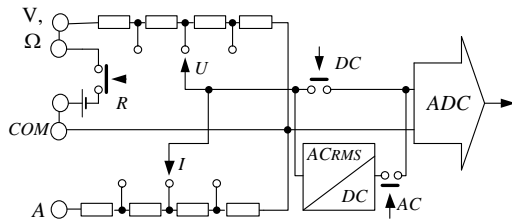


FIGURE 4.108
The input circuit of typical digital measuring instrument

Usually in the case of DC measurements the input circuit is separated by the capacitor. Therefore AC and DC measurements are performed separately and the resultant value is determined according to the formula (2.77). On certain instruments it is indicated (usually as "AC+DC") that it is possible to measure both components of the signal. To measure the AC values in the input circuit is inserted AC/DC converter. If this converter calculates the *rms* value of the AC input signal often such instrument is indicated as "True rms".

The logic circuit controls all functions of the instrument: automatic change of the input ranges (in certain instruments), triggering of the measuring cycle, control of ADC, saving the data into memory, etc. Sometimes the instrument saves a certain number of last measurement results and these data can be transmitted through available interface. More expensive measuring instruments are equipped with

Ethernet interface, cheaper ones with serial interface RS232 or USB. The interface enables not only to transmit the data to other external devices (including computer) but also allows controlling the instrument by the external computer system (for example change of the ranges or functions).

A group of manufacturers have developed a standard command set (language) facilitating the users to control the measuring process. The standard of commands is known as *SCPI – Standard Commands for Programmable Instruments*. It was assumed that this standard should be user friendly (written in the text mode) and can be delivered to the measuring instrument by any interface.

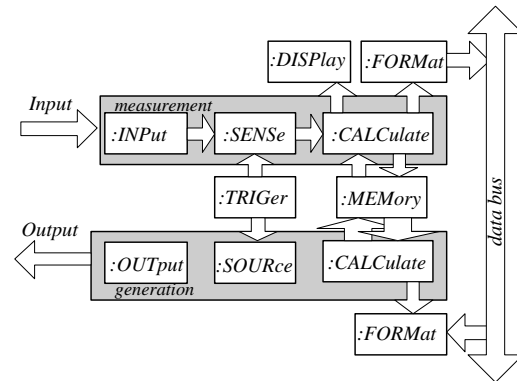


FIGURE 4.109
SCPI instrument model

The SCPI model of measuring instrument is presented in Figure 4.109. The inscriptions in each block describe most important operations:

- *INPut* command controls the signal conditioning: input impedance (:IMPedance), gain (:GAIN), filtering, attenuation or other input operations;
- *SENSe* command describes range, resolution, type of the signal;
- *CALCulate* describes processing of measured data, for example calculation of the *rms* value;
- *OUTput* command defines the parameters of the output signal;
- *SOURce* describes signal parameters, such as frequency, power, modulation;
- *TRIGger* determines the method of synchronization;
- *MEMory* manages the saving procedures;
- *DISPlay* describes the method of presentation of the data.

The structure of commands is hierarchical – the command is followed by the more detailed subcommand, as presented in Figure 4.110.

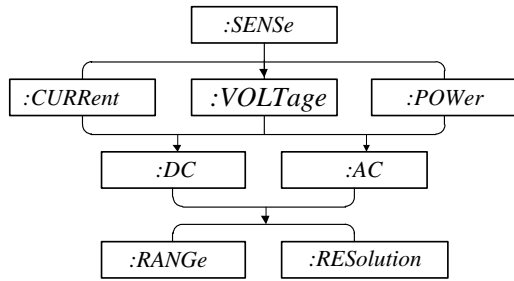


FIGURE 4.110
The example of hierarchical command tree

The commands are separated by colons. The blank space separates the parameter from the command and a semicolon separates commands within the same subsystem. For example the command

`SENS:VOLT:AC:RANG 5`

means the measurement of the AC voltage in the measuring range 5V. In the case of

`CONF:VOLT:DC 100,0.01; READ?`

the voltmeter is configured as the 100V DC voltmeter with resolution 0.01V and the result of the measurement is transferred to the buffer.

The braces enclose the parameter choice while the vertical bar separates multiple parameter choices, for example

`VOLT:DC:RANG {<range > |MIN|MAX}`

Most available measuring instruments are capable of receiving and processing the SCPI commands and detailed command syntax is described in the *User Guides* for each particular device.

Typically digital multimeters enable the measurements of voltage, current, resistance, often also frequency. Sometimes the measurement of capacity is possible as well. In very cheap instruments capacity is measured as the impedance – voltage drop on the tested capacity fed by alternating voltage. It is also possible to measure directly capacity. Figure 4.111 presents two examples of the input circuits designed for capacity measurement. In both circuits the measuring process is divided into two cycles: in the first one (switch in position 1) the measured capacitor is charged from the voltage source U_{ref} connected by the resistance R . In the second cycle (switch in position 2) the capacitor is discharged.

In the first circuit (Figure 4.111a) measured capacity is proportional to the charge Q and

$$C = \frac{Q}{U_{ref}} = \frac{\int_0^T i dt}{U_{ref}} \quad (4.104)$$

Thus in the output of the integrating circuit the signal is proportional to the measured capacity.

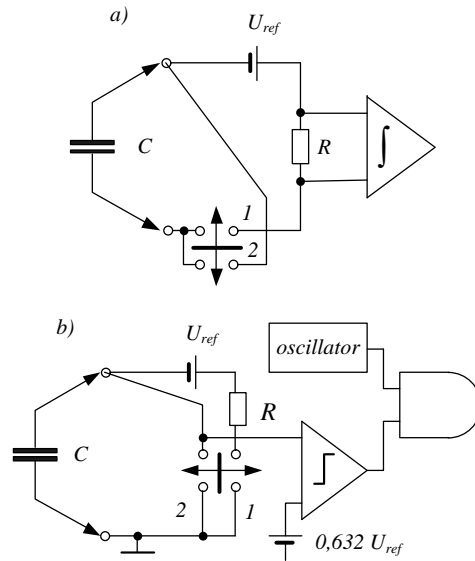


FIGURE 4.111
The example of input circuits for capacity conversion to voltage

In the second circuit (Figure 4.111b). 5.133b) the measured voltage across the capacitor increases exponentially

$$U_c = U_{ref} \left(1 - e^{-t/RC}\right) \quad (4.105)$$

After a time equal to the time constant $\tau = RC$ this voltage reaches value $0.632 U_{ref}$. If the voltage U_c is connected to the one input of the comparator and to the second input is connected to voltage $0.632 U_{ref}$ then the comparator closes the gate after the time equal to the time constant. Thus we obtain conversion of the measured capacity into the time period. If to the gate is connected to a reference oscillator the digital counter directly indicates the measured capacity.

Most of digital multimeters use the dual-slope converters because they use DC voltmeter and long time of conversion is no problem. Advantage of the dual-slope (integrating) converter is very high accuracy and resolution. Moreover this device is insensitive to the interference of frequency corresponding with

integrating time (most often it is 50 Hz interference). Recently dual-slope converters are often supplanted by delta-sigma converters.



FIGURE 4.112
The laboratory multimeter type HP 34401 of Agilent

Figure 4.112 presents one of the most popular digital multimeters, HP 34001 of Agilent. This instrument enables measurements of voltages, currents (both DC and AC), resistances and frequencies with uncertainty of about 0.004% DC and 0.1% AC. In the case of measurements of AC values the instrument operates as a DC voltmeter with AC rms/DC converter. It is also possible to determine a maximal (peak) value of the input signal.

Table 4.5 presents a comparison of typical performances of digital multimeters.

TABLE 4.5
The performances of typical portable, laboratory and precision multimeters.

Type	Portable	Laboratory	Precision
Model	179	34411	2002
Manufacturer	Fluke	Agilent	Keithley
Number of digits	3 3/4	6 1/2	8 1/2
Measure	V, I, R, C, F, T	V, I, R, C, f, T	V, I, R, f
Uncertainty DC [%]	0.09+2	0.0015+0.004	0.0006+0.00008
Uncertainty AC [%]	1+3	0.02+0.02	0.02+0.01
frequency bandwidth	45 Hz – 1 kHz	3 Hz – 300 kHz	1 Hz – 2 MHz
speed [rdg/s]		1000/s	2000/s
memory [rdg]		1 000 000	30 000
interface		LXI, GPIB, USB	GPIB

Another operating principle is used in the time/frequency measurements (electronic counters). Figure 4.113 presents the block diagrams of the frequency meters (Figure 4.113a) or period meters (Figure 4.113b). In the case of frequency meter the

triggering input circuit converts the measured signal to the rectangle waveform and starts counting. The signal of the standard quartz oscillator after frequency division opens the gate for a precisely set period of time. The number of pulses counted in this time period is a direct the measure of frequency.

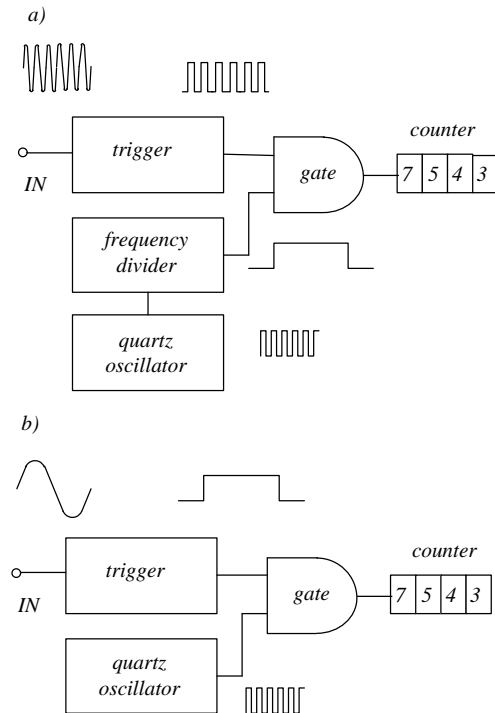


FIGURE 4.113
Digital measurement of the frequency (a) or period (b)

For the low frequency signal the gate should be open for a long time to obtain sufficient resolution (sufficient number of counts). Therefore, for low frequency signals it is better to substitute the frequency measurement by the period measurement. The input signals of the gate are reversed. The measured signal opens the gate for the period or multiple of periods. The pulses of standard oscillator are counted as the measure of the period. Typical frequency meters enable also to measure width of the pulse, phase shift and time.

General purpose digital multimeters measure voltage, current, resistance, frequency, sometimes capacity. To measure other electrical parameters as impedance, inductivity, power, energy it is necessary to use more specialized meters. On the market is available a huge number of various specialized digital measuring instruments of different performances and often with

not clearly explained principle of operation. For these measurements area available:

- impedance analyzers, RLC meters
- wattmeters, energy meters
- power quality analyzers,
- spectrum analyzers,
- sources of signals.

Often in such digital instruments the input circuit is analogue one and only A/D converter is added at the end. For example to detect electric power an analog multiplier can be used or for impedance analysis the synchronous detector is useful. Especially it is reasonable when we use introductory sensor with feedback. In fully digital instruments in such case would be necessary to use additional D/A converter (introducing additional inaccuracy) [Cerman and Ripka, 2003].

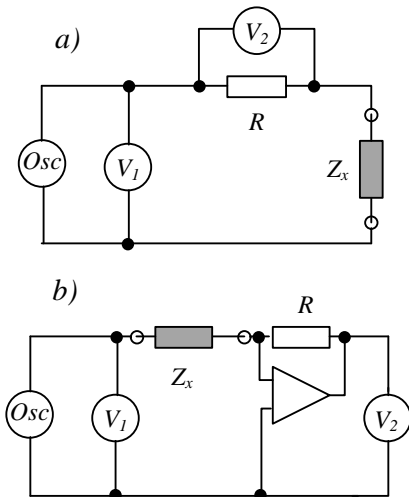


FIGURE 4.114 Two circuits for I-V method of impedance measurement

Due to complex procedure of obtaining the balance the bridge circuits earlier commonly used to impedance measurements are more often substituted by current/voltage I-V method (Figure 4.114). The voltage drops on the resistor R and impedance Z_x are measured and next the impedance is calculated:

$$Z_x = \frac{V_1}{V_2} R \tag{5.95}$$

To calculate ratio V_1/V_2 simply analogue multiplier can be used and next by using synchronous detector both components of impedance can be determined (by using as a reference voltage $V \sin \omega t$ and $V \cos \omega t$ signals).

Instead of using a voltage drop on resistance R the current-to-voltage converter can be used (Figure 4.114b). For high frequencies the current-to-voltage converter can be substituted by more sophisticated circuit consisting of phase detector and integrator [Agilent 2009].

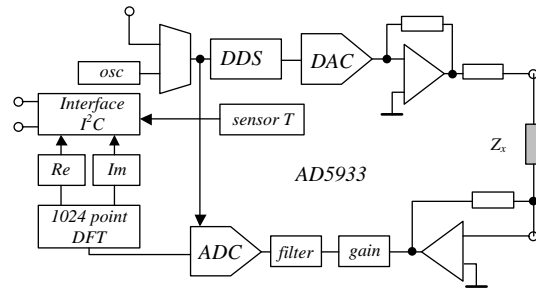


FIGURE 4.115 Digital impedance converter – model AD5933 of Analog Devices

Figure 4.115 presents fully digital impedance analyzer. The device under test DUT is fed by internal oscillator. Direct Digital Synthesis DDS technique enables to establish frequency with sub-Hertz precision. Signal from current-to-voltage amplifier is converted to digital form and next Discrete Fourier Transform DFT is calculated. Knowing voltage it is possible to determine both real and imaginary part of tested impedance:

$$\text{Magnitude} = \sqrt{\text{Re}^2 + \text{Im}^2} \tag{4.106a}$$

$$\text{Phase} = \tan^{-1} (\text{Im} / \text{Re}) \tag{4.106b}$$

The system accuracy is 0.5% in frequency range up to 100 kHz.

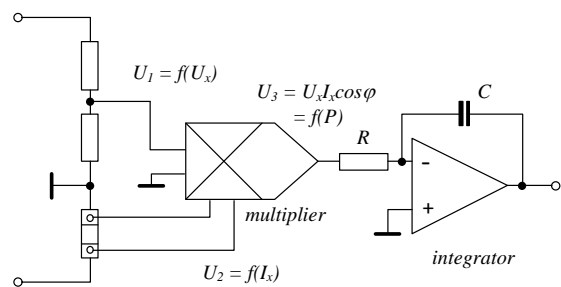


FIGURE 4.116 Power to voltage converter using the analog multiplier

Similarly in the power and energy measurements there are two strategies of digital measurement – hybrid one with analog multiplier connected to digital converter or fully digital. The first one uses power to voltage converters and next there are connected typical digital devices. Figure 4.116 presents the power-to-voltage converter using the analog multiplier device.

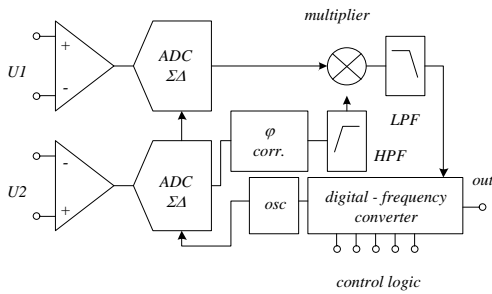


FIGURE 4.117
Power and energy converter – model ADE7757 of Analog Devices

Figure 4.117 presents the IC all-digital power and energy converter. Two input signals after analog-to-digital conversion (delta-sigma 16-bit 450 kHz) are digitally multiplied and at the output there is signal proportional to the power. The frequency output is adapted for electromechanical counters and 2-phase stepper motors. The uncertainty of conversion is 0.1% for power and 0.1° for phase.

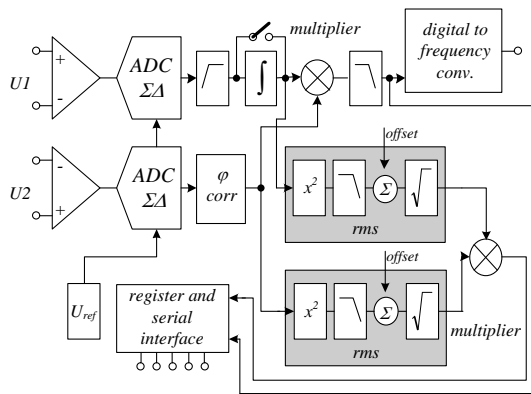


FIGURE 4.118
The active and apparent power and energy converter – model ADE7763 of Analog Devices

Figure 4.118 presents the enhanced version of IC energy and power converter. This circuit is supplemented by two rms converters and an additional multiplier. Due to this add-on elements it is possible to determine also apparent power and energy (VA power),

as well as rms values of current and voltage. It is also possible to determine the period (frequency) of the voltage signal. The circuit is equipped with two outputs – the frequency one for energy counters and a serial one for communication with computer measuring systems.

An interesting extra element is the integrator in one of the channels. This integrator enables the converter to cooperate with inductive sensor of current (for example Rogowski coil) where the output signal is proportional to di/dt .

In XXI century started new technology of generation, transmission and distribution of electrical power known as *smart grid* [Massoud Amin and Wollenberg 2005, Akanayake *et al* 2012, Momoh 2012]. In smart grid technology the power distribution is controlled and managed in intelligent way using computer tools. Of course to introduce such technology the new measuring devices are indispensable. To control and analyze of power quality are now commonly used *power quality analyzers*. In consumers area the old induction type watt-meters are now not acceptable because it is not possible to read and transmit information about power and energy consumption. Electromechanical energy meters are now substituted by computerized *smart meters*.



FIGURE 4.119
An example of the power quality analyzer – three phase energy and power quality analyzer model 437 of Fluke (permission of Fluke Company)

Figure 4.119 presents an example of the power quality analyzer developed by Fluke. This instrument

enables to measure and register main parameters as voltage, current, power (active and reactive), phase shift, distortion, crest factor, waveforms etc. But moreover it investigates and stores information about all important events as flickers, dips and swells of voltage. Figure 4.120 present an example of screen with bar presentation of monitoring of rms voltage, distortion, flickers, dips, interruptions, rapid changes, swells, unbalance and frequency.

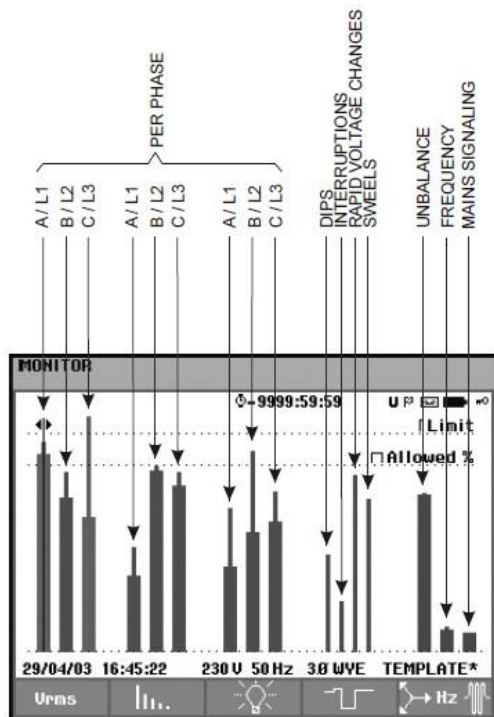


FIGURE 4.120 An example of the screen with power quality monitoring

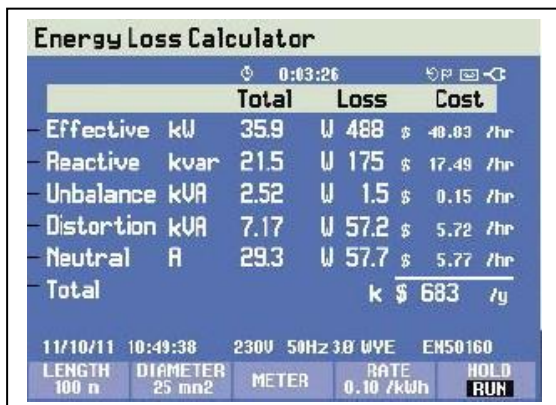


FIGURE 4.120 An example of the screen with loss calculation

It is also possible to analyze the measured data – Figure 4.121 presents an example of intelligent energy loss calculator analyzing wasted kilowatt hours per year.



FIGURE 4.122 An example of smart meter instrument (permission of Efergy)

The full introduction of smart meters it is a very complex operation taking into account the number of devices to replacements and problems of development of communication infrastructure. It is expected that till 2020 most of energy consumers should use such meters. The main difference of smart meters in comparison with other digital energy meters is the possibility to gathering and remote reporting the data to central system of delivery of the energy. Also the private consumer is able to analyze energy consumption as it is presented in Figure 4.122.

4.8 Digital synthesis – source of signals

Digital signal processing used for analysis of the signals can be also used for the synthesis of the signal. The most important development of this technique is visible in high quality sound processing. Most of the audio components are equipped with *digital sound processor DSP* enabling sophisticated processing of the sound (for example supplementing the sound with artificial reverberation). On the market there are available various sound synthetizers. Most personal computers are equipped with a sound board or a chip enabling the software processing and creating of the sound.

There are also available digital instruments for numerically controlled signal generation. Recently, the most popular are three systems: *PLL – phase locked*

loop, DDS – direct digital synthesis and AWG – arbitrary wave generators.

The PLL system is used for very accurate control of frequency of the generated signal. It is used in radio communication systems (including radio broadcasting) as very precise tuned generator.

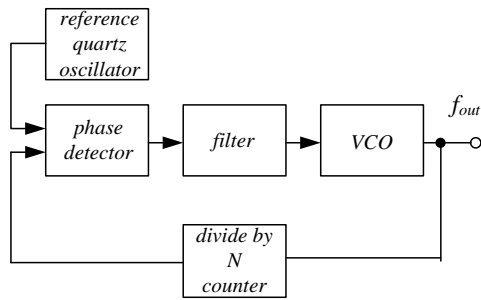


FIGURE 4.123 The principle of PLL frequency synthesis

The principle of the PLL synthesis is presented in Figure 4.123. The output signal f_{out} is compared with precise frequency of the quartz oscillator f_{ref} . As the comparing device the phase frequency detector PFD is used to convert the difference of frequencies to the voltage. This voltage is used to control the voltage controlled oscillator VCO. The value of the output frequency is set by the change of parameters of the frequency divider. The precise setting of the output frequency is guaranteed by the feedback.

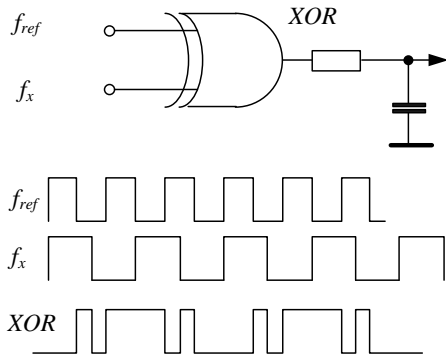


FIGURE 4.124 The example of PFD device

As the simplest phase-frequency detector a XOR type gate can be used – in such a gate the output signal is equal to zero when both inputs are the same (Figure 4.124). In PLL systems also more sophisticated PFD circuits are used, so called PFD type II modules, in

which the output signal is proportional to the phase shift between slopes of two impulses. Usually, an oscillator with the varicap type diode is used as the voltage controlled oscillator. An example of the VCO circuit is presented in Figure 3,37.

There are available integrated circuits of VCO devices as well as the whole PLL systems. As an example in Figure 4.125 is presented the PLL circuit type CD4046 of Texas Instruments. This device can work as the PLL oscillator and as a voltage controlled oscillator.

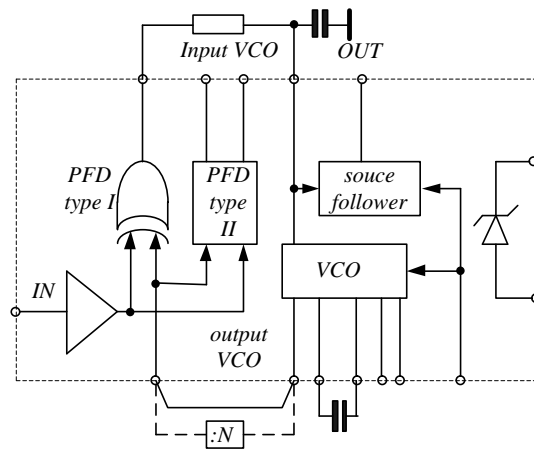


FIGURE 4.125 The example of PLL device – model CD4046 of Texas Instruments

The PLL synthesis is performed in the frequency domain. It is also possible to perform the signal synthesis in the time domain by the DDS system. The direct digital synthesis enables to generate the signal with synthesis of the frequency as well of the wave shape. The principle of operation of DDS system is presented in Figure 4.126.

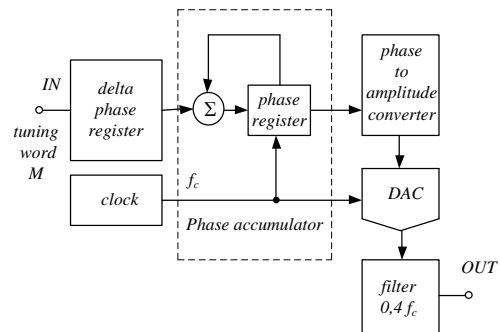


FIGURE 4.126 The principle operation of the DDS synthesis

The DDS system generates the sine wave with the frequency depending on the clock frequency and binary number – *tuning word* M at the input. To generate a fixed frequency sine wave phase increment, which is determined by tuning word, is added to the phase accumulator with each clock cycle.

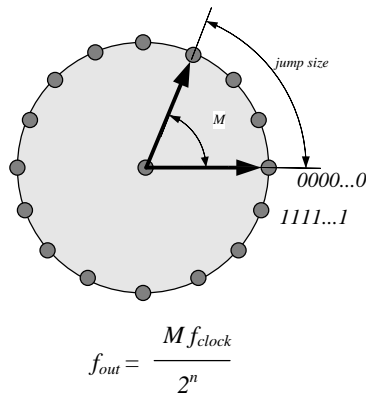


FIGURE 4.127
The phase circle of the DDS system

The phase accumulator acts as a phase wheel presented in Figure 4.127. The sine-wave oscillation can be considered as the vector rotation around the phase circle and each point of the circle corresponds to equivalent point of the wave. One revolution of the vector around the phase wheel means the full sine wave cycle. In the n -bit accumulator the wheel can be divided into 2^n points. Thus for 32-bit register we obtain the resolution of phase equal to 4 294 967 296 points around the wheel.

In the phase accumulator with every pulse of the clock generator the pointer in the wheel is moved by the binary coded input word M . The output frequency is determined by the M word (see Figure 4.127).

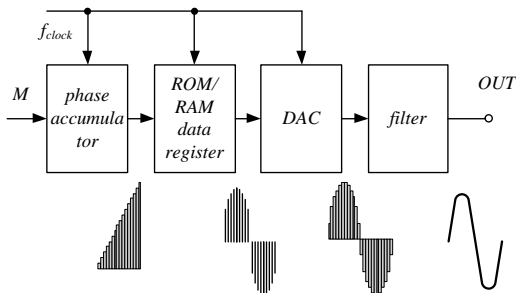


FIGURE 4.128
The signal synthesis in the DDS system

The amplitude of the output signal is formed by the phase to amplitude converter related to the data registered in the RAM memory (Figure 4.128).

The *arbitrary wave generator* AWG is often used as the source of signals of precise adjusted frequency, phase and amplitude waveform. The principle of operation of AWG is presented in Figure 4.129. The user stores the waveform data in the memory and according to the clock signal desired signal is then reconstructed sample by sample and transferred to the DAC.

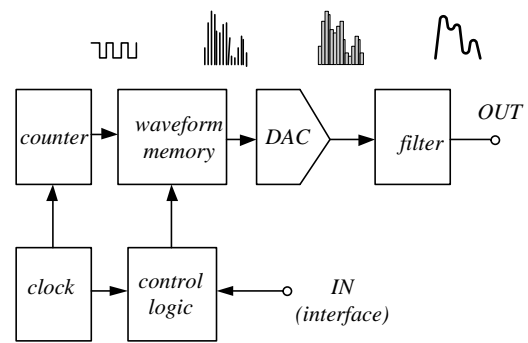


FIGURE 4.129
The principle of operation of the arbitrary wave generator

Also the DDS system can operate as the waveform generator. An example of the arbitrary wave generator utilizing the direct digital synthesis DDS is presented in Figure 4.130.

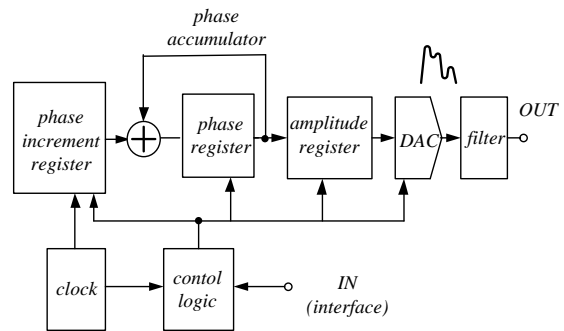


FIGURE 4.130
The DDS system used as the arbitrary wave generator

The arbitrary wave signal is programmable and can be realized from device memory as well as from an external device or computer via a suitable interface.

4.9 Digital storage oscilloscopes DSO

The first oscilloscopes were introduced more than hundred years ago by Ferdinand Braun¹³ in 1897. And until now, these instruments are one of the most important tools in engineering and scientific research. And more – with the era digital instruments many new possibilities appeared.

Modern digital oscilloscopes allow not only displaying the signals, but also recording, analyzing them (for example performing of the spectral analysis) and also appreciating measurements of the signals (Kularatna 2003). LCD digital instruments practically replaced old analog *cathode ray tube CRT* oscilloscopes (also called *cathode ray oscilloscopes CRO*).

If the frequency of the signal is larger than several Hz due to the inertia of our eyesight it is not possible to see such picture of the signal. Therefore the main function of the oscilloscope is to somehow stop the picture on the screen. Due to *trigger function* the oscilloscope instrument creates the illusion that the picture is standing still. We say that the investigated signal is *synchronized* with the frequency of horizontal movement.

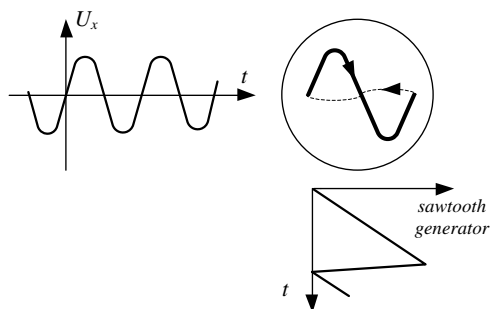


FIGURE 4.131
The principle of displaying of the signal in analog oscilloscope

Figure 4.131 illustrates the principle of displaying the signal in analog oscilloscope. The picture on the screen is obtained in such a way that during the horizontal movement the luminous point is deflected vertically proportionally to the value of the detected signal. The horizontal movement is obtained by the sweep oscillator generating a sawtooth signal (Figure 4.131). If the period of oscillation of the sawtooth signal is the same (or multiple) as the period of investigated signal the successive pictures appear to be the same. This creates the illusion that the picture is

standing still. Of course during their return path the moving point is nonvisible

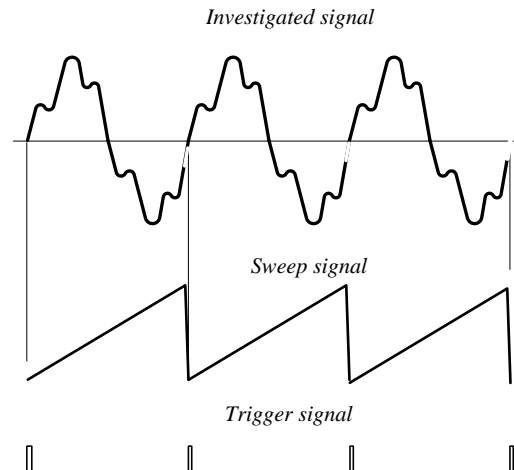


FIGURE 4.132
The principle of synchronization of the tested signal with period of the horizontal movement in analog oscilloscope

Figure 4.132 presents the principle of synchronization of the investigated signal. The sawtooth voltage is initiated by the pulse from triggering system. In the simplest case of the automatic trigger mode this start can occur for the zero value of signal – it is important to start every time in precisely defined point of signal, because only in such case we can obtain standing picture on the screen.

Of course it is possible to set manually the moment of triggering – for example for defined value or for rising or falling slope (trigger level and trigger slope). This moment of start can be observed directly on the screen as the initial point of the signal. The user can manually change the frequency of time base in order to observe one or more periods of investigated signal.

Synchronization is rather easy when the investigated signal is periodical – it is sufficient if the period of horizontal movement is the same or multiple of the period of investigated signal and start of horizontal movement is still for the same point of investigated signal (in most of oscilloscopes is button known as AutoScale).

More complex is the case when investigated signal is periodical but with short pulse time in comparison with the period time of the whole signal (Figure 4.133a) or when it is a single pulse (Figure 4.133b). In such case the trigger mode of synchronization is very helpful. The trigger circuit is connected to the source of trigger signal – this can be either internal or external source. The sweep generator controlled by trigger system starts

¹³ Braun was awarded the Nobel Prize in Physics in 1909 with Marconi for wireless telegraphy.

exactly in defined point, often in initial point of the investigated signal. It is possible to set additionally the hold-off time when the trigger system does not start again. The triggering mode can be periodical (for example in the case presented in Figure 4.133a) or a single sweep mode (single event mode) - for example in the case presented in Figure 4.133b.

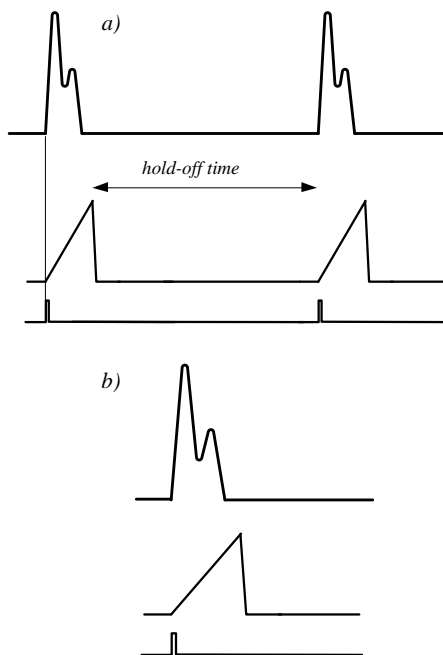


FIGURE 4.133
The triggering of pulse signals – periodic pulses (a) and single pulse (b)

In the single event mode the sawtooth signal is composed from only one tooth – this means that the luminous spot is traveling through the screen horizontally only once. This mode is very convenient to observe non-periodical signals, for example single pulses.

In the case of digital storage oscilloscopes it is not necessary to generate sawtooth signal to force horizontal movement – this movement is governed by clock signal. Moreover signal is sampled, converted by ADC and transmitted to memory as a record of certain number of samples. This record is next processed by microcontroller into the picture. Thus we can trigger start point off-line in any sample of the collected signal. But principle of synchronization is the same – if we demand to obtain stable picture the start point and frequency of horizontal movement should be adjusted to the investigated signal.

Modern oscilloscopes offer many quite sophisticated modes of triggering – not only slope and level but by well-defined event: glitch, pulse width or start bit of frame in serial interface signal.

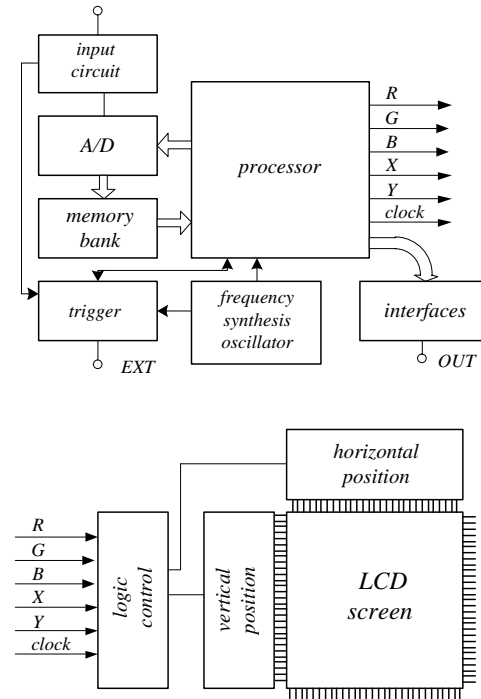


FIGURE 4.134
Block diagram of typical digital oscilloscope)

Figure 4.134 presents the block diagram of a typical digital oscilloscope. We can notice in this diagram similar functions as were present in the analog instruments: triggering circuit and horizontal/vertical position logic. Although there are significant differences of the operation principle of digital and analog oscilloscope, the manufactures take into account certain tradition and equip the digital instrument with very similar functions as were in the analogue instruments.

The main difference between the digital and analog oscilloscope results from storage of data after acquisition. We can process signal saved in memory, we can present it on the screen in any moment (not only in real-time). It does not mean that digital oscilloscopes are fully off-line devices – process of acquisition is very fast, often thousands times per second.

The storage function enables not only simple recording and reproduction of signals, due to the digital processing oscilloscopes are equipped with various

additional functions, such as FFT analysis, averaging function, integration of the signal, measurement of the value and frequency of the signal, etc (Hickman 1997, Kularatna 2003).

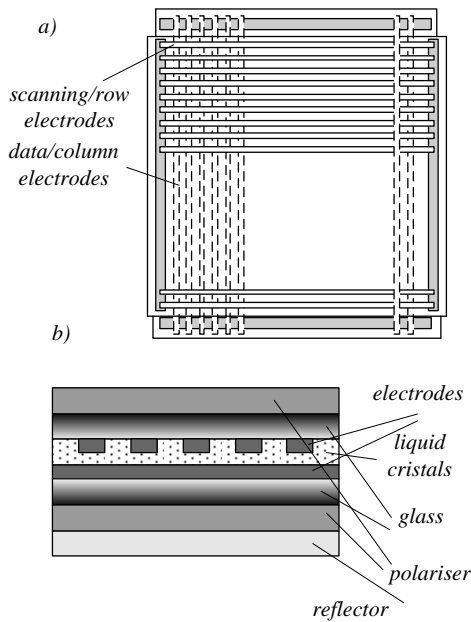


FIGURE 4.135 Planar (a) and cross-sectional view (b) of matrix addressed in LCD [Sarua 2004]

Figure 4.135 presents the design of typical LCD screen used in digital oscilloscopes. Liquid crystal material consists of rod shaped molecules that can be ordered by electrostatic field. The display is divided in small areas called pixels, each of which is driven by an individual electrode. Pixels are organized in the matrix with scanning/row electrodes for horizontal movement control and data/column electrodes for vertical movement control. In the simplest case these electrodes are driven in passive way, but to obtain better parameters the *Active Matrix Addressing AMLCD* is used. In the active system each pixel is driven by thin film transistor *TFT* connected to two capacitors for voltage storage. If a system of filter is added, then it is possible to obtain colored LCD monitor.

Figure 4.136 presents the example of the screen of digital oscilloscope. It is important for user that every time this picture can be sent to printer or saved as a graphic file. Important advantage is that easy it is possible to obtain multicolor picture of investigated signals. Beside the picture of the signals part of the screen is reserved for presentation of data, as for example horizontal and vertical scale.

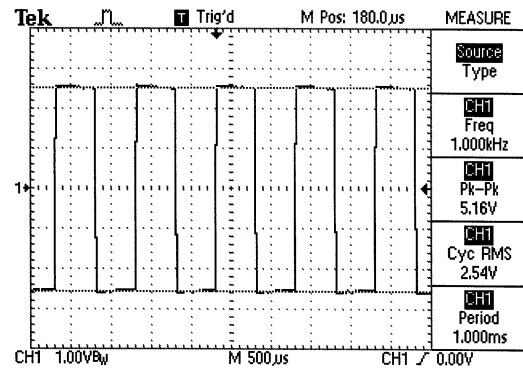


FIGURE 4.136 The sample of the screen of digital oscilloscope

In digital sampling oscilloscope every column in the screen can be represented by a sample (the position in the column by value of the signal). The simplest way to obtain such picture is to convert investigated signal into the set of samples according to the clock impulses (Figure 4.137). This kind of sampling is called *sequential sampling*. We can save this sampling result in memory and then reproduce the signal “sample by sample” on the screen.

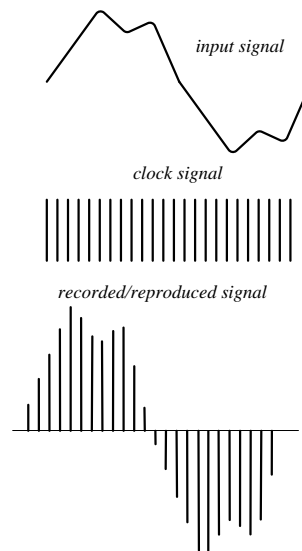


FIGURE 4.137 The signal before and after sequential sampling

In the input circuit apart from conventional attenuators/amplifiers there should be inserted a sample-and-hold circuit and an anti-alias filter. This filter is very important, because if the frequency of sampling is too small due to the aliasing effect the

processor can fit to the sample an incorrect signal (as illustrated in Figure 4.138). The observer will see the signal of other frequency than frequency of correct signal (continuous and dashed lines in Figure 4.138).

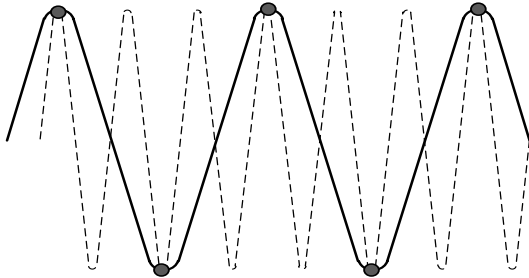


FIGURE 4.138
The aliasing effect in digital oscilloscope

One of the important problems of digital oscilloscopes is a presence of a dead (blind) time zone. If some event, for example very short pulse appears between the samples it can be not detected or detected in false way. Figure 4.139 presents the signal interpretation for two different positions of the rise slope. Depending on the pulse placement (with respect to the sampling pulses) we can obtain various results – for the pulse *a* we approximate the slope by the *A* line, while for the pulse *b* by the *B* line.

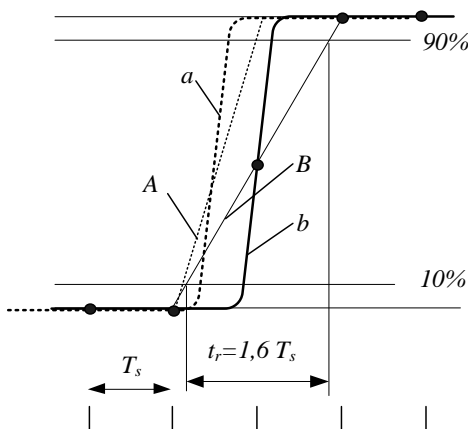


FIGURE 4.139
The interpretation of short pulse

Placement of pulse *b* exactly in the same time as the sampling pulse results in the interpretation of the rise time as the $1.6 T_s$. This is the most disadvantageous case. Thus the shortest detectable rise time is

$$t_r = 1.6 \cdot T_s = \frac{1.6}{f_s} \quad (4.107)$$

Thus it is obvious that to obtain short dead zone the sampling frequency should be as high as possible. Microcontroller is also used to perform interpolation of detected signal from the samples. We can say that the higher the sampling frequency the easier it is to reconstruct the signal because we have more samples. It is assumed that the *useful storage bandwidth USB* depends on the sampling frequency

$$USB = \frac{f_s}{C} \quad (4.108)$$

where $C = 2.5 - 25$ is the coefficient depending on the method of wave interpolation. When we do not interpolate the wave (the shape is reconstructed from the sampled points) the coefficient $C = 25$. When the points are connected by line (linear interpolation) it is assumed that $C = 10$ guarantee correct reconstruction. When we interpolate the sampling results by the sine wave, $C = 2.5$ is sufficient. But we can use the sine interpolation only when we are sure that the investigated signal is close to a sine wave (for the rectangle pulses the error of sine wave interpolation can be significant).

Thus in digital oscilloscopes the sampling frequency is a very crucial parameter to obtain satisfying performances. But from chapter 4.2 results that the fastest analog-to-digital converters have the sampling frequency not higher than 1.5 GHz¹⁴. In the meantime signals of modern technique exceed frequency 20 GHz. And such requirements are fulfilled – the best oscilloscope of Tektronix model DSA73304D exhibits frequency bandwidth as high as 33 GHz and time rise 9 ps with sampling frequency 50 GS/s – 1TS/s (!)¹⁵.

There are certain tricks enabling to obtain such high sampling frequency of ADC. First of all in analog to digital converters there are two time consuming processes – sampling and quantization. In digital oscilloscopes these both processes can be performed separately – sampling rate can be very high, the record can be transmitted to memory and next more slowly converted to digit.

Another commonly used technique is increasing the number of samples by *multiple-point random sampling* (or random equivalent time sampling) in which the

¹⁴ The fastest 6 Bit ADC of Rockwell Scientific model RAD008 enables sampling with frequency 4 Gb/s.

¹⁵ Similarly Agilent oscilloscope model DSAX96204Q exhibits frequency bandwidth 63 GHz with sampling rate 160 GS/s.

same signal is sampled several times with randomly shifted samples (Figure 4.140). In such technique very important is to reference the sampled wave to the trigger point. In this technique instead of one AD converter for sampling the dozen parallel connected converters can be used.

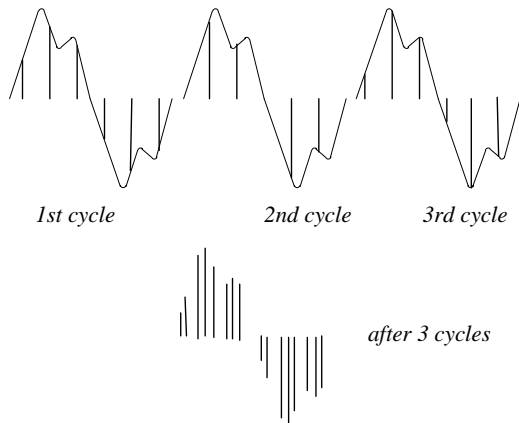


FIGURE 4.140
Random equivalent time sampling technique enabling increase of the effective sampling rate

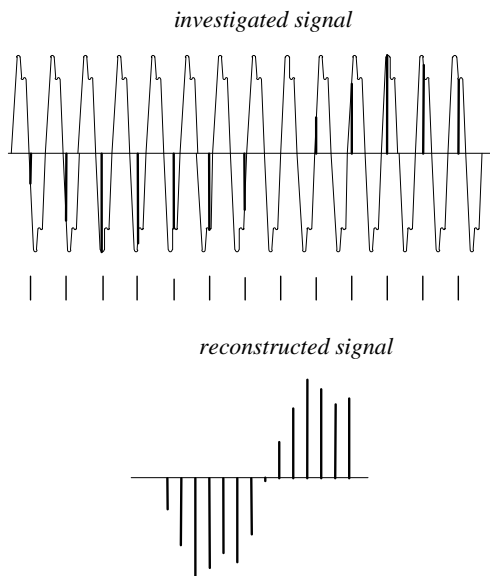


FIGURE 4.141
Sequential equivalent time sampling technique enabling reconstruction of periodic signal for small number of samples (per period)

Another technique enabling signal reconstruction even for one sample per period (below Nyquist-Shanon requirements), known as *sequential equivalent time sampling* is presented in Figure 4.141. Every trigger pulse is shifted by precise fixed time increment versus

previous pulse. In this way each time other point of signal is sampled. Knowing the time increment it is possible to reconstruct the signal. This method can be used only for periodic signals.

Very high frequency bandwidth can be obtained in special oscilloscopes known as *Digital Sampling Oscilloscopes*. In these oscilloscopes the position of attenuator/amplifier and ADC are reversed – the investigated signal is first connected to analog to digital converter. In this way to amplifier is connected signal of much lower frequency than input signal. Of course such oscilloscopes have limited value of input signal.

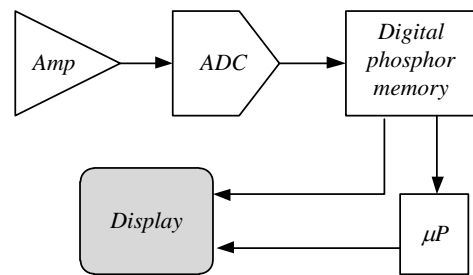


FIGURE 4.142
The parallel processing of the signal in Digital Phosphor Oscilloscope

The dead zone can be significantly decreased by increase of the *waveform capture ratio* expressed by number of acquired records per second. To increase this parameter to even thousand per second the special architecture known as Digital Phosphor Oscilloscope was developed. In this oscilloscope (Figure 4.142) the signal is bypassing the microprocessor. This way the snapshots of the signal are sent directly to the display without stopping the acquisition. The observer obtains on the screen “normally” processed signal of higher light intensity and parallel sent signals of lower color intensity. The name of this oscilloscope refers to the analog chemical phosphor luminance of prolonged time of lighting (afterglow). This way displayed signal is three-dimensional: time, amplitude and history (distribution even single random short events in time).

Oscilloscopes are not just tools designed for observation the signals. The setting parameters *time base* and *vertical deflection* are scaled in *sec/div* or *volts/div*, respectively. Thus it is easy to calculate the value of the signal (for example the value of magnitude) or value of the time (for example to determine the phase shift between two signals or frequency of the signal). Thus the oscilloscope is a complete measuring device, especially valuable in the high frequency range. Moreover modern oscilloscopes can directly indicate most important parameters of the signal.

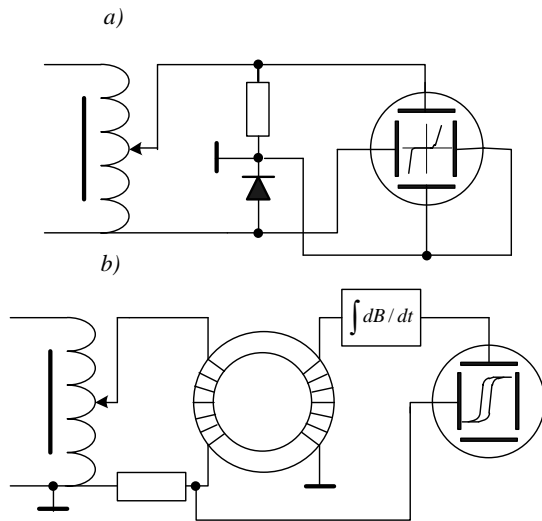


FIGURE 4.143
The XY mode of operation of oscilloscope used for: determination of the diode characteristic (a) or for determination of the hysteresis loop (b)

Usually the oscilloscope displays the time varying signals, thus the horizontal axis is the time axis. But it is also possible to connect another signal to the horizontal deflection system. In such mode of operation we can display on the screen the function $Y=f(X)$. Figure 4.143 presents two examples of X-Y operation. In the first example, the signal proportional to the current (voltage drop on the resistor) is applied to the vertical axis while the signal proportional to the voltage on the diode is connected to the horizontal axis. Thus we obtain the characteristic $I=f(U)$ of the diode on the screen of oscilloscope.

The second example (Figure 4.143b) illustrates the possibility of investigating the hysteresis loop ($B-H$ loop). To the horizontal axis the signal proportional to the magnetic field strength (that is proportional to the magnetizing current) is connected while to the vertical axis the signal proportional to the flux density (the voltage E induced in the winding after integration, because $E = f(dB/dt)$) is used. Thus we can observe the $B=f(H)$ loop on the screen.

Figure 4.144 presents typical digital oscilloscope. On the front panel are visible typical switches and buttons for acquisition channels, for time base and for trigger part. Usually digital oscilloscopes use extended screen menu. Even very sophisticated devices can be not very large.



FIGURE 4.144
The example of typical digital oscilloscope

The LCD screen enables to construct even portable, battery fed oscilloscopes. Very useful solution is to joint both function – oscilloscope and digital multimeter in one device – as it is presented in Figure 4.145.



FIGURE 4.145
The portable instrument joining function of multimeter and oscilloscope – Scopemeter of Fluke (permission of the Fluke Corporation)

Recently it is possible to design even very complex digital instruments by applying data acquisition board DAS and commonly available software, as for example LabView. Thus the market of manufacture prepared instruments has alternative. But there are some advantages of commercially available measuring

devices. In the case of digital oscilloscopes especially for high frequency important is also appliance – exclusively prepared probes, high frequency resistors in the input attenuator or specifically designed AD converters.

Commercially available digital measuring instruments, as for example multimeters usually have certificate with detailed described and guarantee accuracy. In the case of self-made instruments, we can also estimate accuracy taking into account the accuracy of data acquisition board DAS but in the case of problems or conflicts with customer only certificate of reputable manufacturer is really valid.

References

- AD8551 – The data sheet of the AN 8551 amplifier of Analog Devices
- Agilent impedance measurement handbook, 2009
- Antoniou A. 2005 Digital Signal Processing, McGraw-Hill
- Bauch A., 2003, Caesium atomic clocks: functions, performances and applications, Meas. Sc. Technol., 14, 1159-1173
- Bez S.P., Hamilton C.A., 2004, Application of the Josephson effect to voltage metrology, Proc IEEE, 92, 1617-1629
- Bovik A., 2000, Handbook of image and video processing, Academic Press
- Bracewell R.N. 1999 The Fourier Transforms and its Applications, McGraw-Hill Science
- Candy J.C., Temes G.C. 1991 Oversampling Delta Sigma Data Conversion, Wiley & Sons
- Cerman A, Ripka P, 2003, Towards fully digital magnetometer, Sens. Act., A106, 34-37
- Chevtchenko O.A., et al, 2005, Realization of a quantum standard for AC voltage: overview of a European Research Project, IEEE Trans. Instr. Meas., 54, No.2, 628-631
- Chu E., George A., 2000, Inside the FFT black box, CTC Press
- Coughlin R.F., Driscoll F.F. 2000 Operational Amplifiers and Linear Integrated Circuits, Prentice Hall
- Coley J.W., Tukey J.W. 1965 An Algorithm for the Machine Calculation of Complex Fourier Series, Math. Computation, 19, pp. 297-301
- Czyzewski A. 1998 Digital Sound (in Polish), Exit
- Deziel J.P. 2000 Applied Digital Signal Processing, Prentice Hall
- Duff M., Towey J., 2010, Two ways to measure temperature using thermocouples feature simplicity, accuracy and flexibility, Analog Dialogue, 44-10, 1-6
- Gilbert B., 1975, Translinear circuits: a proposed classification, Electron. Lett. 11, 14-16
- Guy C. Ffytche D., 2005, A introduction of the principles of medical imaging, Imperial College Press
- Ekanayake von J., Jenkins N., Liyange K., Wu Jianzhong, Smart grid: technology and applications, John Wiley & Sons
- Fraden J., 2003, Handbook of modern sensors, Springer
- Franco S. 2001 Design with Operational Amplifiers and Analog Integrated Circuits, McGraw-Hill
- Hagel R., Zakrzewski J., 1984, Dynamic measurements (in Polish), WNT
- Hamilton C.A., Burroughs J., Benz S.P., 1997, Josephson voltage standard – a review, IEEE Trans. Appl. Superconductivity, 7, 3756-3761
- Hickman I., 1997, Digital Storage Oscilloscopes, Newnes
- Huelsman L.P. 1993 Active and Passive Filter Design, McGraw-Hill
- Jackson L.B. 1995 Digital Filter and Signal Processing with Matlab Exercises, Springer
- Jähne B., 2004, Practical handbook of image processing for scientific and technical applications, CRC Press
- Jamal R., Steer R. 2003 Filters, Chapter 22 in Electrical Measurements, Signal Processing and Displays, CRC Press
- James J.F. 2002 A Students Guide to Fourier Transform, Cambridge Univ. Press
- Jeckelmann B., Jeanneret B., 2001, The quantum Hall effect as an electrical resistance standard, Rep. Prog. Phys., 64, 1603-1655
- Jung W.G. 2004 Op Amp Application handbook, Newnes
- Kak A.C., Slaney M., 1988, Principles of computerized tomographic imaging, IEEE Press
- Kester W., 2005, The data conversion handbook, Newnes
- King G., Fukushima T., 2004, RTD interfacing and linearization using an ADuC8xx microconverter, Analog Devices AN-709
- Kitchin C., Counts L., 1986, RMS to DC conversion application guide, Analog Devices
- Kitchin C., Counts J., 2006, A designers guide to instrumentation amplifiers, Analog Devices
- Kohlmann J., Behr R., Funck T., 2003, Josephson voltage standards, Meas. Sc. Technol., 14, 1216-1228
- Kularatna N., 2003, Digital and analogue instrumentation, Institute of Electrical Engineers
- Lai E. 2004 Practical Digital Signal Processing, Newnes
- Levensen M.T., Chiao R.Y., Feldman M.J., Tucker B.A., 1977, An inverse AC Josephson effect voltage standard, Appl. Phys., Lett., 31, 776
- Lutovac M.D., Tosic D.V., Evan B.L. 2000 Filter Design for Signal Processing using MATLAB and Mathematica, Prentice Hall
- Lyons R.G. 2004 Understanding Digital Signal Processing, Prentice Hall
- Madisetti V.K., Willimas D.B. (Editors), 1998, The digital signal processing handbook, CRC Press
- Malik R., 2010, Thermocouple linearization when using the AD8497, AN-1087 Application Note of Analog Devices
- Maloberti F., 2007, Data converters, Springer
- Manabendra Bhuyan, 2011, Intelligent instrumentation, CTC Press
- Mancini R., 2002, OpAmps for Everyne, Texas Inst. Appl. Note
- Massoud Amin S., Wollenberg B.F., 2005, Towards a smart grid, IEEE Power and Energy Magazine, 3 (5), 34-41
- Maxim 2003, Analog Filter Design Demystified, Maxim (Dallas Semiconductors) Technical Note No. 1795

- McClellan J.H., Schafer R.W., Yoder M.A. 1998 DSP First – a Multimedia Approach, Prentice Hall
- Mitra S.K. 2002 Digital Signal Processing, McGraw Hill
- Moghimi R., 2011, To chop or auto-zero: that is the question, Analog Devices Technical Note, MS-2062
- Momoh von J., 2012, Smart grid: fundamentals of design and analysis, John Wiley & Sons
- MT-066, 2009, In-Amp bridge circuit error budget analysis, Analog Devices Tutorial
- Nash E., Greichen J., 1999, Revolutionary RF IC performs rms to DC conversion, Microwaves & RF, 38, 140-149
- NIST 1458 2003 NIST Measurement Service for DC Standard Resistors, NIST Technical Note 1458
- Northrop R.B. 1997 Introduction to Instrumentation and Measurements, CRC Press
- Norsworthy S.R., Temes G.C. 1996 Delta Sigma Data Converters, IEEE Computer Society
- Novoselov K.S. et al, 2007, Room temperature quantum Hall effect in graphene, Science, 315, No. 5817, 1739
- Nuce D.S., 2004, Linear position sensors, Wiley Interscience
- Okazakio Y., Yanase S., Nakamura Y., Maeno R., 2009, Magnetic shielding by grain-oriented electrical steel sheet under alternating fields up to 100 kHz, Przegł. Elektr., 85, No.1, 55-59
- Ott H.W. 1988 Noise Reduction in Electronic System, John Wiley & Sons
- Padmanabhan T.R., 2000, Industrial instrumentation, Springer
- Pallas-Areny, Webster, 1999, Analog signals processing, John Wiley & Sons
- Pallas Areny R., Webster J.G., 2001, Sensors and signal conditioning, John Wiley & Sons
- Park P.G., Kim Y.G., Shifrin V.Y., 2005, Maintenance of magnetic flux density standards on the basis of proton gyromagnetic ratio at KRISS, IEEE Trans. Instr. Meas., 54, No.2, 734-737
- Rak R., Majkowski A., 2004, Time-frequency signal analysis, Przegład Elektrotechniczny, 515-520
- Rich A. 2005 Shielding and Guarding, Analog Devices Application Note AN-347
- Sarma K.R., 2004, Liquid Crystal Displays, Chapter 31 in Electrical Measurements, Signal Processing and Displays of CRC Press
- Schaumann R. 2001 Design of Analog Filters, Oxford University Press
- Scholes R., 1970, Application of operational amplifiers to magnetic measurements, IEEE Trans. Magn., 6, 289-291
- Schott C., Blanchard H., Popovic R., Racz R., Hrejsa J., 1997, High accuracy analog Hall probe, IEEE Trans. Instr. Meas., 46, 613-616
- Schreier R. Temes G. 2005 Understanding Delta Sigma Converters, Wiley & Sons
- Scofield J.H. 1994 A frequency domain description of a lock-in amplifier, American Journal of Physics, 62, pp. 122-133
- Seebeck T., 1822, Magnetische polarization der Metalle und Erze durch Temperature Differenz, Abh. Der Preussischen Academic der Wissenschaft
- Smith S.W. 2003 Digital Signal Processing, Newnes
- Sneddon I.N. 1995 Fourier Transform, Dover Publ
- Stanley W.D. 2001 Operational Amplifiers and Linear Integrated Circuits, Prentice Hall
- Stata R., 1967, Operational integrators, Analog Dialogue, 1, 11-16
- Stranney D. 2001 Digital Signal Processing, Newnes
- Thede L. 2004 Practical Analog and Digital Filter Design, Artech House
- Tran Tien Lang 1987 Electronics of Measuring Systems, Wiley & Sons
- Van Putten A.F.P., 1996, Electronic measurement systems, IOP Publishing
- Vaseghi S., 2007, Multimedia signal processing, John Wiley & Sons
- Volkenburg M.E. 1995 Analog Filter Design, Oxford University Press
- Wassenar R., Seevinck E., van Leeuwen M.G., Speelman C.J., Holle E., 1988, New technologies for high frequency rms to DC conversion based on a multifunctional V to I converter, IEEE J. Solid State Circuits, 23, No.3, 802-814
- Weyand K., 2001, Magnetic field standards – trace to the maintained units, Int. J. Apl. Electromagnetism and Mechanics, 13, 195-202
- Williams J., 1988, Thermocouple measurement, AN28 Application Note of Linear Technology
- Winder S. 2002 Analog and Digital Filter Design, Newnes
- Witt T.J., 1998, Electrical resistance standards and the quantum Hall effect, Rev. Sc. Instr., 69, No.8, 2823-2843
- Wong V., 2011, Lowest noise zero drift amplifier has 5.6 nV/rtHz voltage noise density, Analog Device Application Note AN-1114
- Yamazaki K., Muramatsu K., Hirayama M., Haga A., Torita F., 2006, Optimal structure of magnetic and conductive layers of a magnetically shielded room, IEEE Trans. Magn., 42, 3524-3526
- Zhang Y., Tan Y.W., Stormer H.L., 2005, Experimental observation of the quantum Hall effect and Berry's phase in grapheme, Nature, 438, 201-204
- Zumbahlen H. (Ed), 2008, Linear circuit design handbook, Elsevier